

Lagrangian transport and mixing in fluids from geometric, probabilistic, and topological perspectives

Shane Ross

Department of Biomedical Engineering and Mechanics, Virginia Tech

with A. BozorgMagham, S. Naik, P. Nolan, P. Tallapragada, P. Grover,
D. Schmale, M. Stremmer, P. Kumar, F. Lekien, P. Vlachos

Numerical Analysis and Predictability of Fluid Motion

University of Pittsburgh, May 3, 2016



1520825
1150456
0966125

shaneross.com
@RossDynamicsLab
sdross@vt.edu



Motivation: complex fluid motion, mixing, and control

fluid particle motion, $\dot{x} = u(x, t)$

Oceans¹

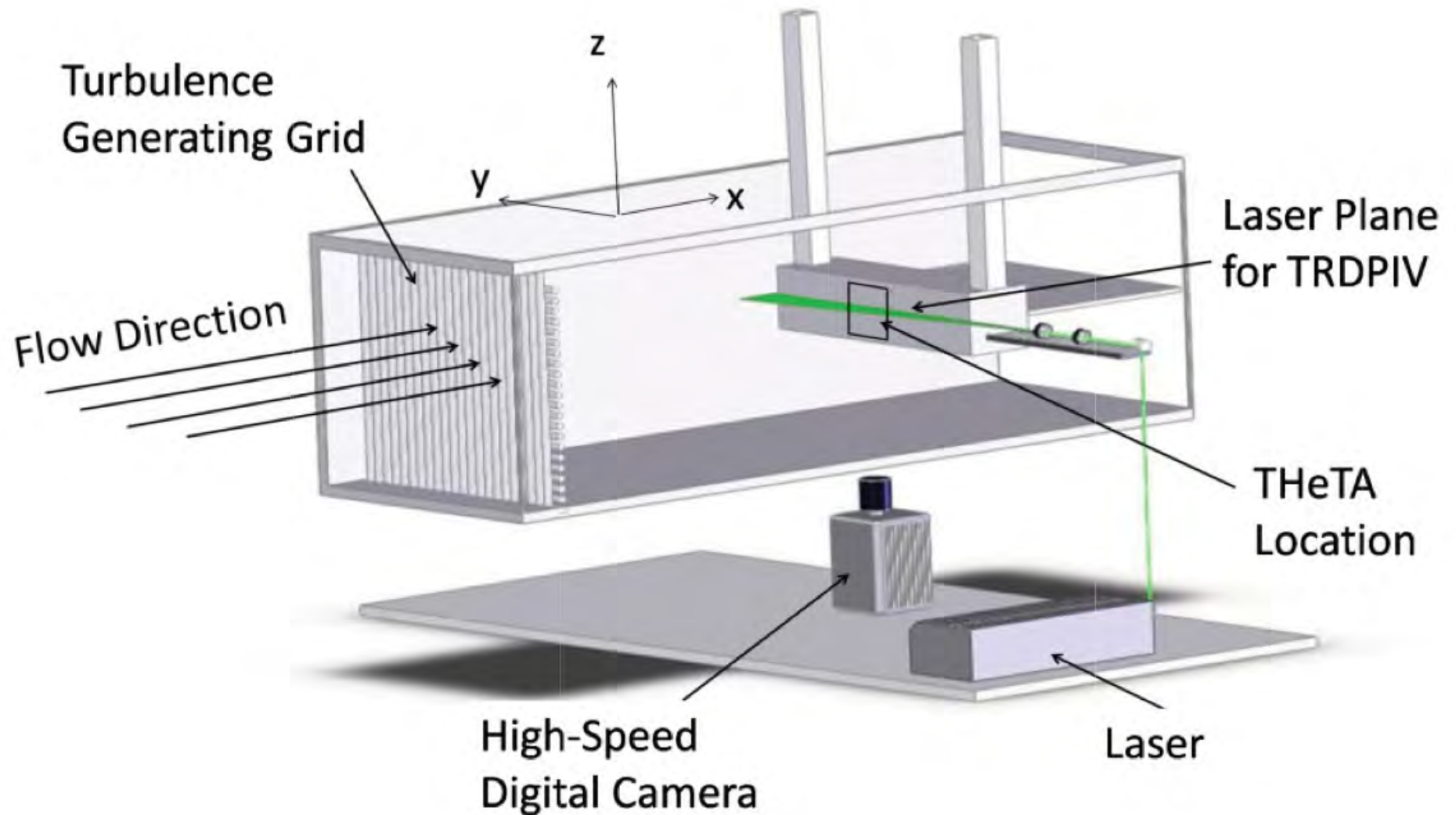
Atmosphere²

¹ Special material surfaces in an ocean model (Harrison, Siegel, Mitarai [2013])

² Special material surfaces over North America: orange = repelling, blue = attracting

Lagrangian transport in fluid experiments

A particle image velocimetry (PIV) fluid experiment — Vlachos lab (Virginia Tech/Purdue)



Raben, Ross, Vlachos [2014, 2015] Experiments in Fluids

Lagrangian transport in fluid experiments

Eulerian analysis

Lagrangian analysis

Motivation: application to real fluid data

- Fixed points, periodic orbits, or other invariant sets and their stable and unstable manifolds **form cores of fluid deformation patterns**
- Many systems defined from data or large-scale simulations — experimental measurements, observations
- e.g., from geophysical fluids, ecology, fluid experiments
- Data-based, aperiodic, finite-time, finite resolution — generally no fixed points, periodic orbits, etc. to organize phase space
- **Geometric methods** to analyze Lagrangian particle transport for — velocity field defined analytically (time-periodic, 2D domain) — velocity field from geophysical fluid numerical simulation (a-periodic)
- Other tools (e.g., **probabilistic, topological**) useful in some settings

Chaotic phase space transport in a 2D map

- Suppose our dynamical system is a **discrete map**¹

$$f : \mathcal{M} \longrightarrow \mathcal{M},$$

eg: $f = \phi_t^{t+T}$, time- T flow map of periodic **vector field**,

$$\dot{x} = u(x, t) \quad \text{where} \quad u(x, t) = u(x, t + T),$$

where $x \in \mathcal{M}$ and \mathcal{M} is a differentiable, orientable, two-dimensional manifold e.g., $\mathcal{M} \subset \mathbb{R}^2$

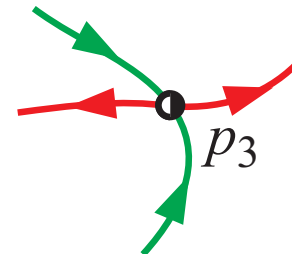
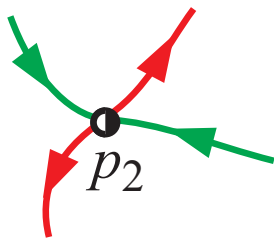
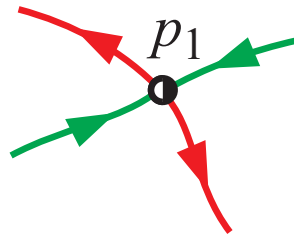
- To understand the transport of points under map f , consider invariant manifolds of unstable fixed points
 - Let $p_i, i = 1, \dots, N_p$, denote **saddle points** of f

¹Following Rom-Kedar and Wiggins [1990]

Partition phase space into regions

□ Natural way to partition phase space

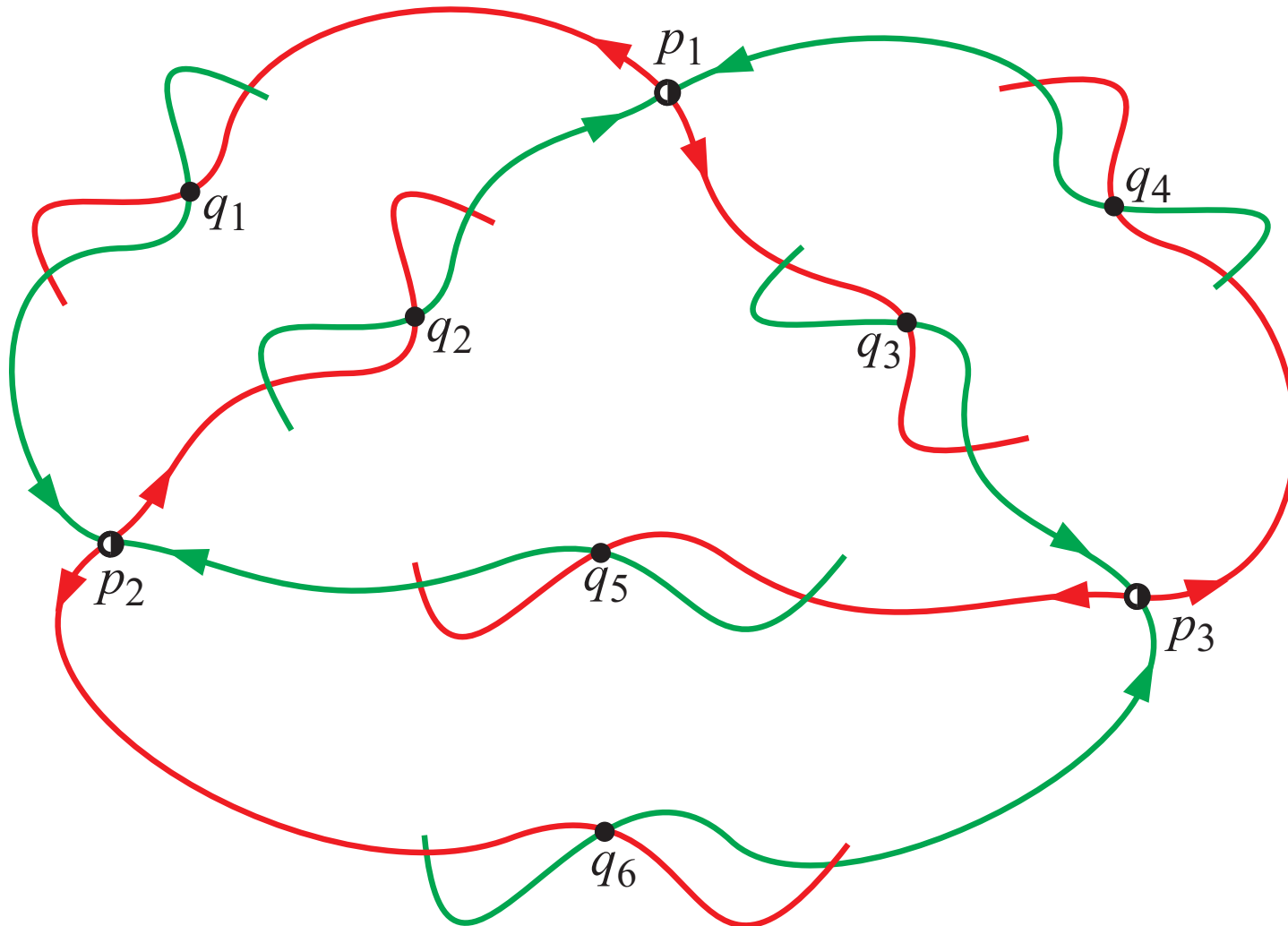
- Unstable and stable manifolds ($W^u(p_i)$, $W^s(p_i)$) partition \mathcal{M} .



Unstable ($W^u(p_i)$) and stable ($W^s(p_i)$) manifolds in **red** and **green**, resp.

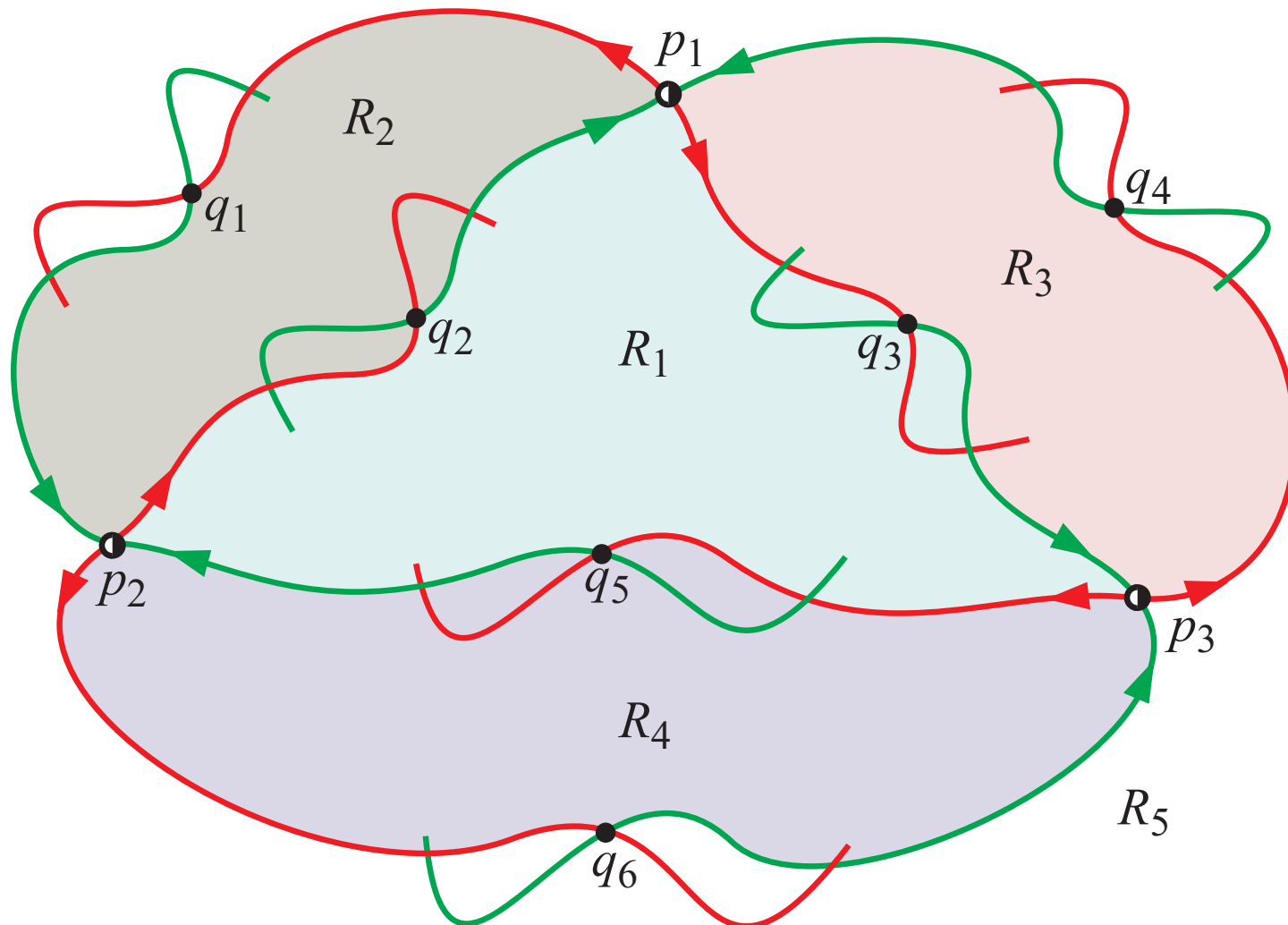
Partition phase space into regions

- Intersection of unstable and stable manifolds define **boundaries**.



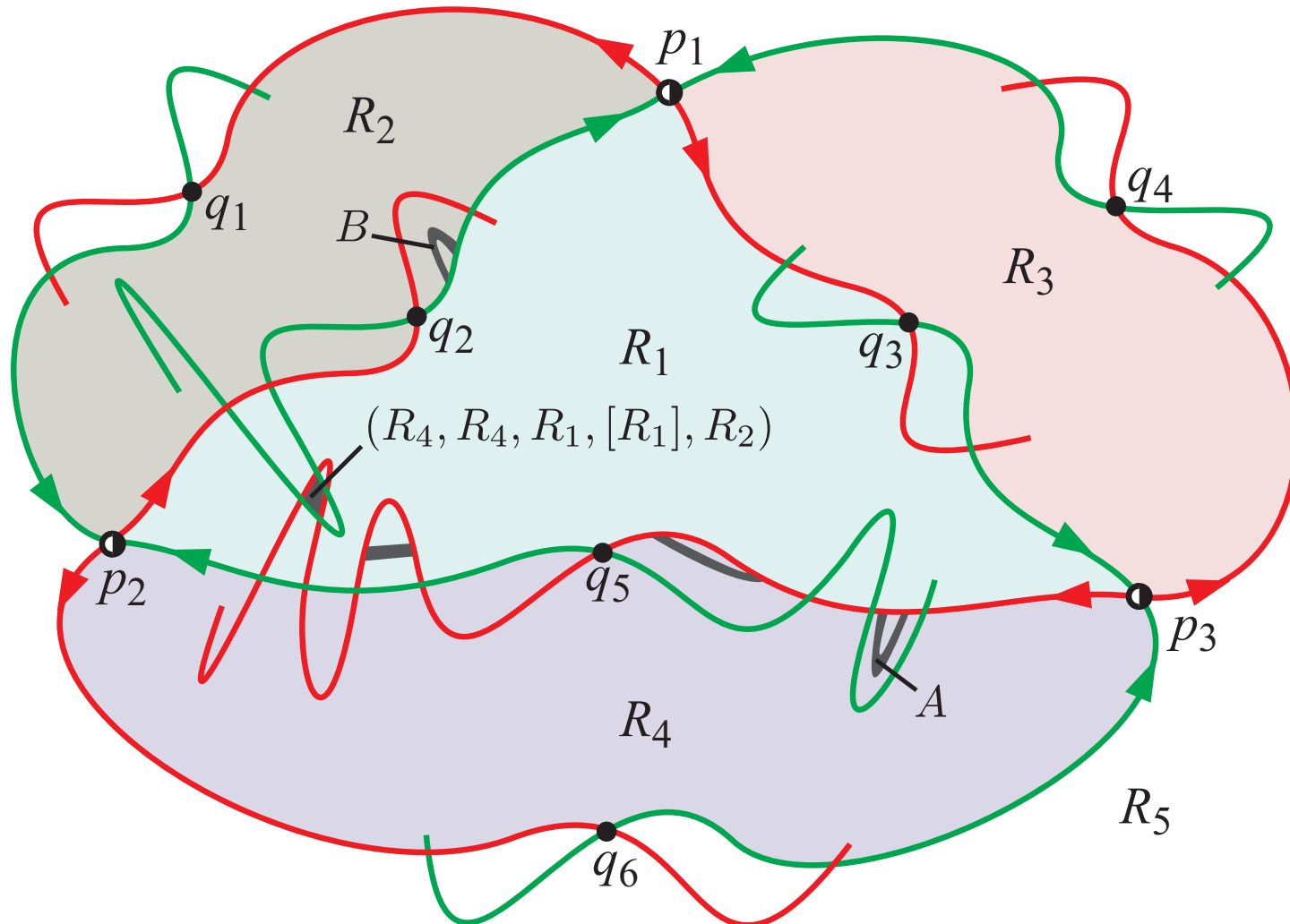
Partition phase space into regions

- These boundaries divide the phase space into **regions**



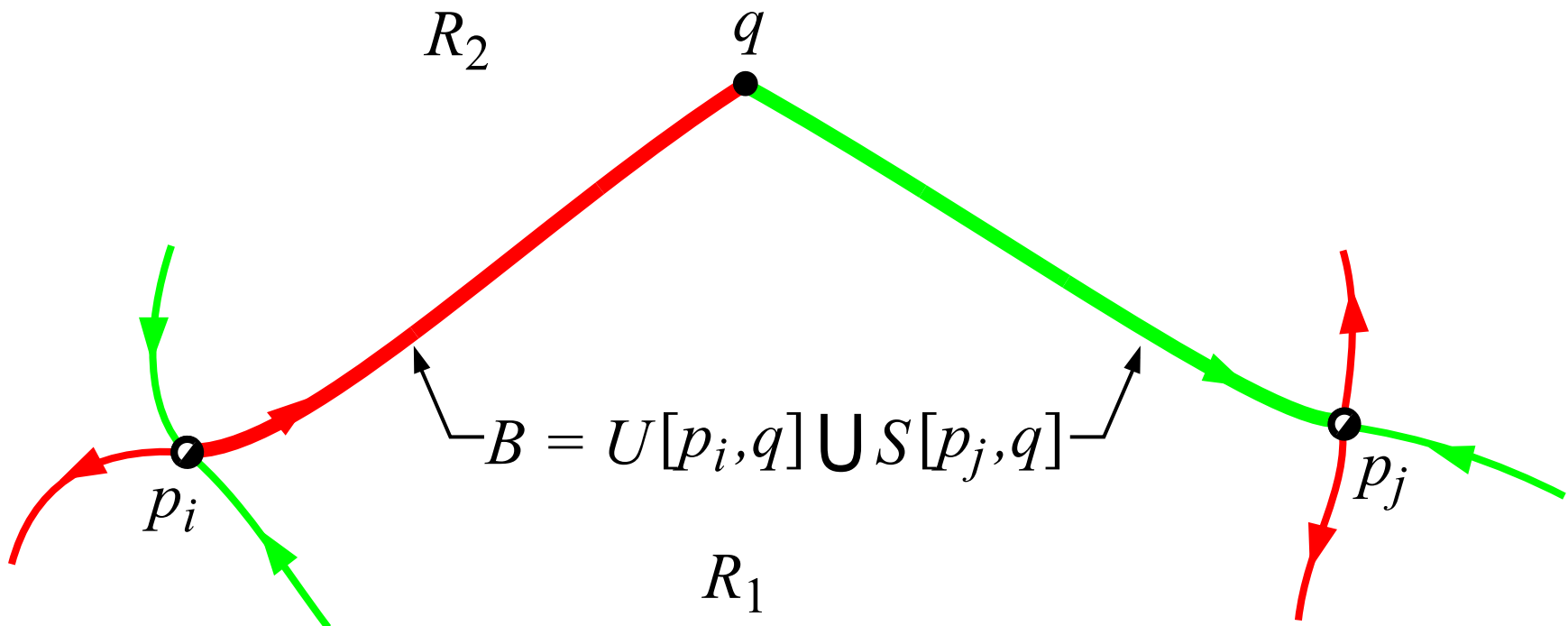
Label subregions: 'atoms' of transport

- Can label mobile subregions based on their past and future whereabouts under iterates of the map, e.g., $(R_4, R_4, R_1, [R_1], R_2)$



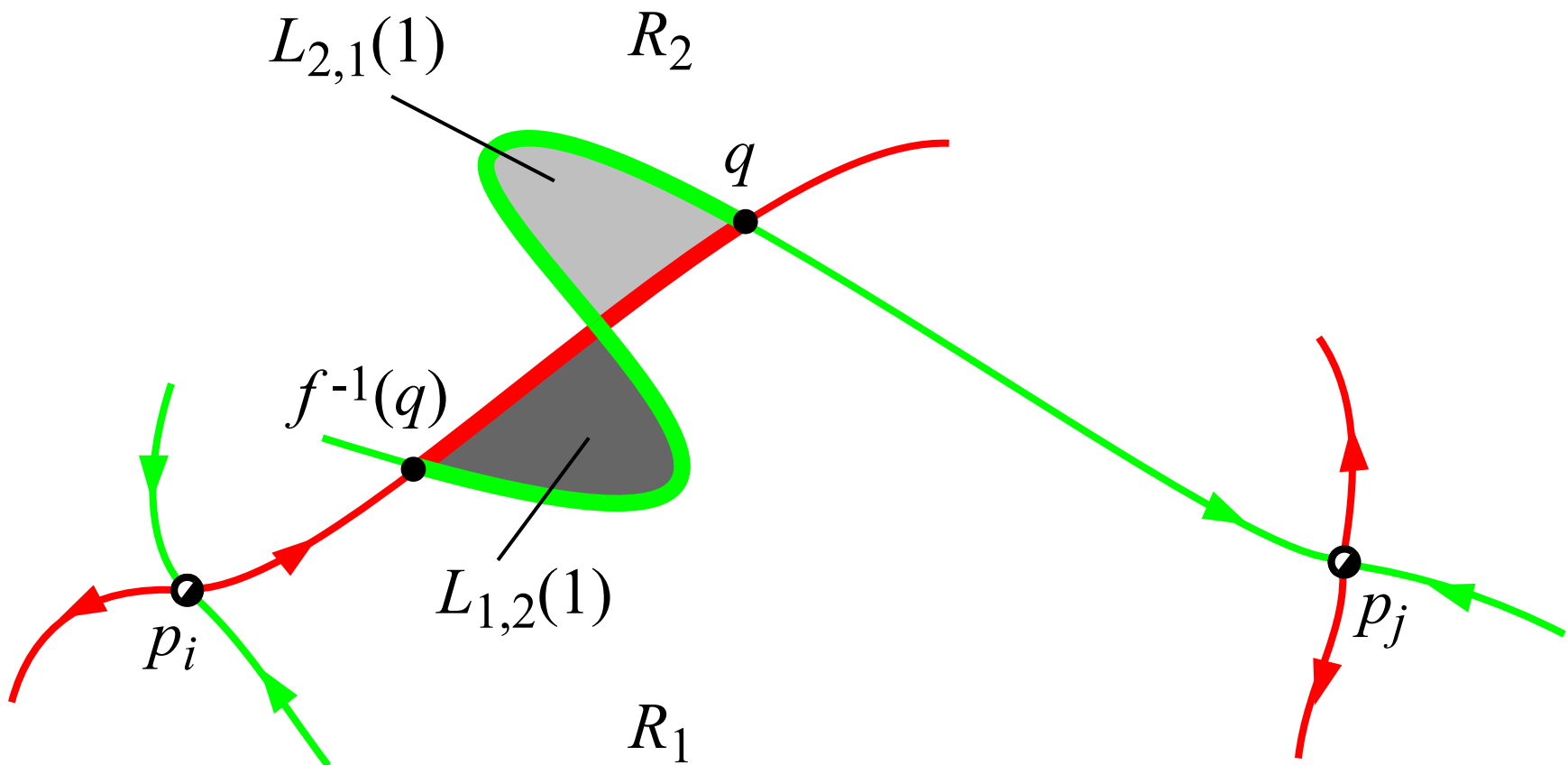
Lobe dynamics: transport across a boundary

- Suppose $W^u(p_i)$ and $W^s(p_j)$ intersect in point q . Define $B \equiv U[p_i, q] \cup S[p_j, q]$ as a **boundary** between “two sides,” R_1 and R_2 .



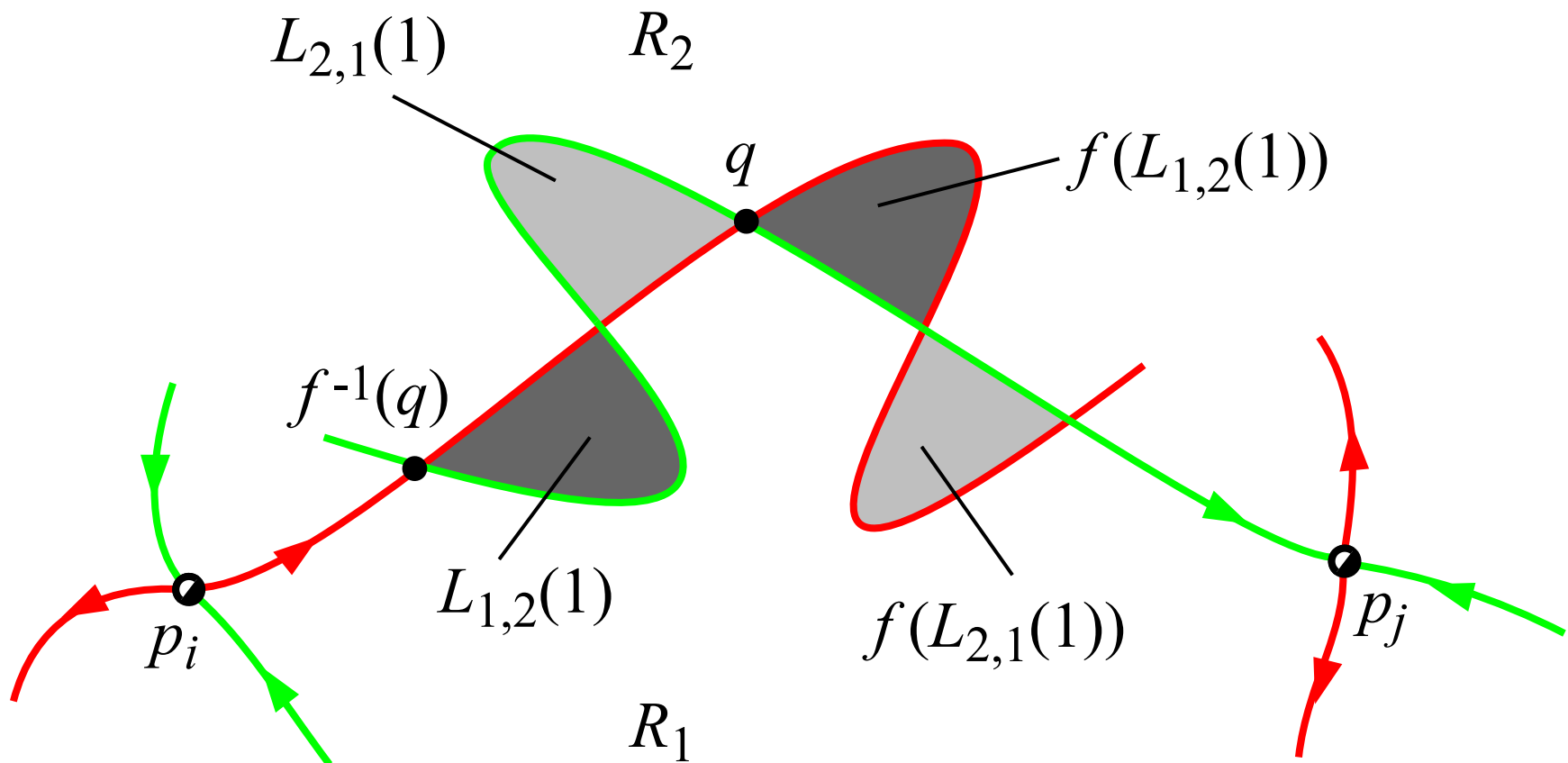
Lobe dynamics: transport across a boundary

- $W^u[f^{-1}(q), q] \cup W^s[f^{-1}(q), q]$ forms boundary of two lobes; one in R_1 , labeled $L_{1,2}(1)$, or equivalently $([R_1], R_2)$, where $f(([R_1], R_2)) = (R_1, [R_2])$, etc. for $L_{2,1}(1)$



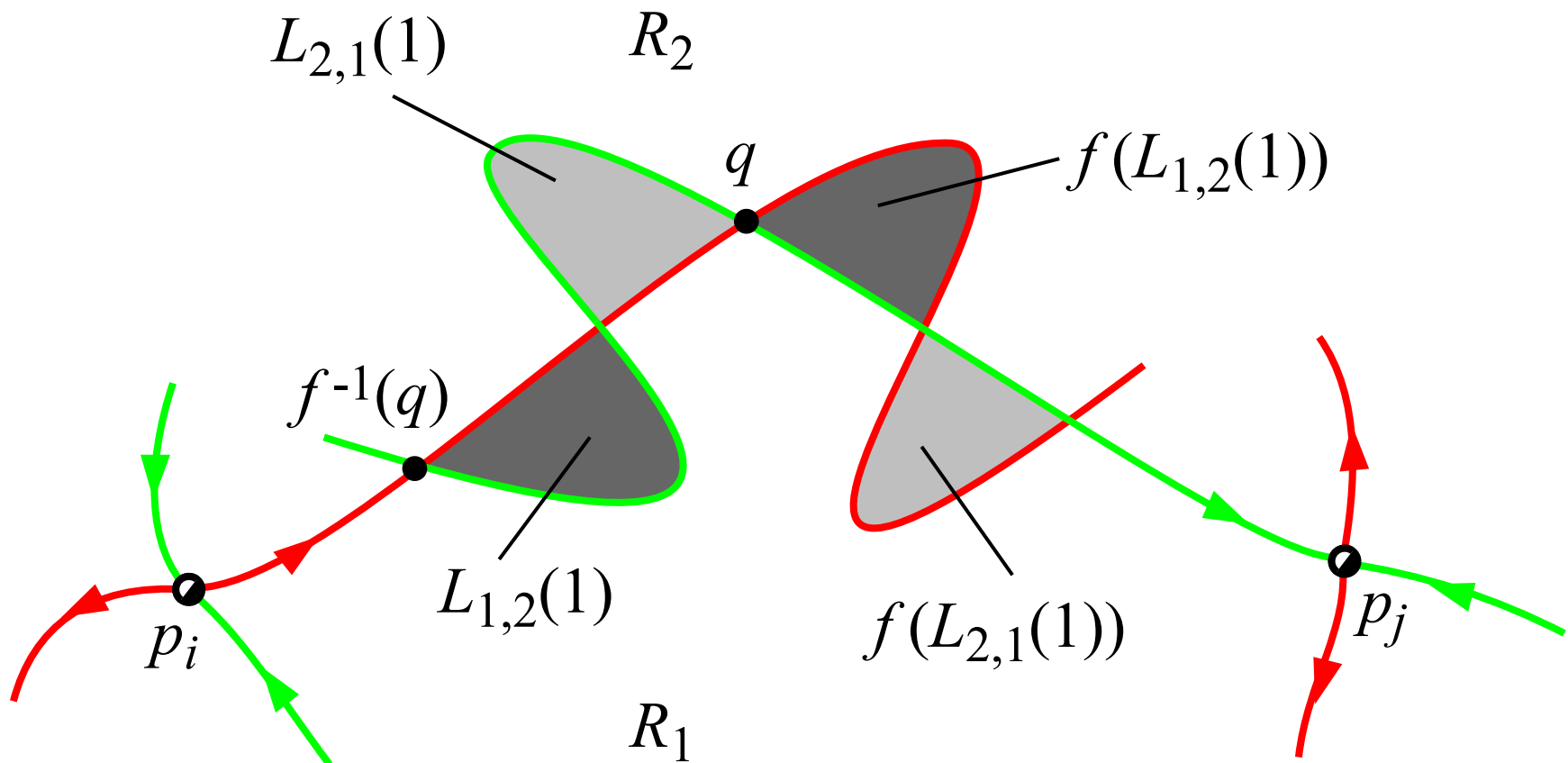
Lobe dynamics: transport across a boundary

- Under one iteration of f , **only points in $L_{1,2}(1)$** can move from R_1 into R_2 by crossing their boundary, etc.
- The two lobes $L_{1,2}(1)$ and $L_{2,1}(1)$ are called a **turnstile**.



Lobe dynamics: transport across a boundary

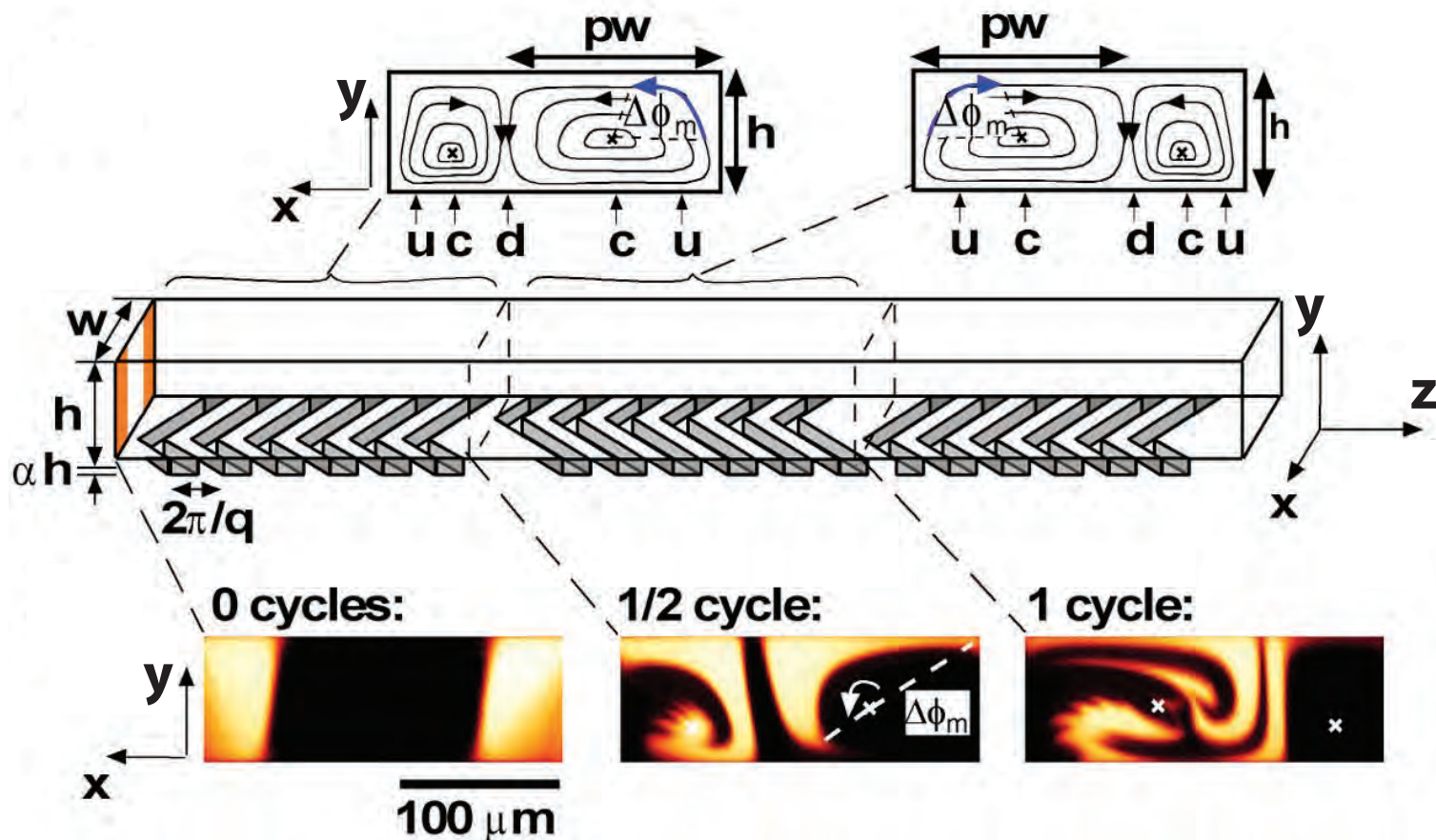
- Essence of lobe dynamics: **dynamics associated with crossing a boundary is reduced to the dynamics of turnstile lobes associated with the boundary.**



Lobe dynamics: intimately related to transport

A time-periodic 2D fluid

- A microchannel mixer: microfluidic channel with **spatially periodic** flow structure, e.g., due to grooves or wall motion²

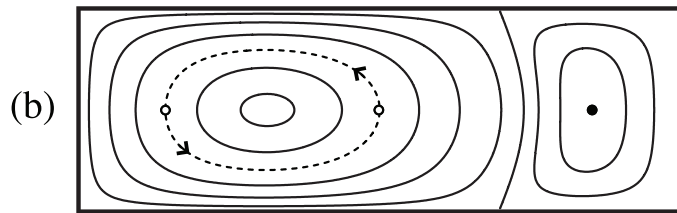
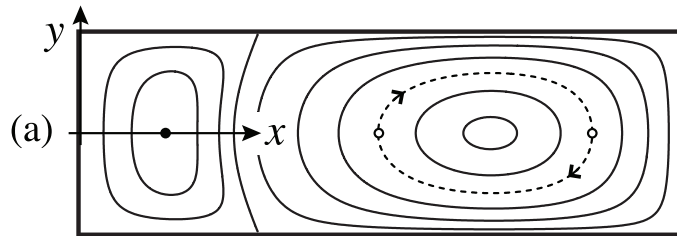


- How does behavior change with parameters?

²Stroock et al. [2002], Stremler et al. [2011]

A time-periodic 2D fluid

- A microchannel mixer: modeled as **time-periodic** Stokes flow



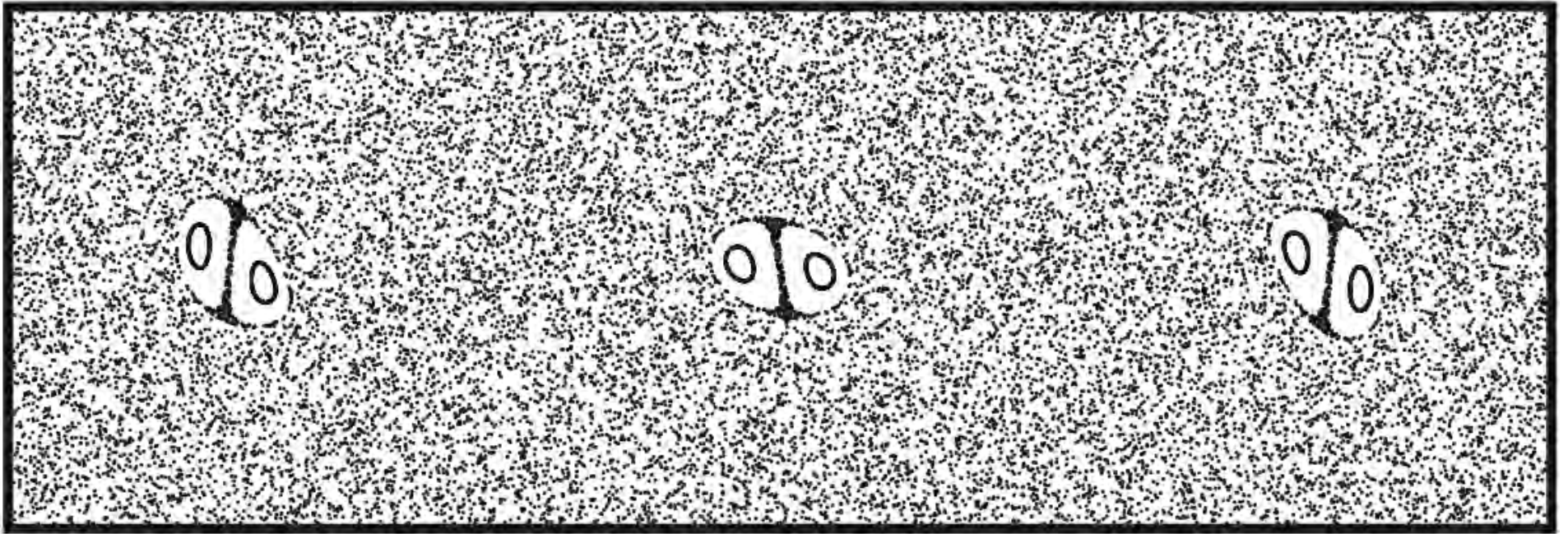
streamlines for $\tau_f = 1$

tracer blob ($\tau_f > 1$)

- piecewise constant vector field (repeating periodically)
top streamline pattern during first half-cycle (duration $\tau_f/2$)
bottom streamline pattern during second half-cycle (duration $\tau_f/2$), then repeat
- System has parameter τ_f , period of one cycle of flow, which we treat as a bifurcation parameter — there's a critical point $\tau_f^* = 1$

A time-periodic 2D fluid

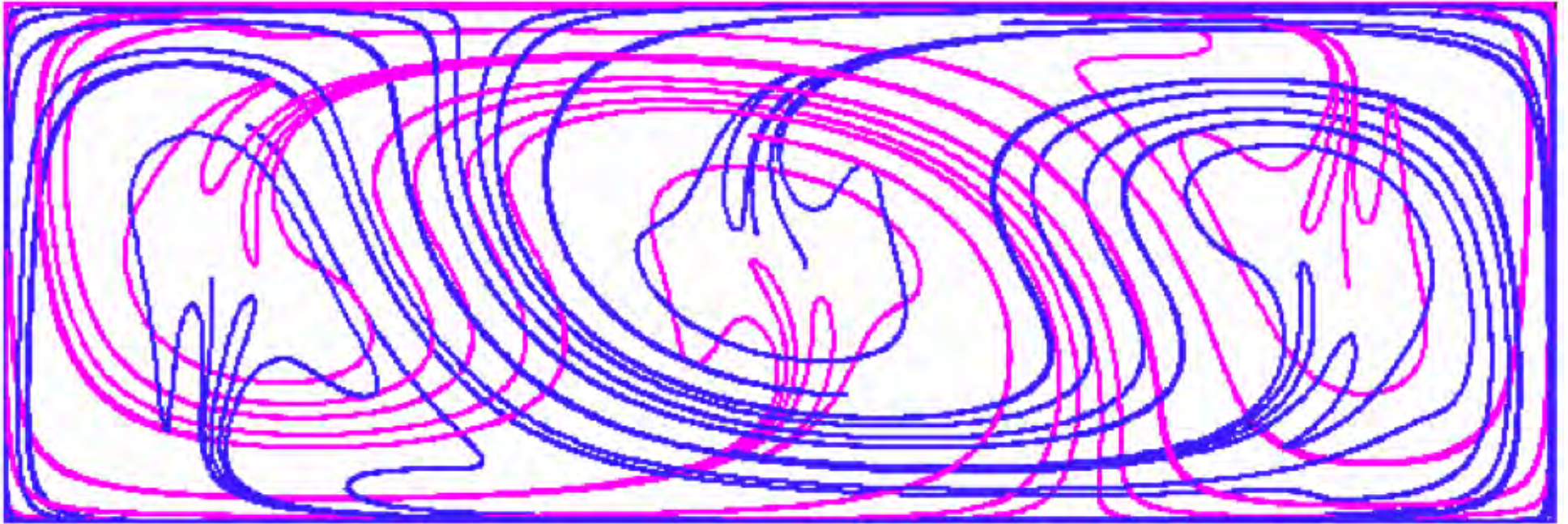
□ Poincaré map for $\tau_f > 1$



period-3 points bifurcate into groups of elliptic and saddle points, each of period 3

A time-periodic 2D fluid

- Structure associated with saddles, lobes



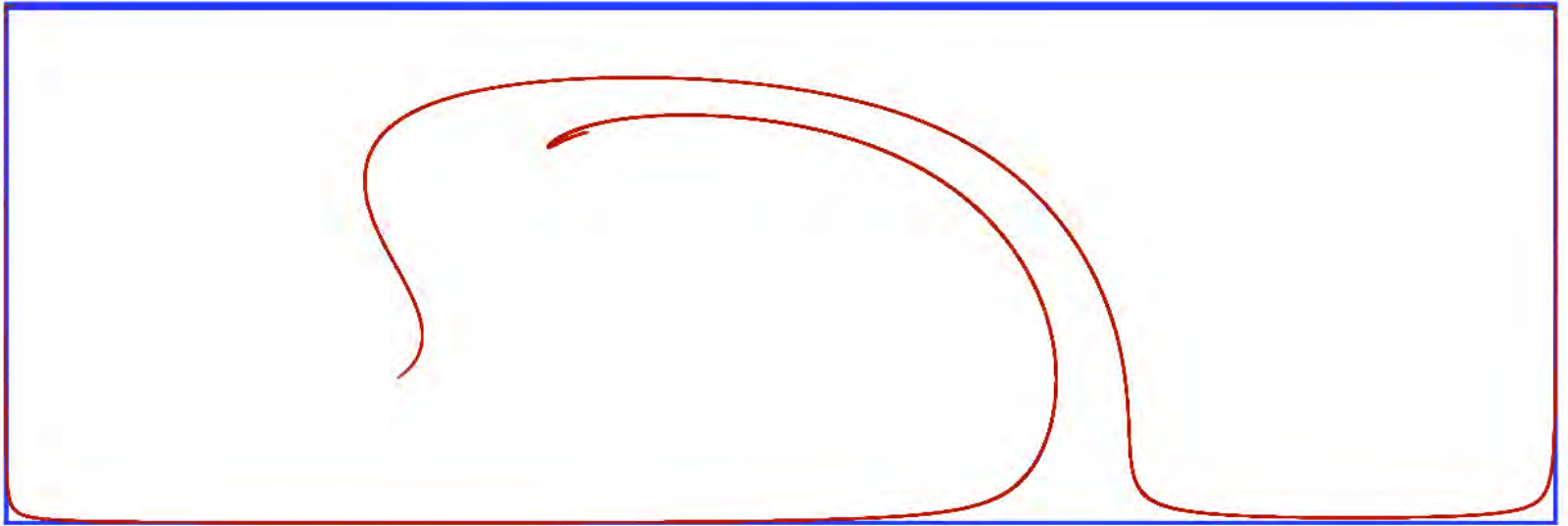
some invariant manifolds of saddles

Stable/unstable manifolds and lobes in fluids



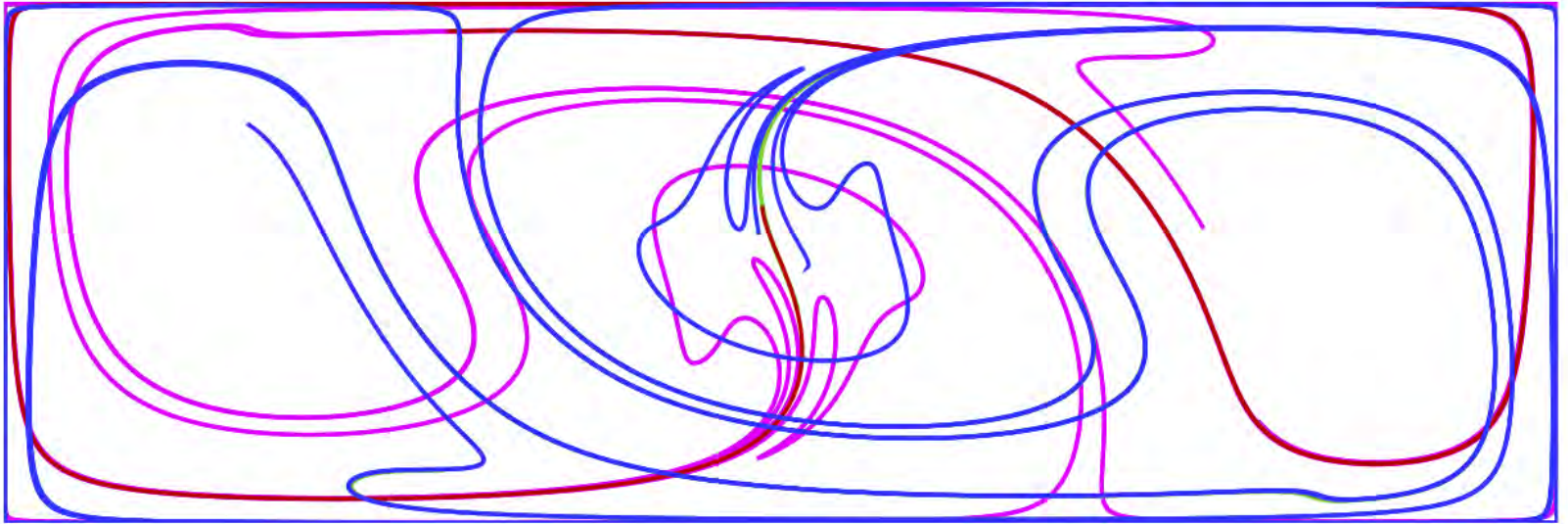
material blob at $t = 0$ periods

Stable/unstable manifolds and lobes in fluids



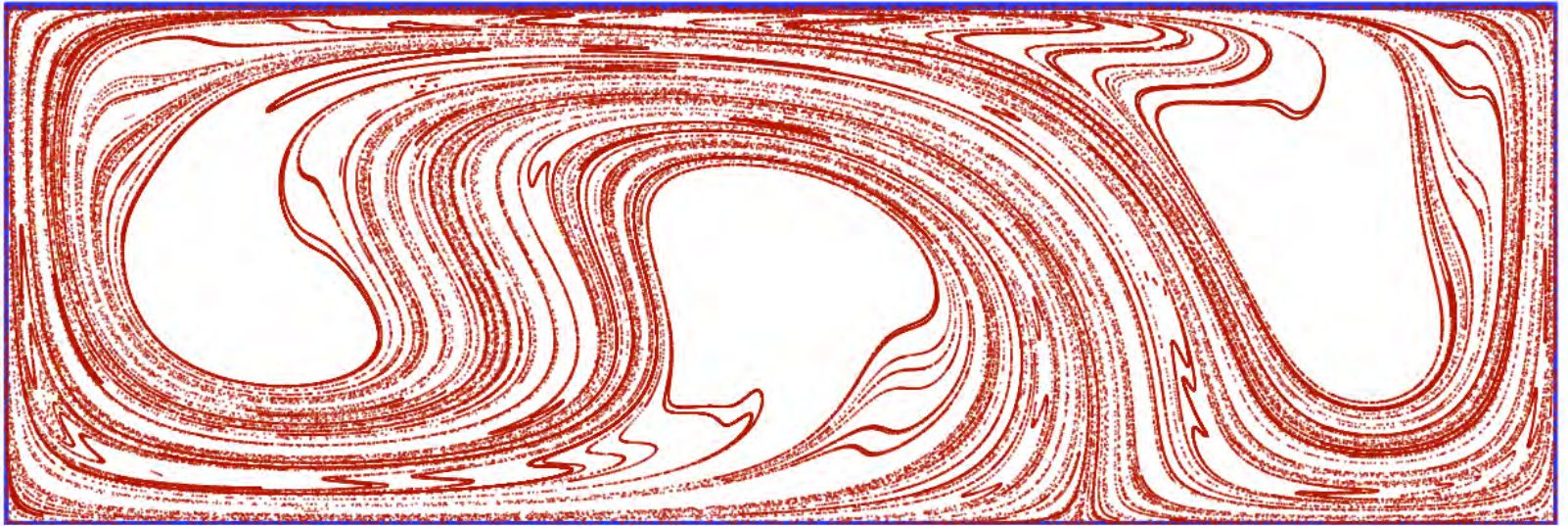
material blob at $t = 2$ periods

Stable/unstable manifolds and lobes in fluids



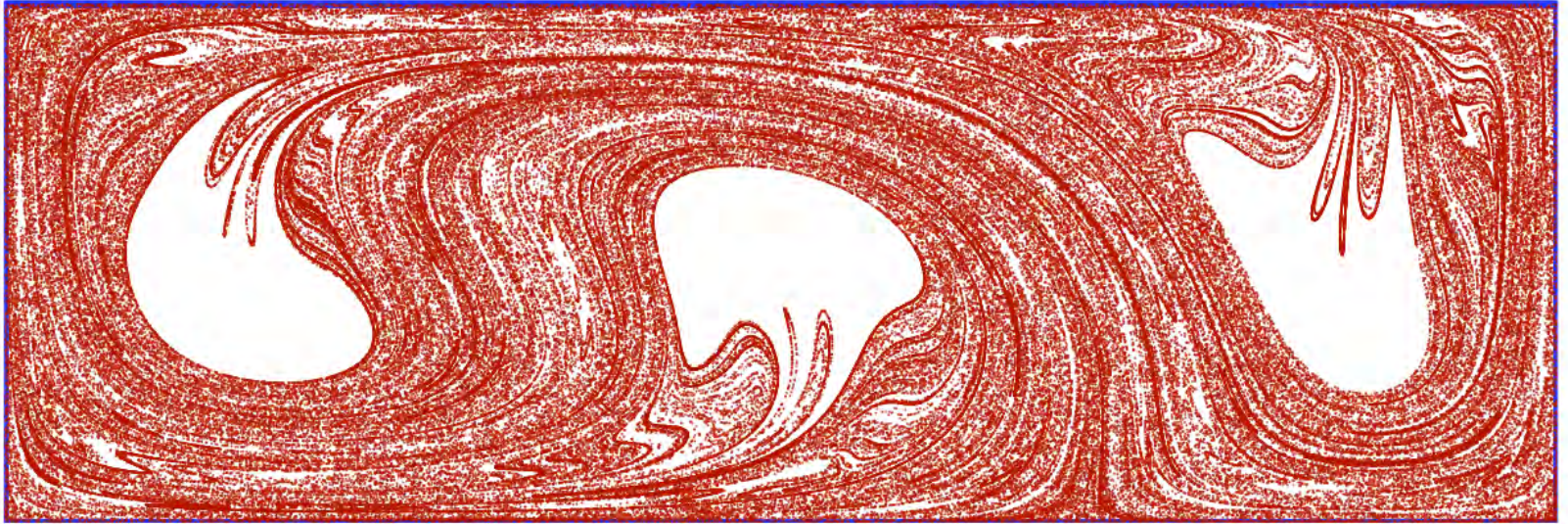
some invariant manifolds of saddles

Stable/unstable manifolds and lobes in fluids



material blob at $t = 4$ periods

Stable/unstable manifolds and lobes in fluids



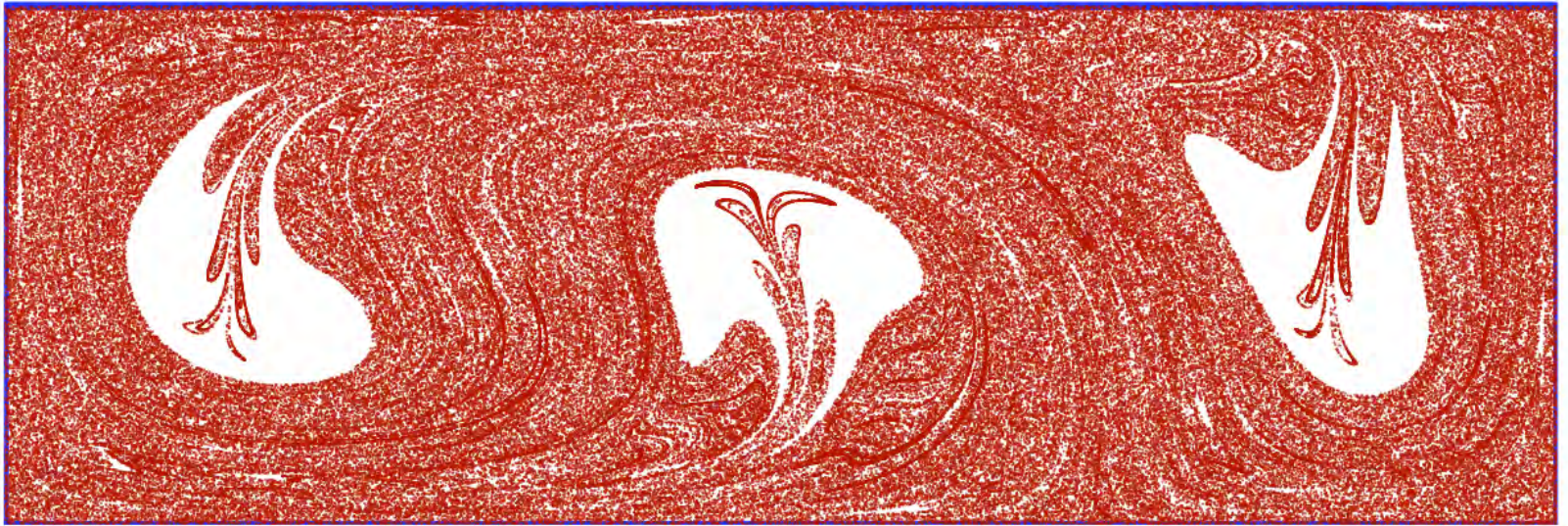
material blob at $t = 8$ periods

Stable/unstable manifolds and lobes in fluids



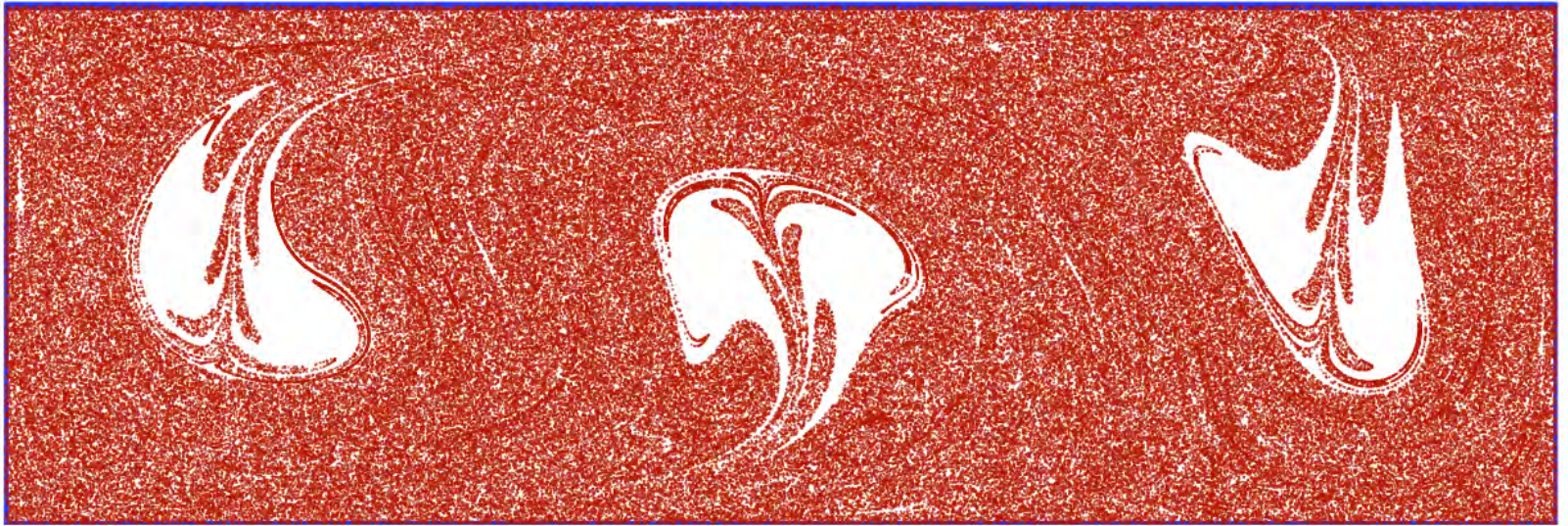
material blob and manifolds

Stable/unstable manifolds and lobes in fluids



material blob at $t = 10$ periods

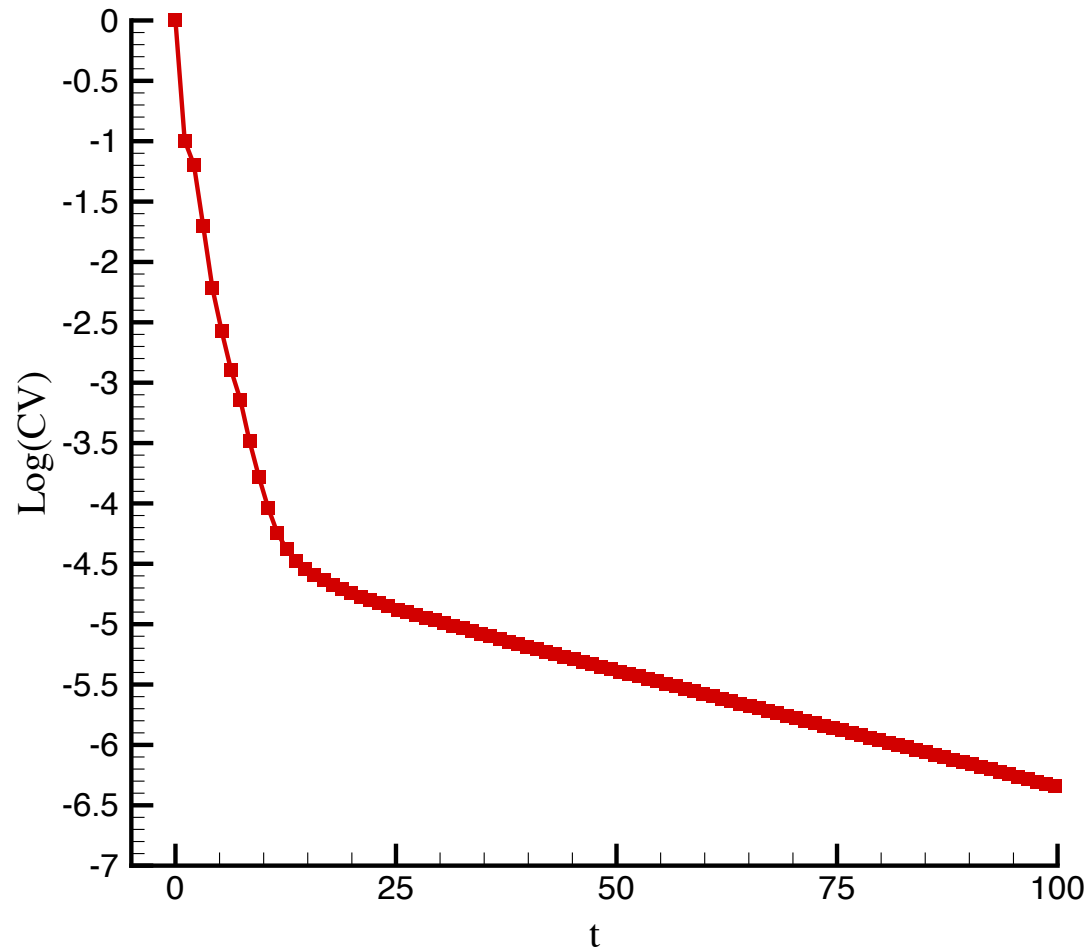
Stable/unstable manifolds and lobes in fluids



material blob at $t = 12$ periods

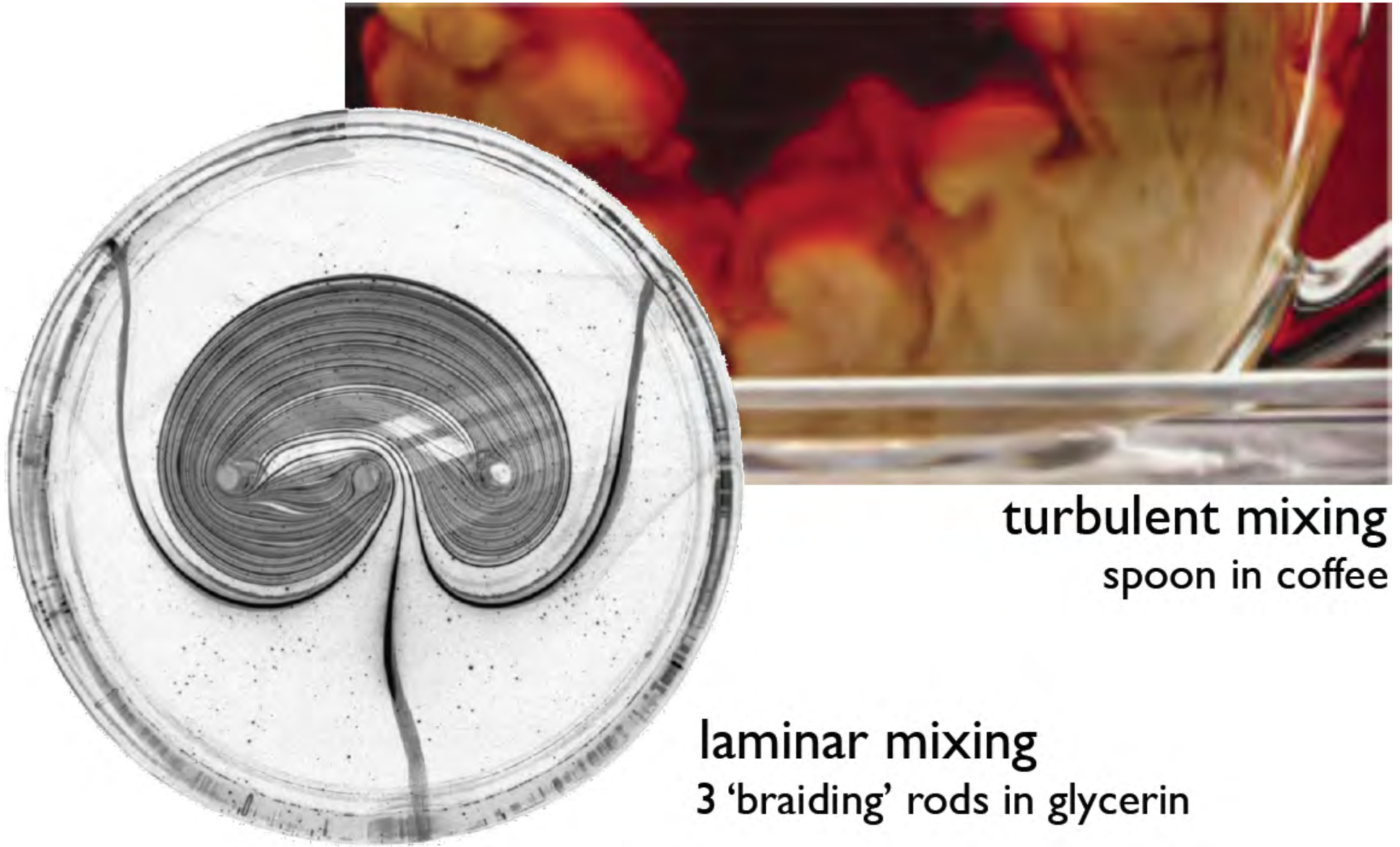
Stable/unstable manifolds and lobes in fluids

□ Concentration variance; a measure of homogenization



- Homogenization has two exponential rates: slower one related to lobes
- Fast rate due to large-scale stirring ...

Stirring fluids, e.g., with solid rods

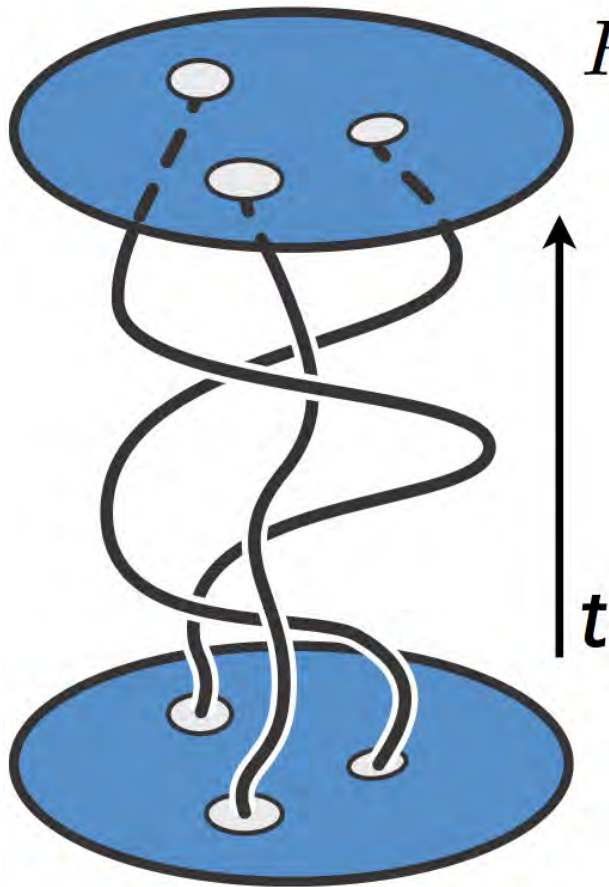


turbulent mixing
spoon in coffee

laminar mixing
3 'braiding' rods in glycerin

Topological chaos through braiding of 'stirrers'

- Topological chaos is 'built in' to the flow due to the topology of boundary motions



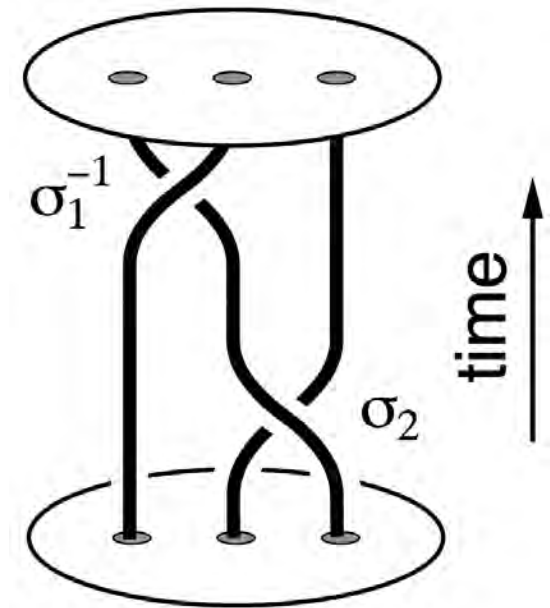
R_N : 2D fluid region with N stirring 'rods'

- stirrers move on periodic orbits
- stirrers = solid objects or *fluid particles*
- stirrer motions generate diffeomorphism
 $f : R_N \rightarrow R_N$
- stirrer trajectories generate braids
in 2+1 dimensional space-time

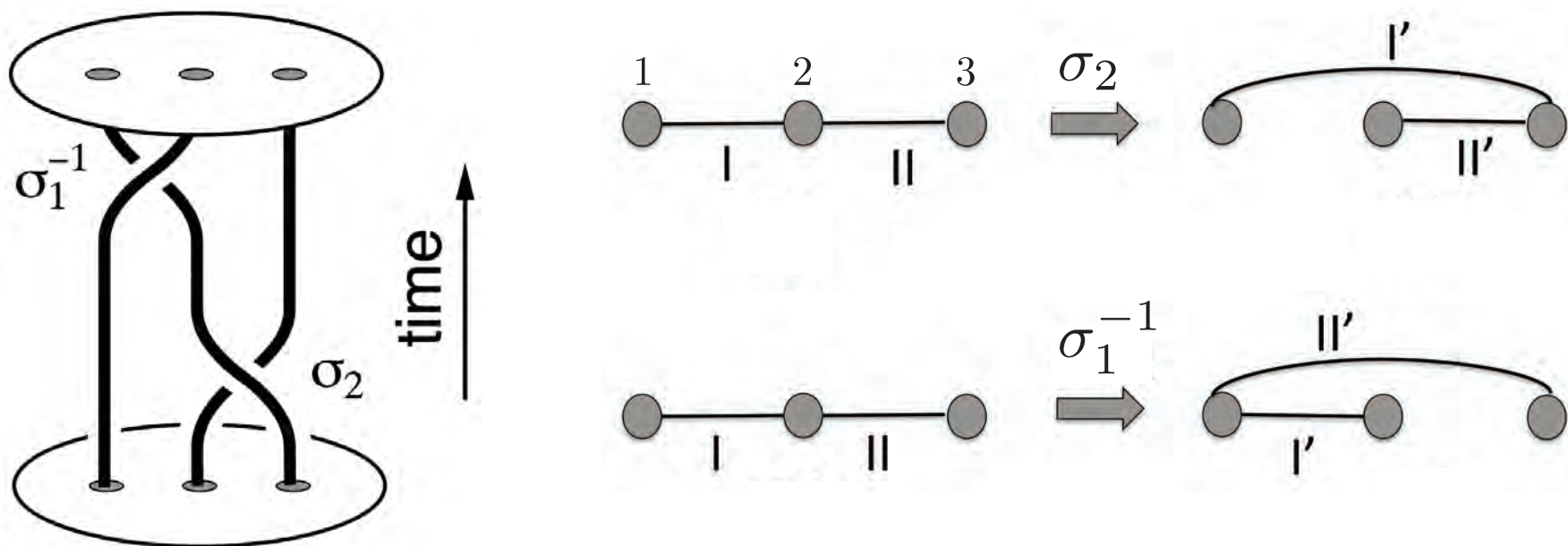
Thurston-Nielsen classification theorem (TNCT)

- Thurston (1988) Bull. Am. Math. Soc.
- A stirrer motion f is isotopic to a stirrer motion g of one of three types (i) finite order (f.o.): g^n is the identity, for some n (ii) pseudo-Anosov (pA): g has Markov partition with transition matrix A , **topological entropy** $h_{\text{TN}}(g) = \log(\lambda_{\text{PF}}(A))$, where $\lambda_{\text{PF}}(A) > 1$ (iii) reducible: g contains both f.o. and pA regions

- h_{TN} computed from **braid word**, e.g., $\sigma_1^{-1}\sigma_2$
- h_{TN} provides a **lower bound** on the true topological entropy h_{flow}



Action of a braid, e.g., $\sigma_1^{-1}\sigma_2$



repeated application gives stretching and folding

that's the essence of a pseudo-Anosov braid

Viscous fluid experiment with this pA braid

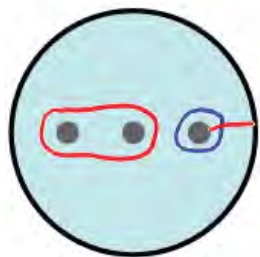
Move 3 rods on 'figure-8' paths through glycerin

Boyland, Aref & Stremler (2000) *J. Fluid Mech.*

- stirrers move on periodic orbits in two steps
- Thurston-Nielsen theorem gives a lower bound on stretching:

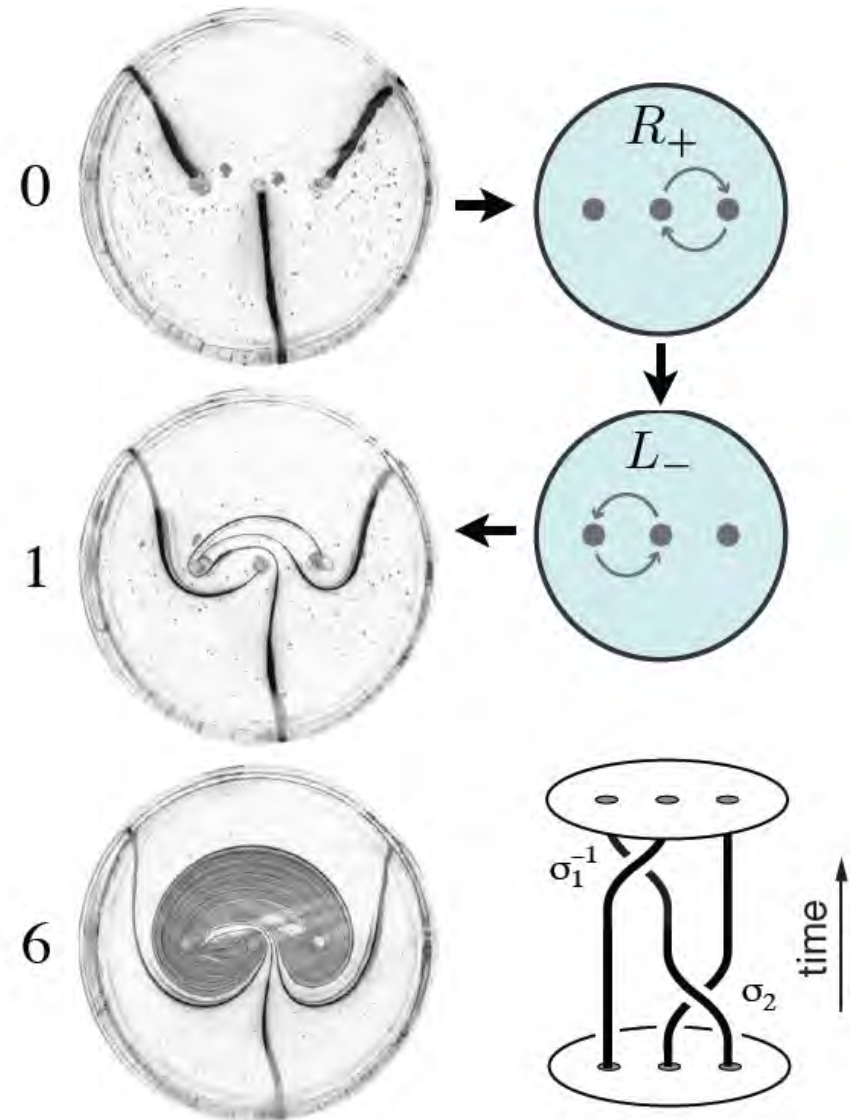
$$\lambda_{\text{TN}} = \frac{1}{2} (3 + \sqrt{5})$$

$$h_{\text{TN}} = \log(\lambda_{\text{TN}}) = 0.962 \dots$$

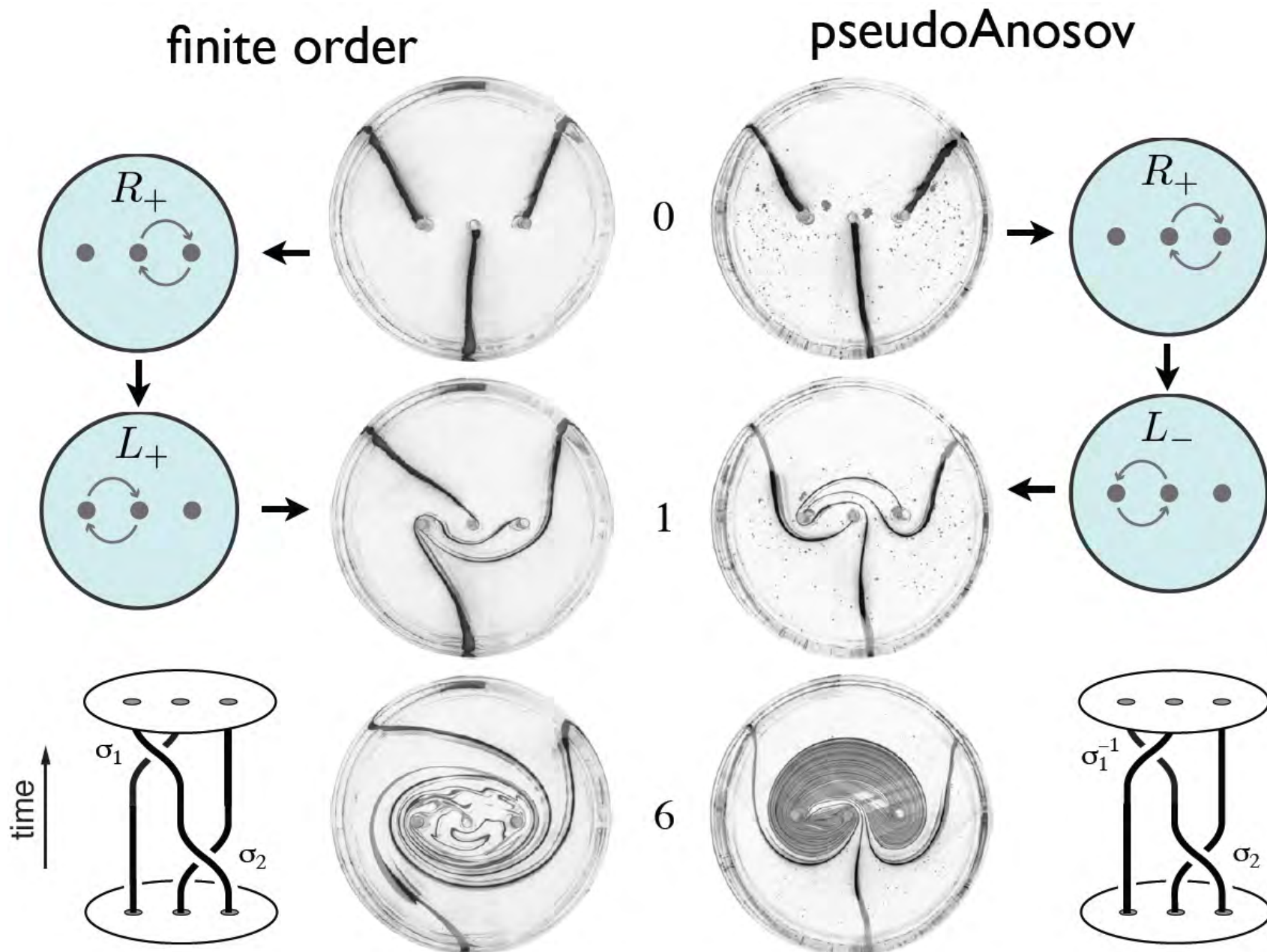


non-trivial material lines
grow like $l \sim l_0 \lambda^n$

$$\lambda \geq \lambda_{\text{TN}}$$



Viscous fluid experiment: f.o. and pA braid



Stirring with periodic orbits, i.e., ‘ghost rods’

point vortices in a periodic domain

Boyland, Stremler & Aref (2003) *Physica D*

one rod moving on an epicyclic trajectory

Gouillart, Thiffeault & Finn (2006) *Phys. Rev. E*



Fluid is wrapped around ‘ghost rods’ in the fluid

– *flow structure assists in the stirring*

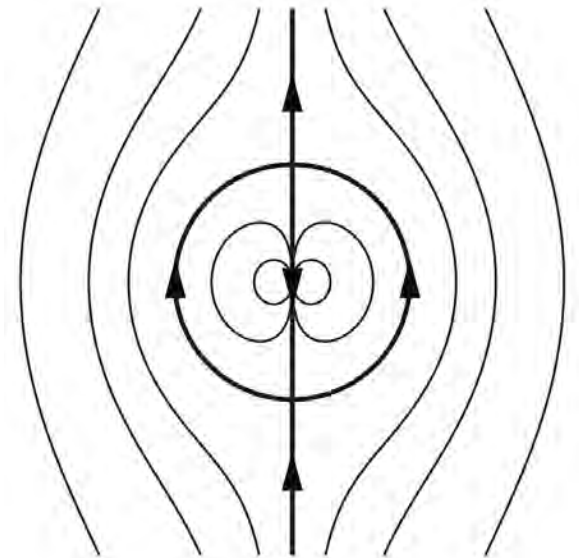
Stirring with periodic orbits, i.e., 'ghost rods'

A combination of 'ghost rods' (particle periodic orbits) and solid rods can form a braid for application of TNCT

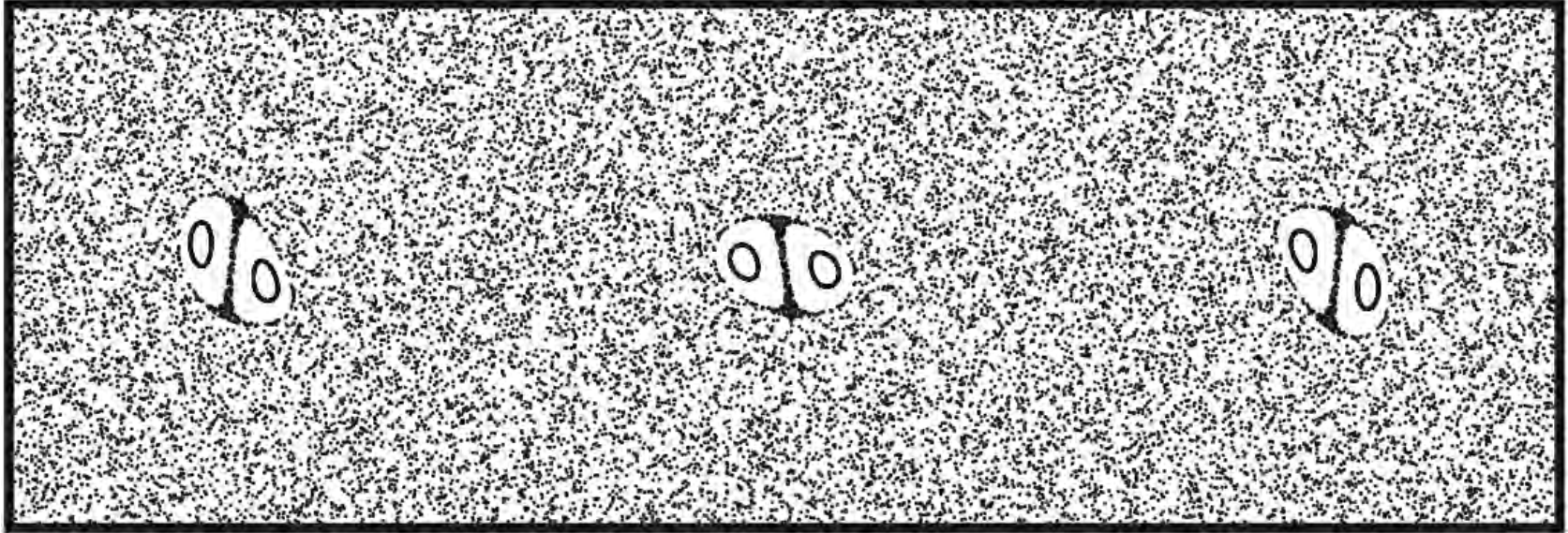
Identifying periodic points in channel flow example

tracer blob for $\tau_f \approx 1.02$

- $\tau_f > 1$, **elliptic / saddle points** of period 3
— streamlines around groups resemble fluid motion around a solid rod \Rightarrow

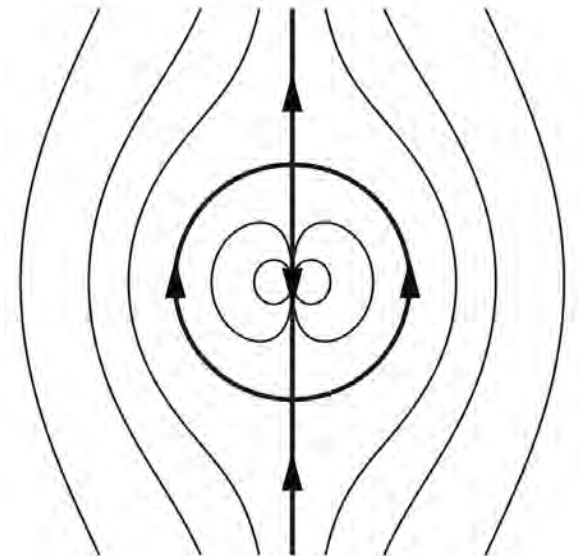


Identifying periodic points in channel flow example

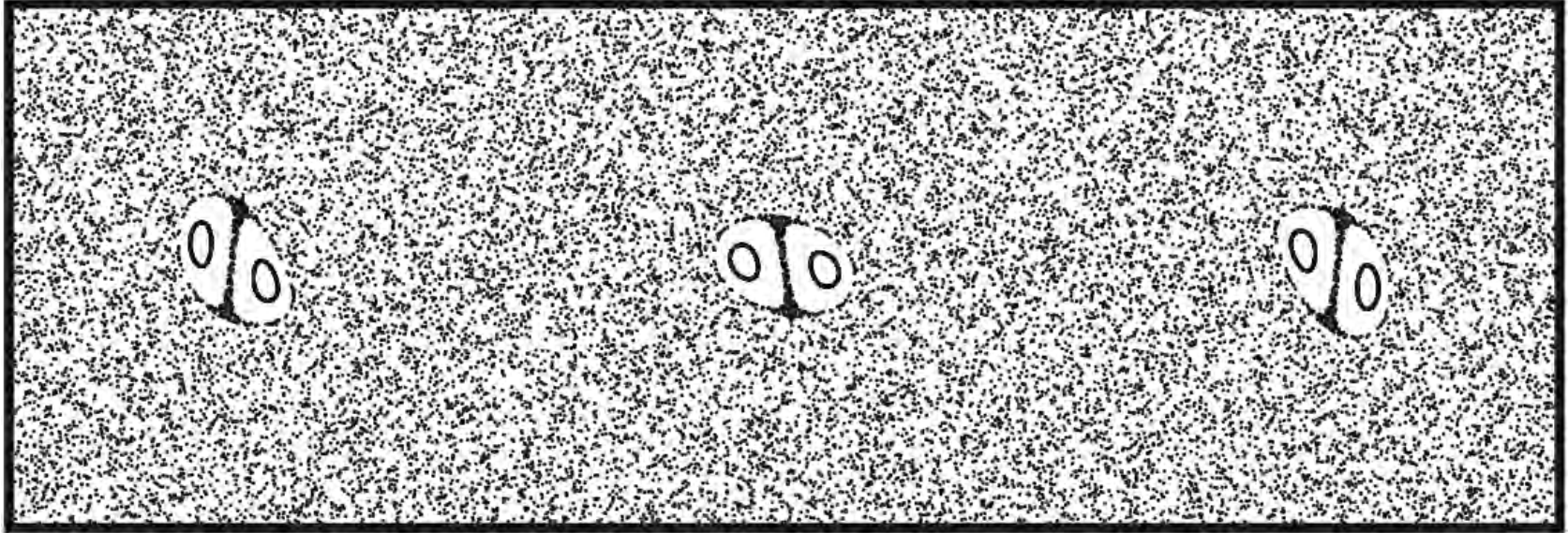


period- τ_f Poincaré map for $\tau_f \approx 1.02$

- $\tau_f > 1$, **elliptic / saddle points** of period 3
— streamlines around groups resemble fluid motion around a solid rod \Rightarrow

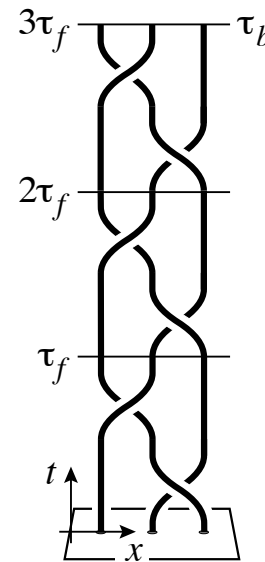


Stirring protocol \Rightarrow braid \Rightarrow topological entropy

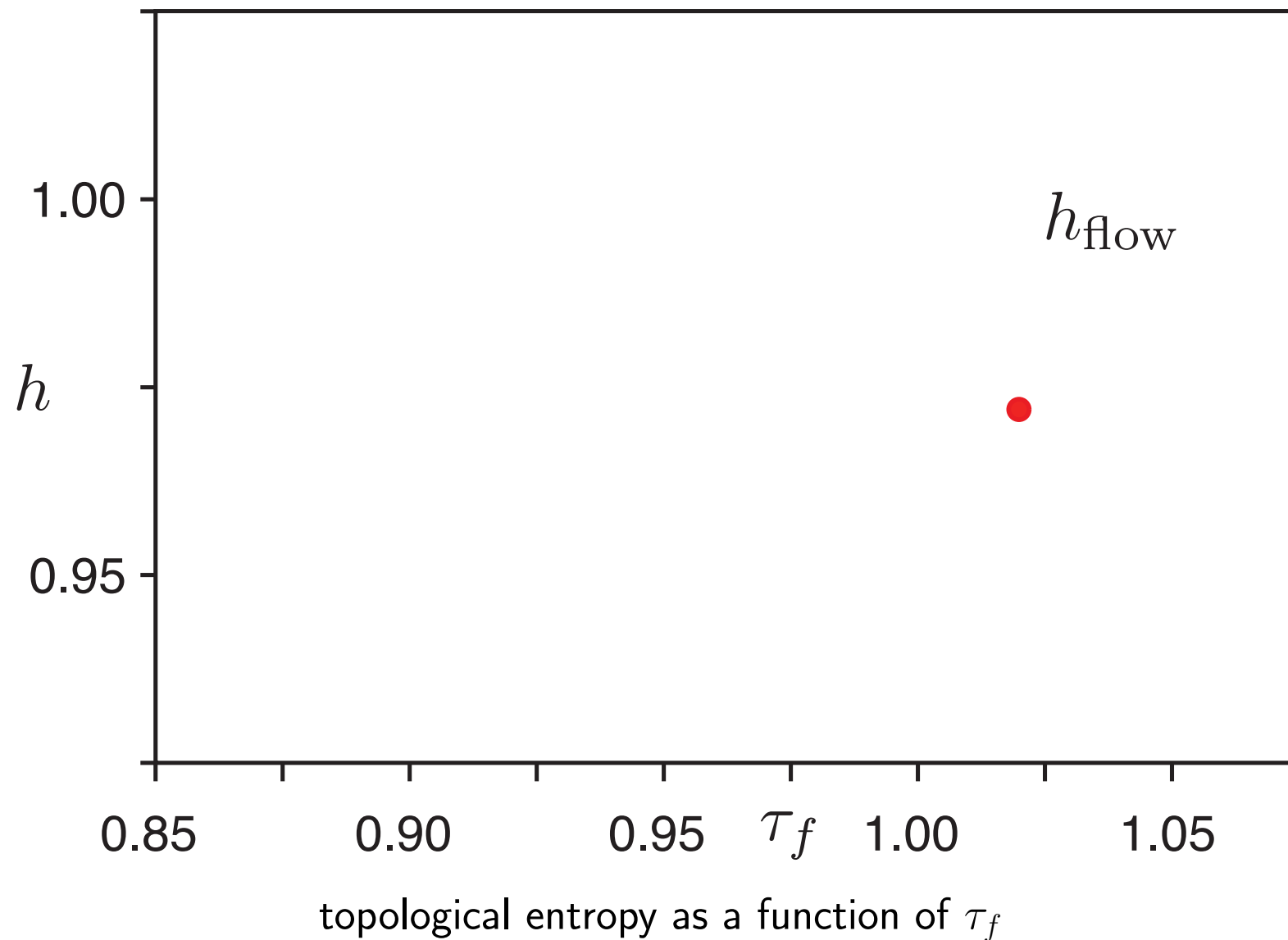


period- τ_f Poincaré map for $\tau_f \approx 1.02$

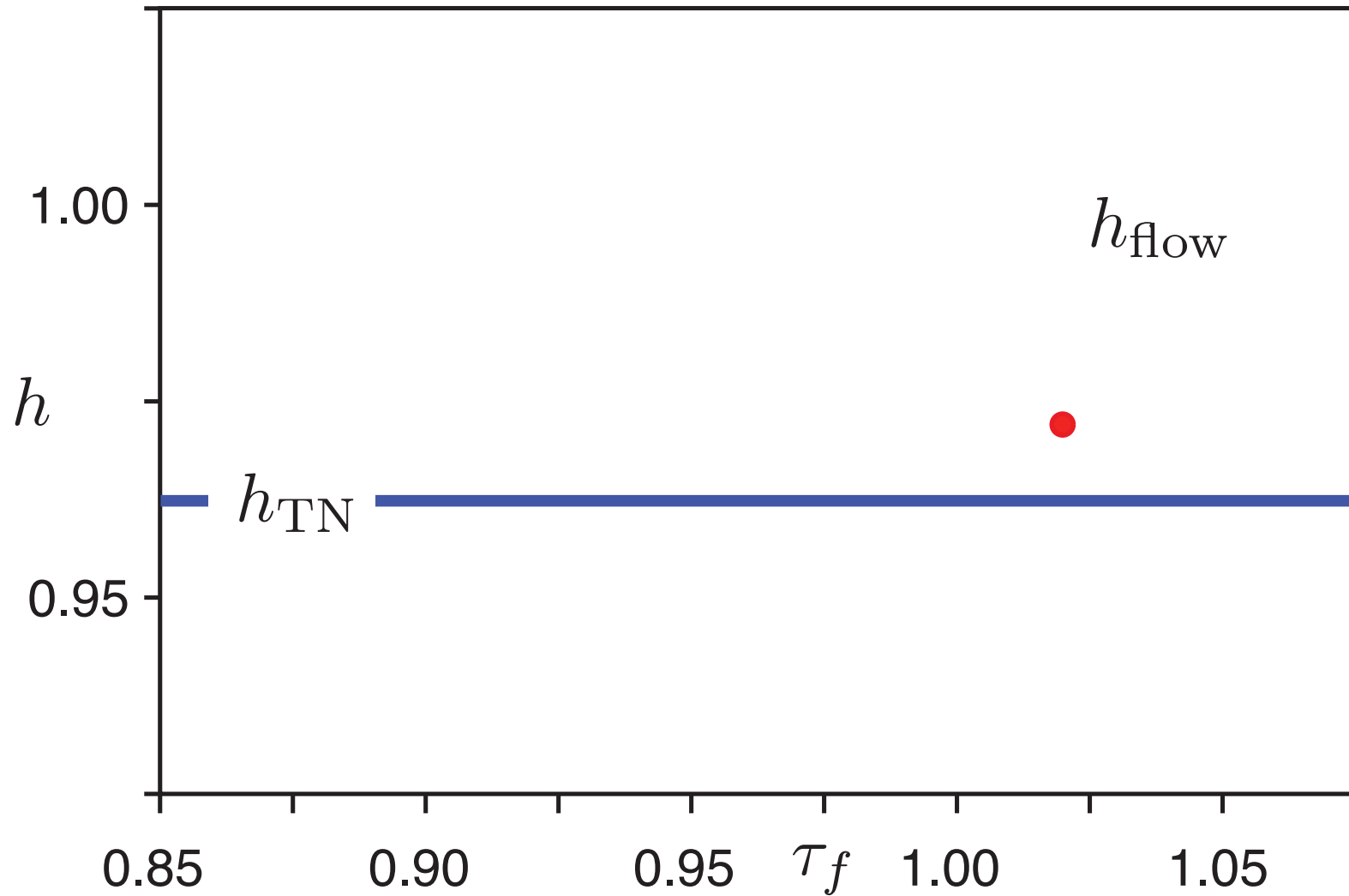
- Braid on 12 strands (periodic orbits) reducible to braid on 3 strands, the 'ghost rods'
- 3-strand braid has $h_{\text{TN}} = 0.962$ from TNCT
- Actual for flow is $h_{\text{flow}} = 0.964$
- $\Rightarrow h_{\text{TN}}$ is an excellent lower bound



Topological entropy continuity across critical point



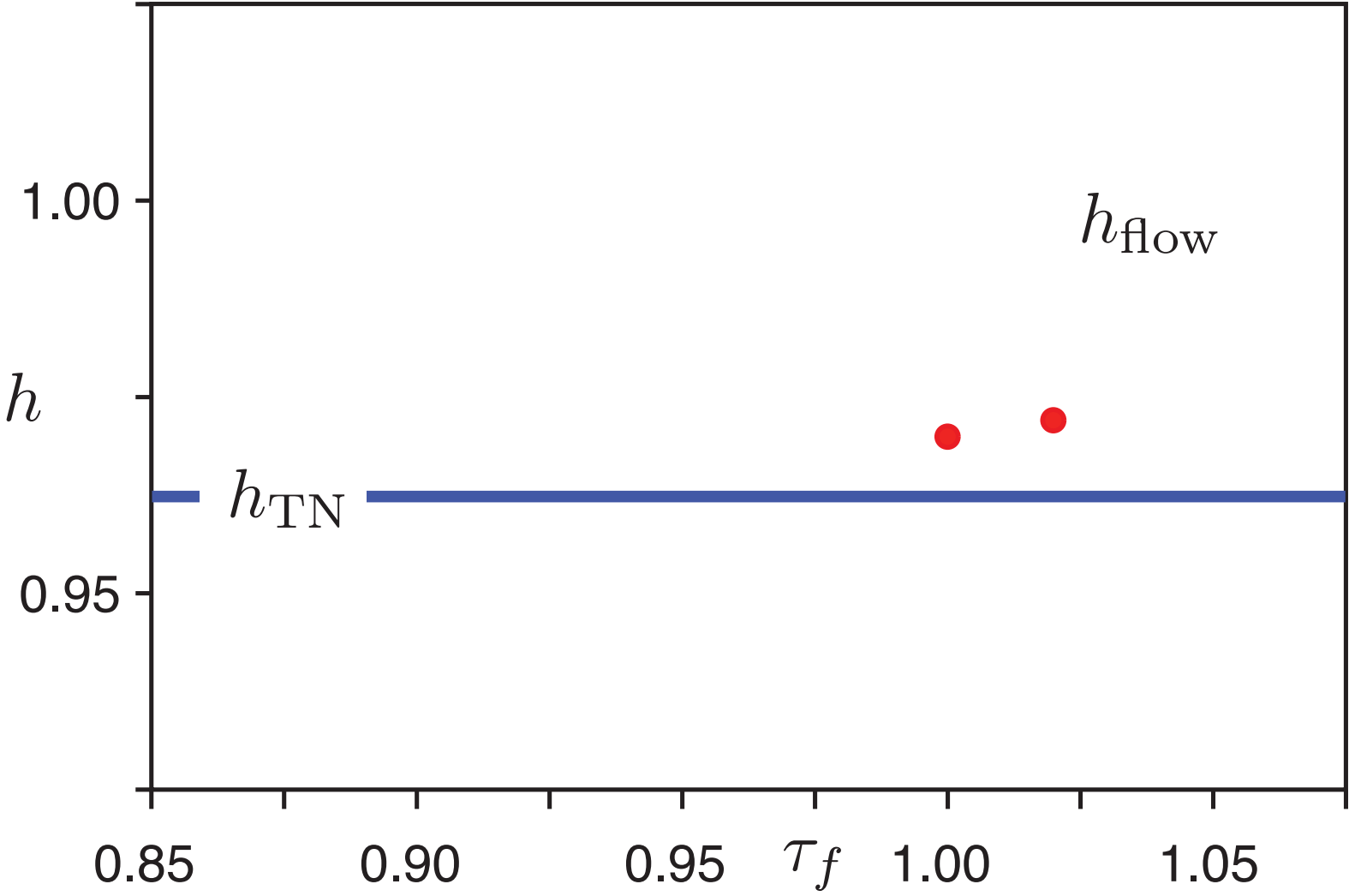
Topological entropy continuity across critical point



topological entropy as a function of τ_f

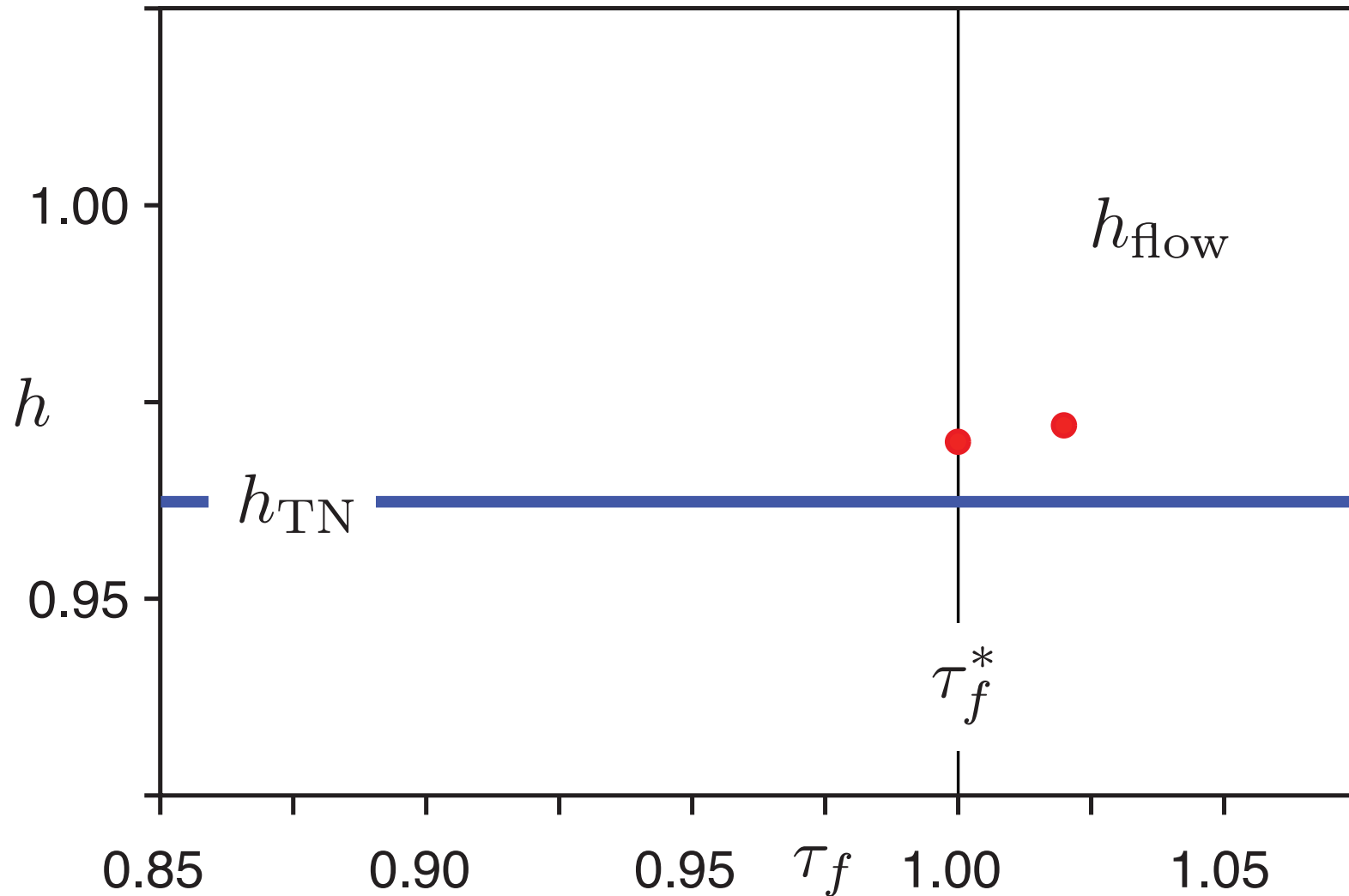
also showing Thurston-Nielson lower bound h_{TN} due to the braid on 3 strands

Topological entropy continuity across critical point



topological entropy as a function of τ_f
also showing Thurston-Nielson lower bound h_{TN} due to the braid on 3 strands

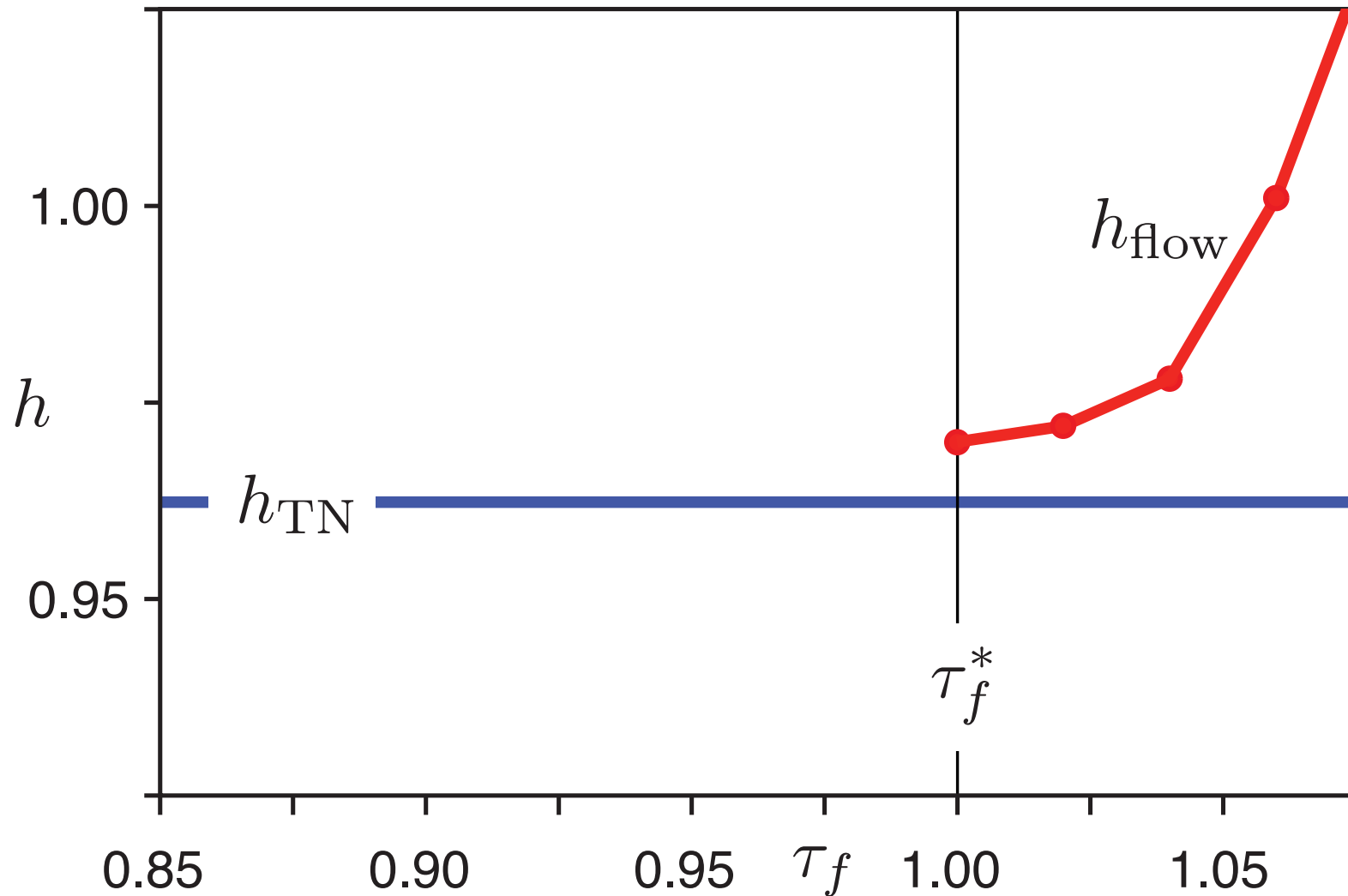
Topological entropy continuity across critical point



topological entropy as a function of τ_f

also showing Thurston-Nielson lower bound h_{TN} due to the braid on 3 strands

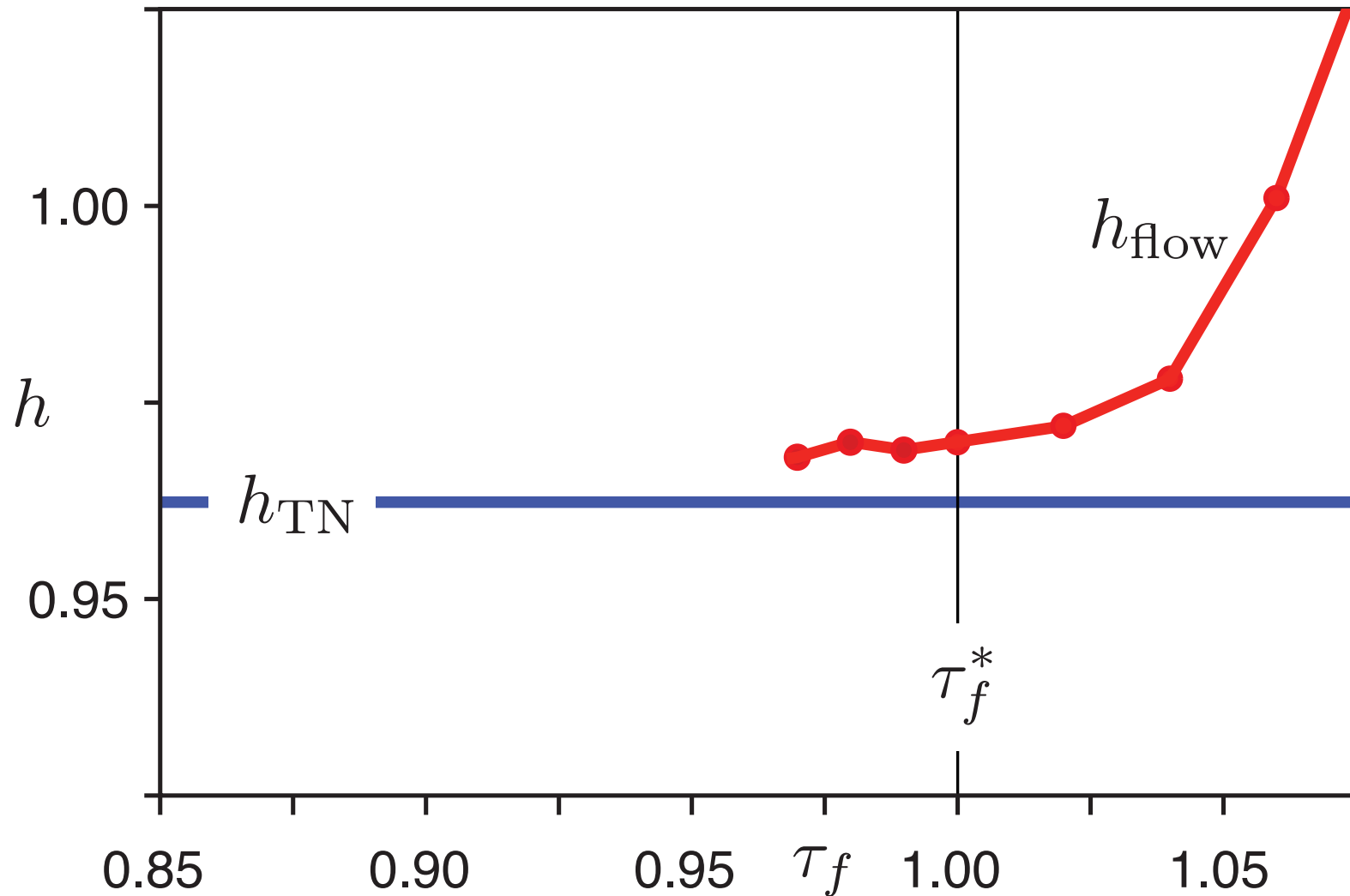
Topological entropy continuity across critical point



topological entropy as a function of τ_f

h_{TN} is a lower bound for values above critical, $\tau_f \geq 1$

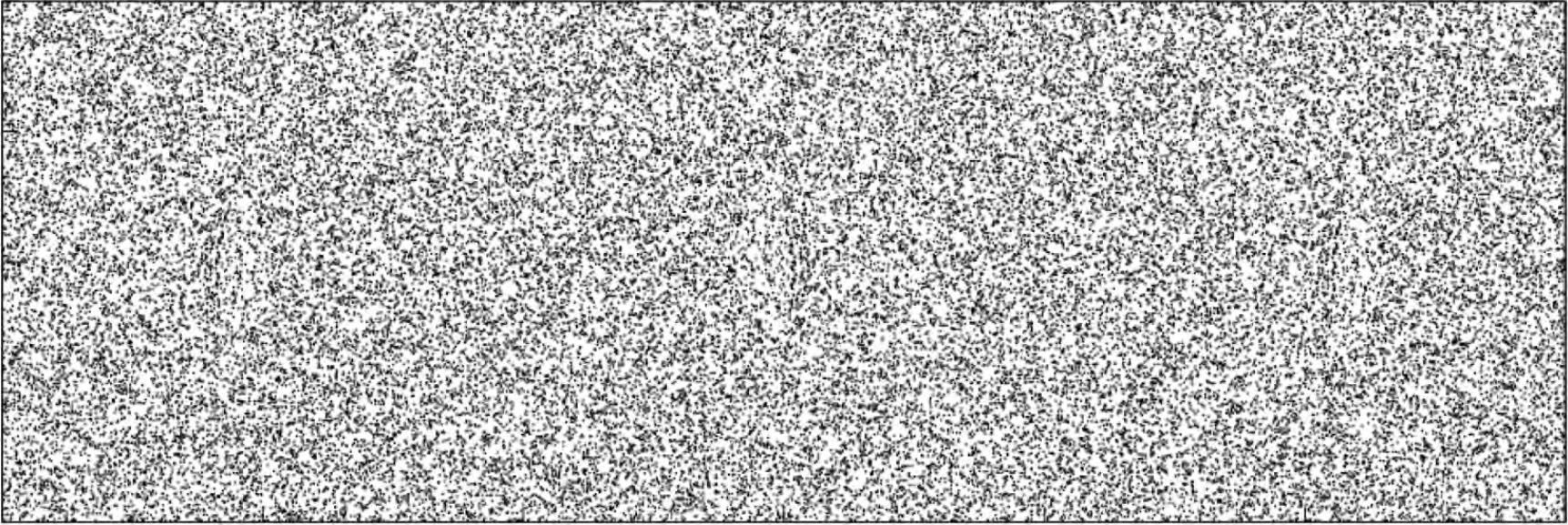
Topological entropy continuity across critical point



topological entropy as a function of τ_f

h_{TN} continues to be a lower bound just below critical, $\tau_f < 1$

Identifying 'ghost rods' ?



Poincaré section for $\tau_f < 1 \Rightarrow$ no obvious structure!

- At $\tau_f = 1$, parabolic period 3 points of map
- For $\tau_f < 1$, **periodic points vanish**
- Is the phase space featureless?

Equilibrium-like ghosts and bottlenecks

Strogatz [1994] *Nonlinear Dynamics and Chaos*

When stable and unstable equilibrium points collide, they leave behind an 'equilibrium-like' region, which Strogatz coincidentally called a 'ghost' or 'bottleneck' of high residence time

Ott [1993] called it a 'tunnel'

Occurs in vector fields or maps

Ghosts and Bottlenecks

The square-root scaling law found above is a *very general feature of systems that are close to a saddle-node bifurcation*. Just after the fixed points collide, there is a saddle-node remnant or **ghost** that leads to slow passage through a bottleneck.

For example, consider $\dot{\theta} = \omega - a \sin \theta$ for decreasing values of a , starting with $a > \omega$. As a decreases, the two fixed points approach each other, collide, and disappear (this sequence was shown earlier in Figure 4.3.3, except now you have to read from right to left.) For a slightly less than ω , the fixed points near $\pi/2$ no longer exist, but they still make themselves felt through a saddle-node ghost (Figure 4.3.5).

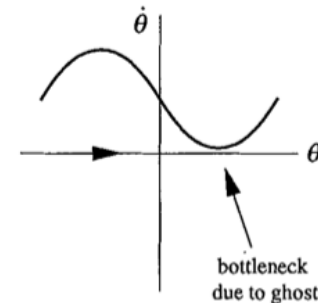


Figure 4.3.5

A graph of $\theta(t)$ would have the shape shown in Figure 4.3.6. Notice how the trajectory spends practically all its time getting through the bottleneck.

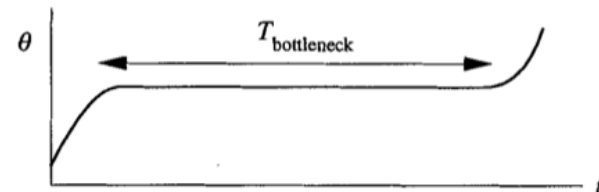
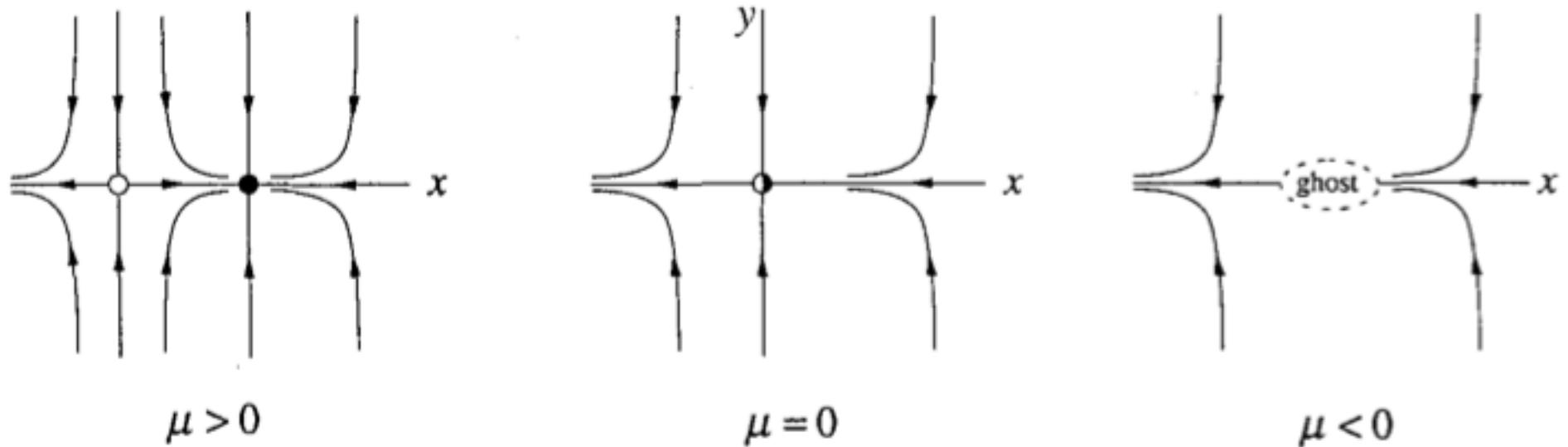


Figure 4.3.6

Equilibrium-like ghosts and bottlenecks

Strogatz [1994] *Nonlinear Dynamics and Chaos*



Passing through a saddle-node bifurcation in 2D, which leaves behind a 'ghost'

- In our system, we can find analogous 'ghosts' for periodic orbits
- Perhaps they braid, making them 'ghost rods' (or rather 'ghost ghost rods')

Probabilistic approach

- Take probabilistic point of view
- Partition phase space into **regions of high residence time**
- Use the approach of **almost-invariant sets**³

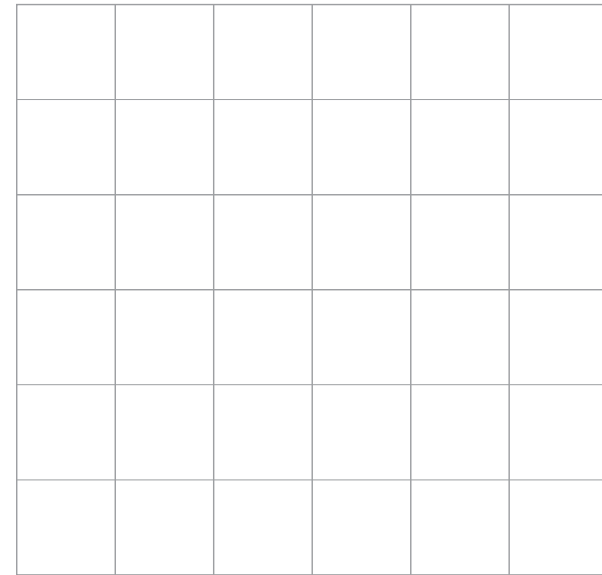
³ Dellnitz, Junge, Koon, Lekien, Lo, Marsden, Padberg, Preis, Ross, Thiere [2005] Int. J. Bif. Chaos

Almost-invariant sets / almost-cyclic sets

- How to identify **almost-invariant sets** (AISs)
- Relatedly, **almost-cyclic sets** (ACSs)¹
- Create box partition of phase space $\mathcal{B} = \{B_1, \dots, B_q\}$, with q large
- Consider a q -by- q **transition (Ulam) matrix**, P , where

$$P_{ij} = \frac{m(B_i \cap f^{-1}(B_j))}{m(B_i)},$$

the *transition probability* from B_i to B_j using, e.g., $f = \phi_t^{t+T}$, often computed numerically



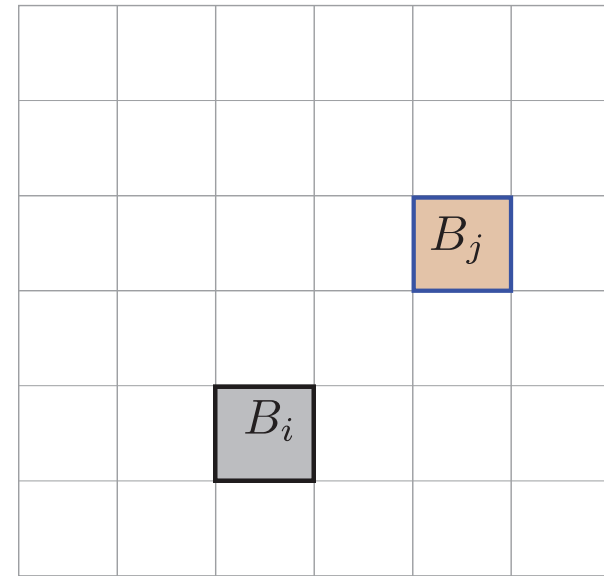
¹Dellnitz & Junge [1999], Froyland & Dellnitz [2003]

Almost-invariant sets / almost-cyclic sets

- How to identify **almost-invariant sets** (AISs)
- Relatedly, **almost-cyclic sets** (ACSs)¹
- Create box partition of phase space $\mathcal{B} = \{B_1, \dots, B_q\}$, with q large
- Consider a q -by- q **transition (Ulam) matrix**, P , where

$$P_{ij} = \frac{m(B_i \cap f^{-1}(B_j))}{m(B_i)},$$

the *transition probability* from B_i to B_j using, e.g., $f = \phi_t^{t+T}$, often computed numerically



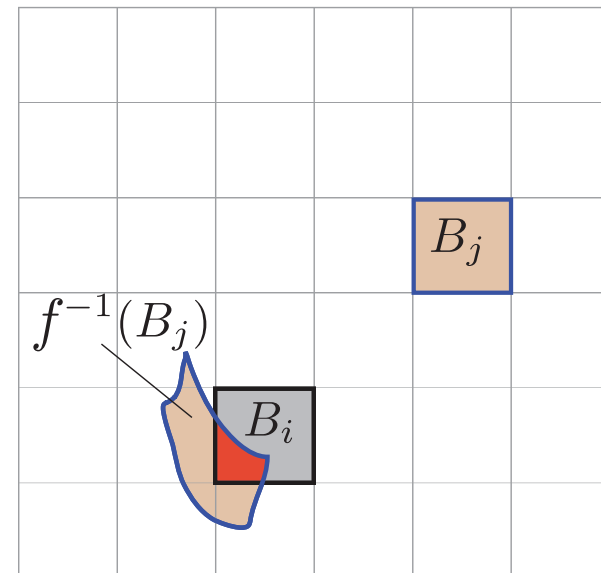
¹Dellnitz & Junge [1999], Froyland & Dellnitz [2003]

Almost-invariant sets / almost-cyclic sets

- How to identify **almost-invariant sets** (AISs)
- Relatedly, **almost-cyclic sets** (ACSs)¹
- Create box partition of phase space $\mathcal{B} = \{B_1, \dots, B_q\}$, with q large
- Consider a q -by- q **transition (Ulam) matrix**, P , where

$$P_{ij} = \frac{m(B_i \cap f^{-1}(B_j))}{m(B_i)},$$

the *transition probability* from B_i to B_j using, e.g., $f = \phi_t^{t+T}$, often computed numerically



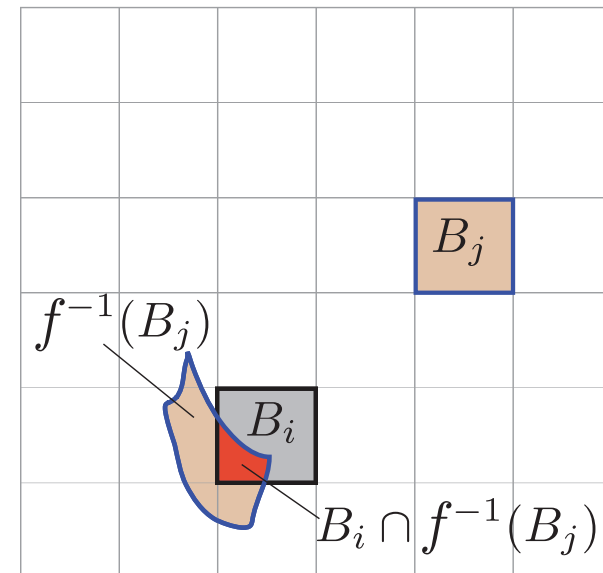
¹Dellnitz & Junge [1999], Froyland & Dellnitz [2003]

Almost-invariant sets / almost-cyclic sets

- How to identify **almost-invariant sets** (AISs)
- Relatedly, **almost-cyclic sets** (ACSs)¹
- Create box partition of phase space $\mathcal{B} = \{B_1, \dots, B_q\}$, with q large
- Consider a q -by- q **transition (Ulam) matrix**, P , where

$$P_{ij} = \frac{m(B_i \cap f^{-1}(B_j))}{m(B_i)},$$

the *transition probability* from B_i to B_j using, e.g., $f = \phi_t^{t+T}$, often computed numerically



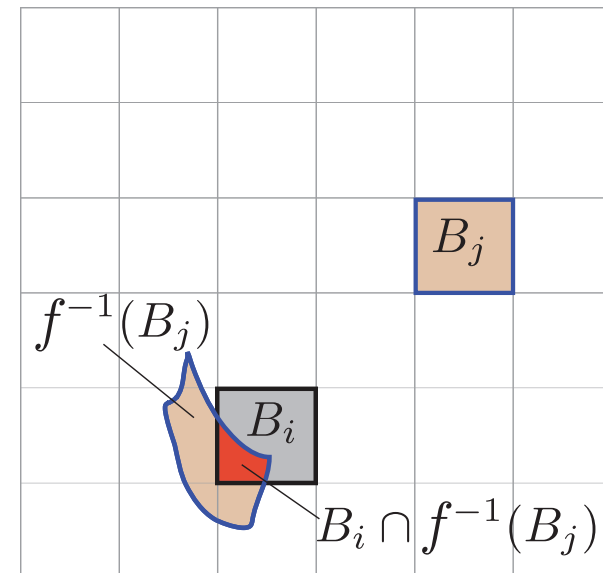
¹Dellnitz & Junge [1999], Froyland & Dellnitz [2003]

Almost-invariant sets / almost-cyclic sets

- How to identify **almost-invariant sets** (AISs)
- Relatedly, **almost-cyclic sets** (ACSs)¹
- Create box partition of phase space $\mathcal{B} = \{B_1, \dots, B_q\}$, with q large
- Consider a q -by- q **transition (Ulam) matrix**, P , where

$$P_{ij} = \frac{m(B_i \cap f^{-1}(B_j))}{m(B_i)},$$

the *transition probability* from B_i to B_j using, e.g., $f = \phi_t^{t+T}$, often computed numerically



- P approximates \mathcal{P} , Perron-Frobenius **transfer operator** — which evolves densities, ν , over one iterate of f , as $\mathcal{P}\nu$
- Typically, we use a reversibilized operator R , obtained from P

¹Dellnitz & Junge [1999], Froyland & Dellnitz [2003]

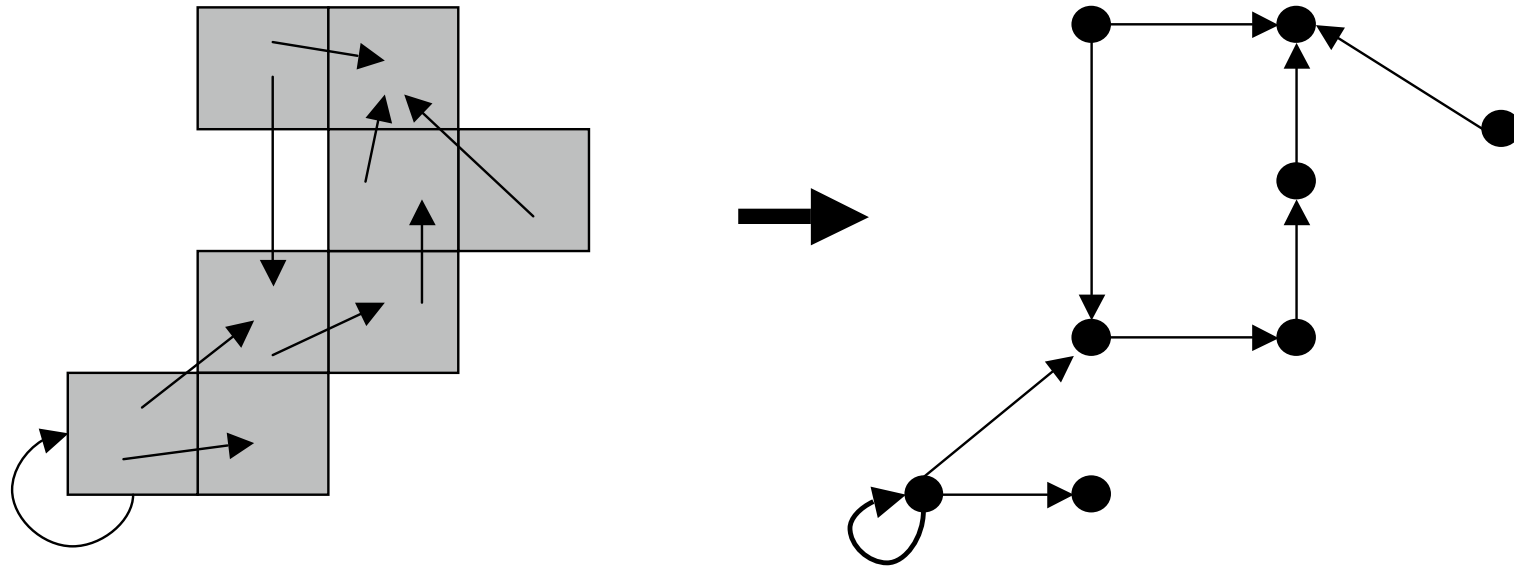
Almost-invariant sets / almost-cyclic sets

- Set B is an **almost-invariant set** (AIS) under the map f if the invariance ratio

$$\rho(B) = \frac{m(B \cap f^{-1}(B))}{m(B)} \approx 1$$

- Can maximize value of ρ over all possible combinations of sets $B \subset \mathcal{B}$.

Identifying AISs by graph- or spectrum-partitioning

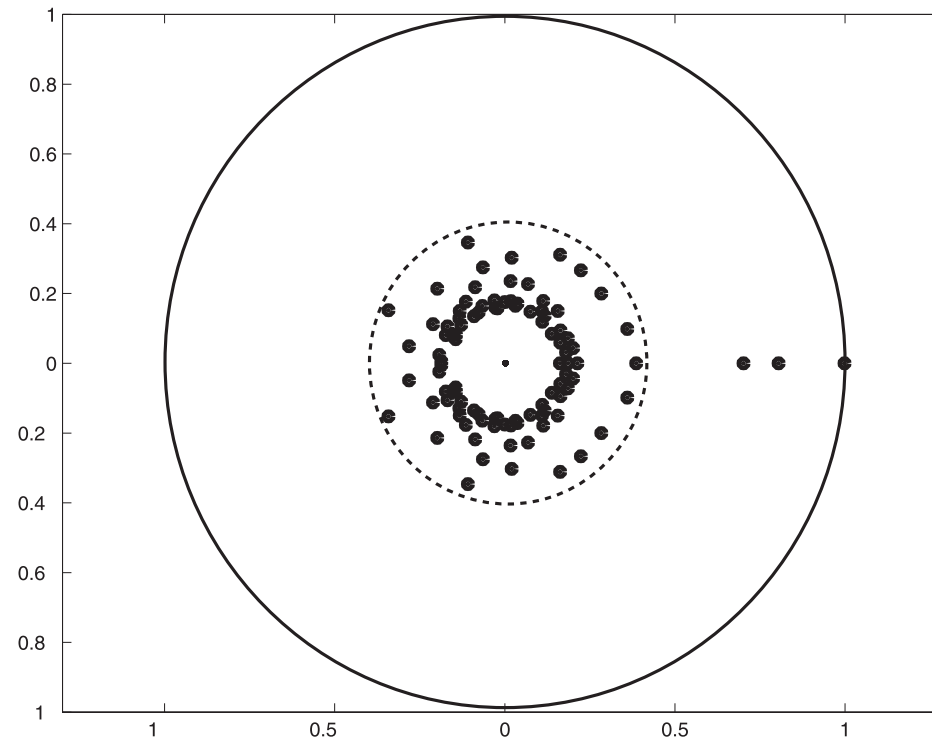


- P admits graph representation where nodes correspond to boxes B_i and transitions between them are edges of a directed graph
- Graph partitioning methods can be applied¹
- can obtain AISs/ACSs and transport between them
- spectrum-partitioning as well (eigenvectors of large eigenvalues)²

¹Dellnitz, Junge, Koon, Lekien, Lo, Marsden, Padberg, Preis, Ross, Thiere [2005] Int. J. Bif. Chaos

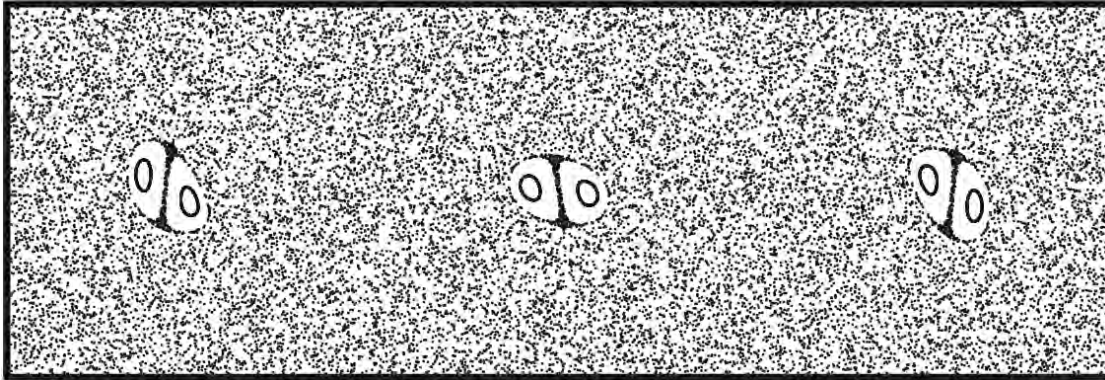
²Dellnitz, Froyland, Sertl [2000] Nonlinearity

Identifying AISs by graph- or spectrum-partitioning



- **Invariant** densities are those fixed under P , $P\nu = \nu$, i.e., eigenvalue 1
- Essential spectrum lies within a disk of radius $r < 1$ (dashed) which depends on the weakest expansion rate of the underlying system.
- Other real eigenvalues close to 1 identify **almost-invariant** sets via **sign structure** of corresponding eigenvectors

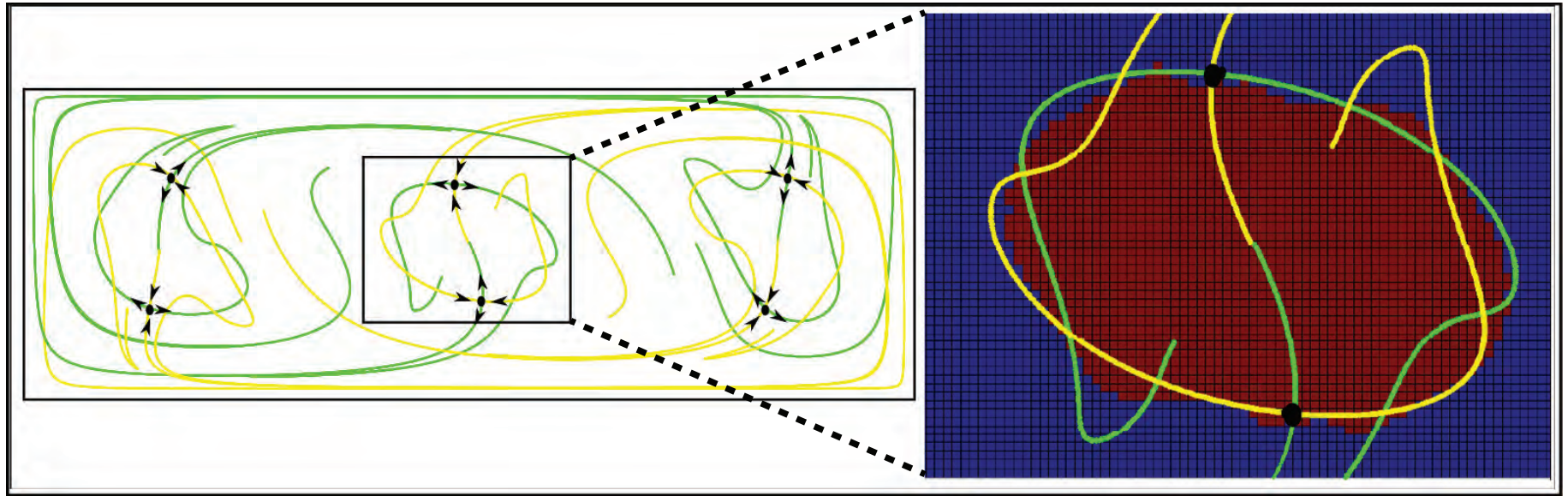
Identifying 'ghost rods': almost-cyclic sets



- For $\tau_f > 1$ case, where periodic points and manifolds exist...
- Agreement between ACS boundaries (zero contour of 2nd eigenvector) and manifolds of periodic saddle points
- Known previously¹ and applies to more general objects than periodic points, i.e. normally hyperbolic invariant manifolds (NHIMs)

¹ Dellnitz, Junge, Koon, Lekien, Lo, Marsden, Padberg, Preis, Ross, Thiere [2005] Int. J. Bif. Chaos

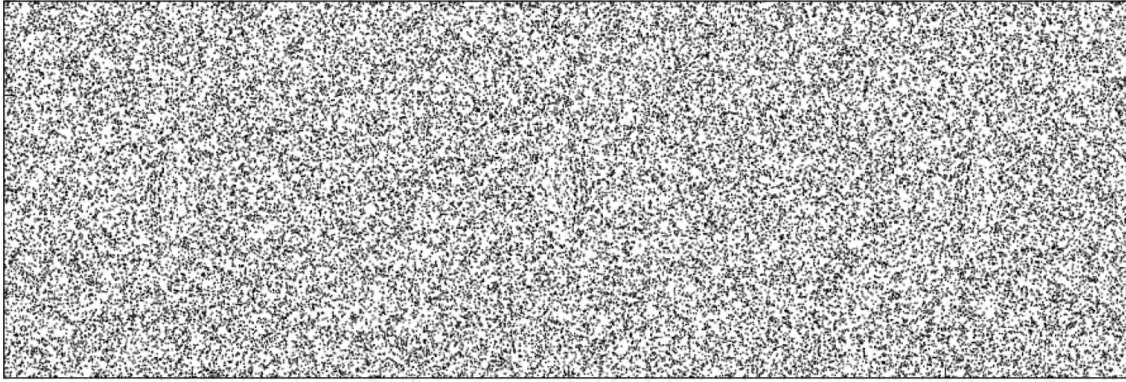
Identifying 'ghost rods': almost-cyclic sets



- For $\tau_f > 1$ case, where periodic points and manifolds exist...
- Agreement between ACS boundaries (zero contour of 2nd eigenvector) and manifolds of periodic saddle points
- Known previously¹ and applies to more general objects than periodic points, i.e. normally hyperbolic invariant manifolds (NHIMs)

¹ Dellnitz, Junge, Koon, Lekien, Lo, Marsden, Padberg, Preis, Ross, Thiere [2005] Int. J. Bif. Chaos

Identifying 'ghost rods': almost-cyclic sets

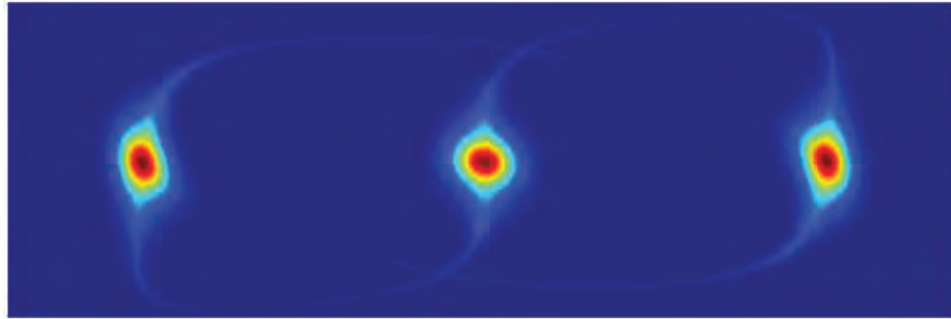


Poincaré section for $\tau_f < 1 \Rightarrow$ no obvious structure

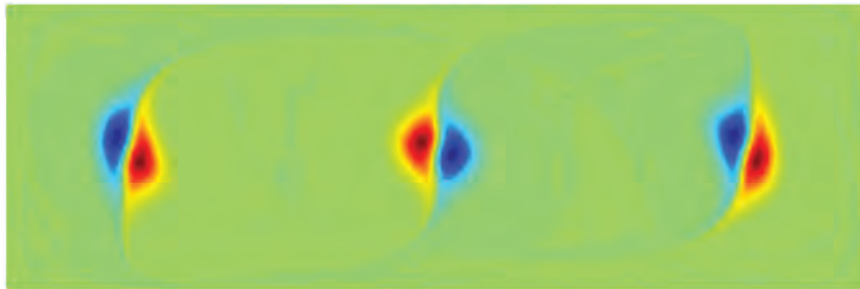
- Return to $\tau_f < 1$ case, where no periodic orbits of low period known
- What are the AISs and ACSs here?
- Consider $R_t^{t+\tau_f}$ induced by family of period- τ_f maps $\phi_t^{t+\tau_f}$, $t \in [0, \tau_f)$

Identifying 'ghost rods': almost-cyclic sets

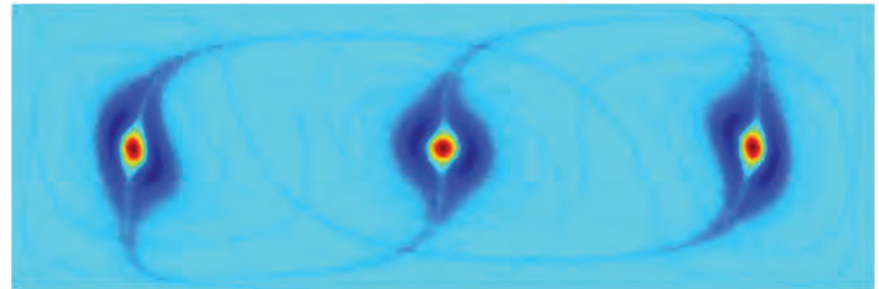
Top eigenvectors of $R_0^{0+\tau_f}$ for $\tau_f = 0.99$ reveal structure



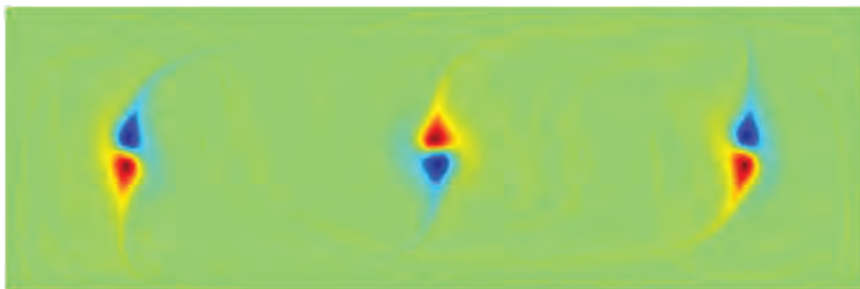
ν_2



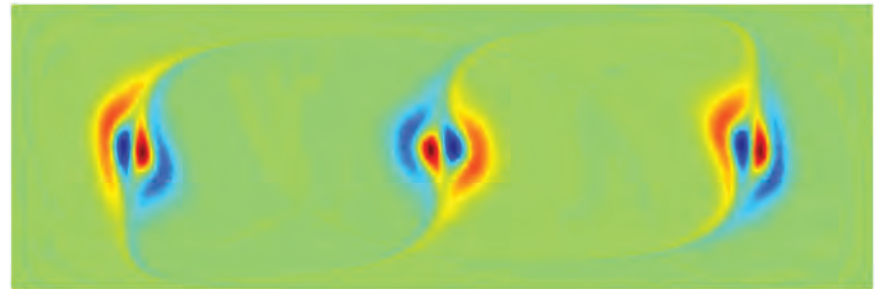
ν_3



ν_4

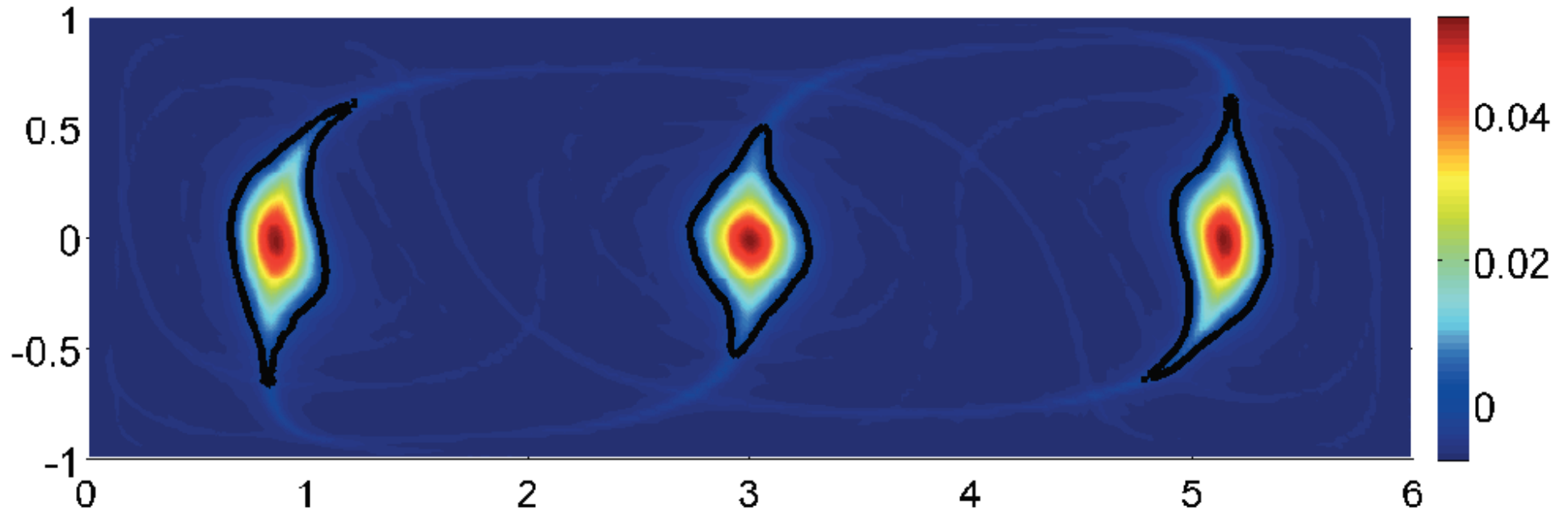


ν_5



ν_6

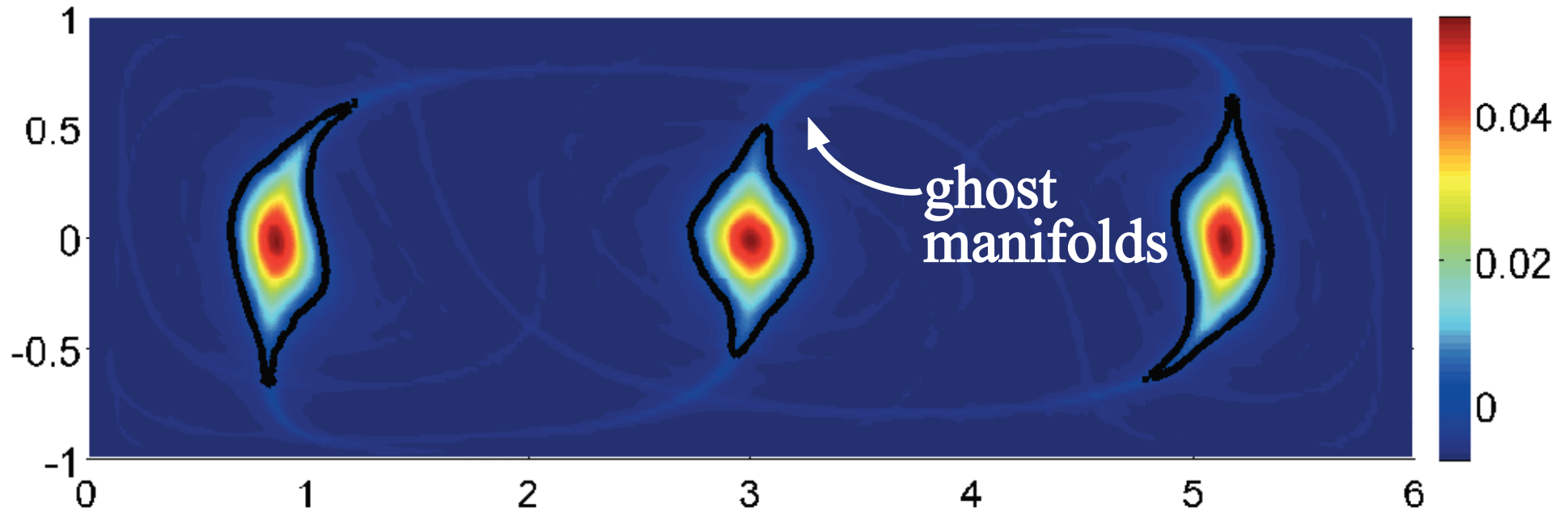
Identifying 'ghost rods': almost-cyclic sets



The zero contour (black) is the boundary between the two almost-invariant sets.

- Three-component AIS made of 3 ACSs each of period 3

Identifying 'ghost rods': almost-cyclic sets



The zero contour (black) is the boundary between the two almost-invariant sets.

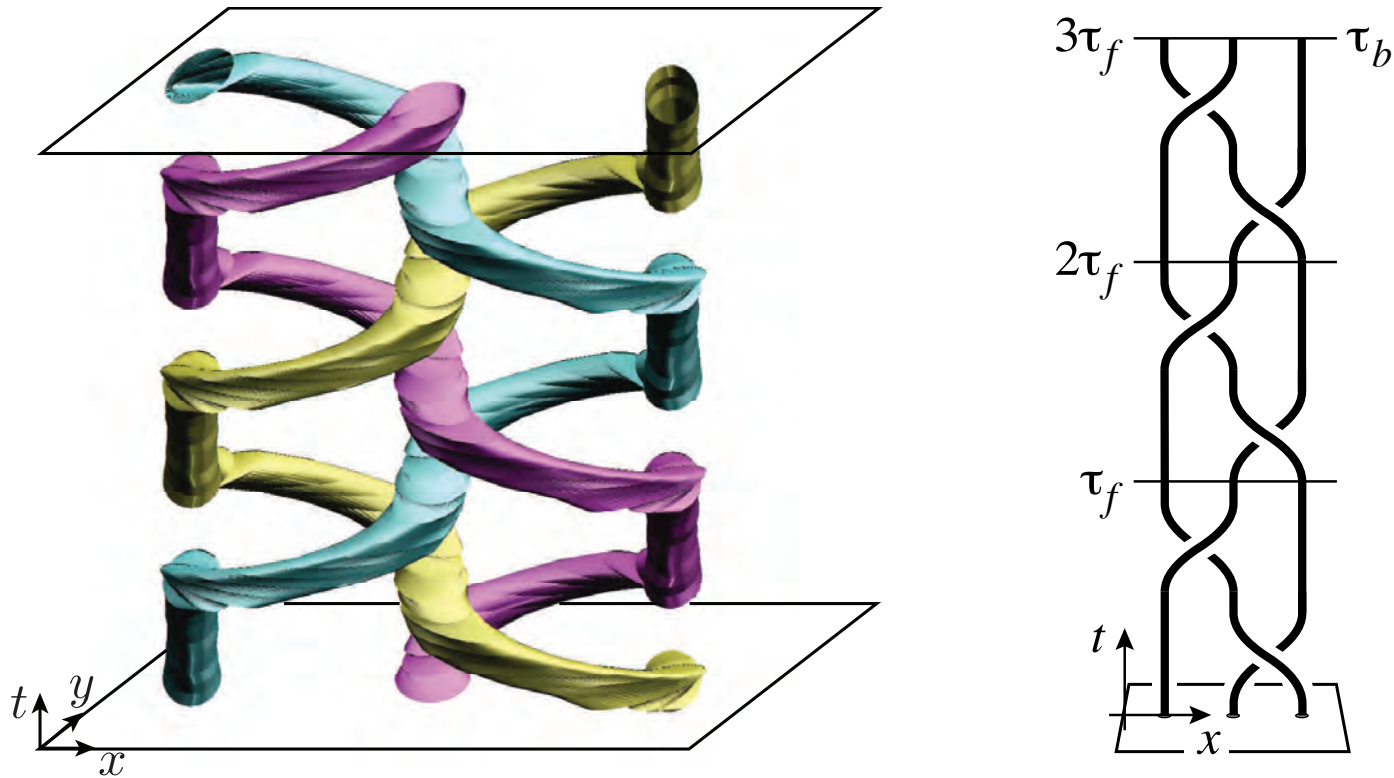
- Three-component AIS made of 3 ACSs each of period 3
- Also: we see a **remnant of the 'stable and unstable manifolds' of the saddle points**, despite no saddle points – 'ghost manifolds'?

Identifying 'ghost rods': almost-cyclic sets

Almost-cyclic sets, in effect, stir the surrounding fluid like 'ghost rods'

Movie shown is 2nd eigenvector for $R_t^{t+\tau_f}$ (movie loops through $t \in [0, \tau_f)$)

Identifying 'ghost rods': almost-cyclic sets



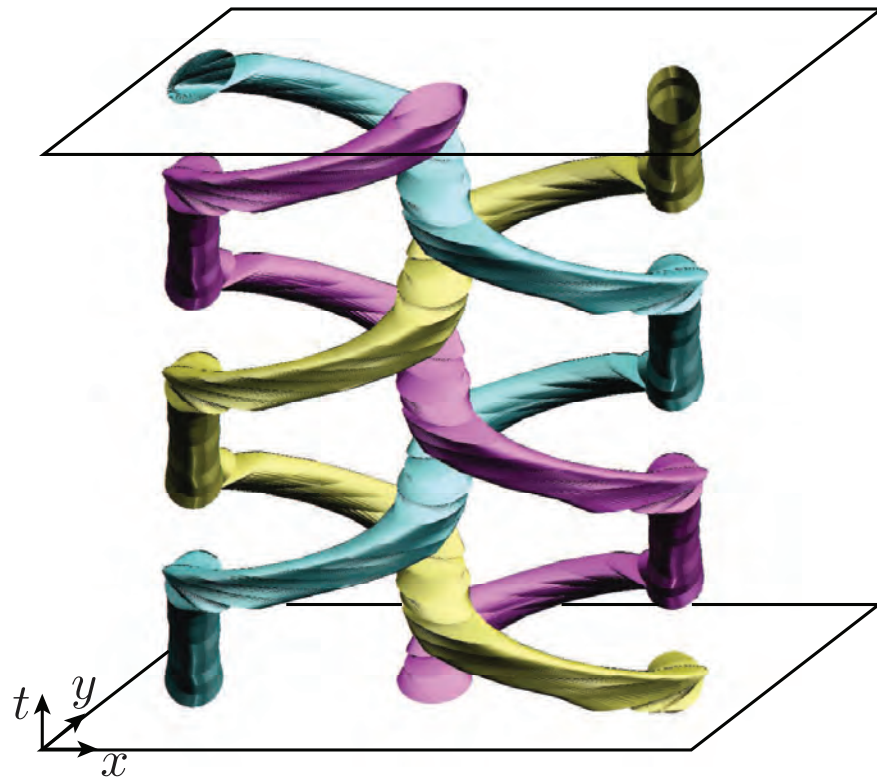
Thurston-Nielsen theorem applies only to periodic points

— But framework seems to work for approximately cyclic regions¹

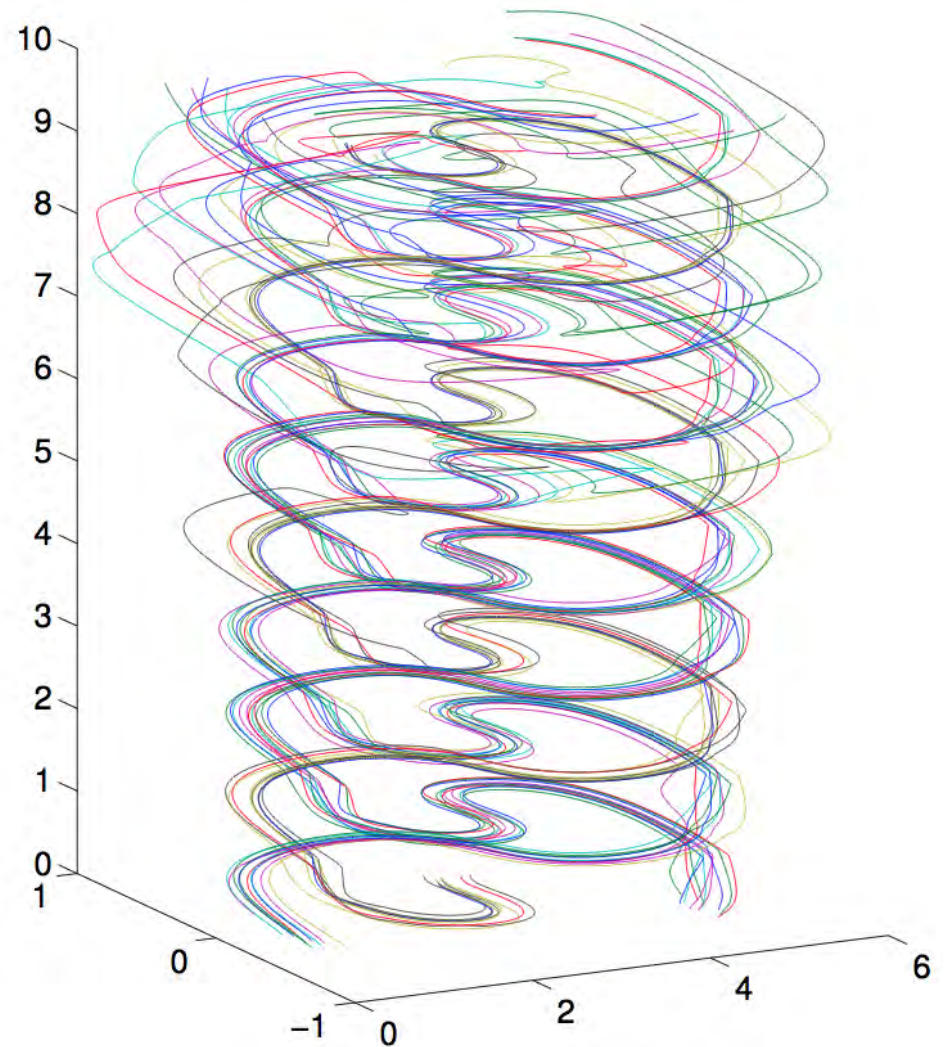
¹Stremler, Ross, Grover, Kumar [2011] Phys. Rev. Lett.

Almost-cyclic sets are 'leaky'

Particles starting in an ACS will eventually escape

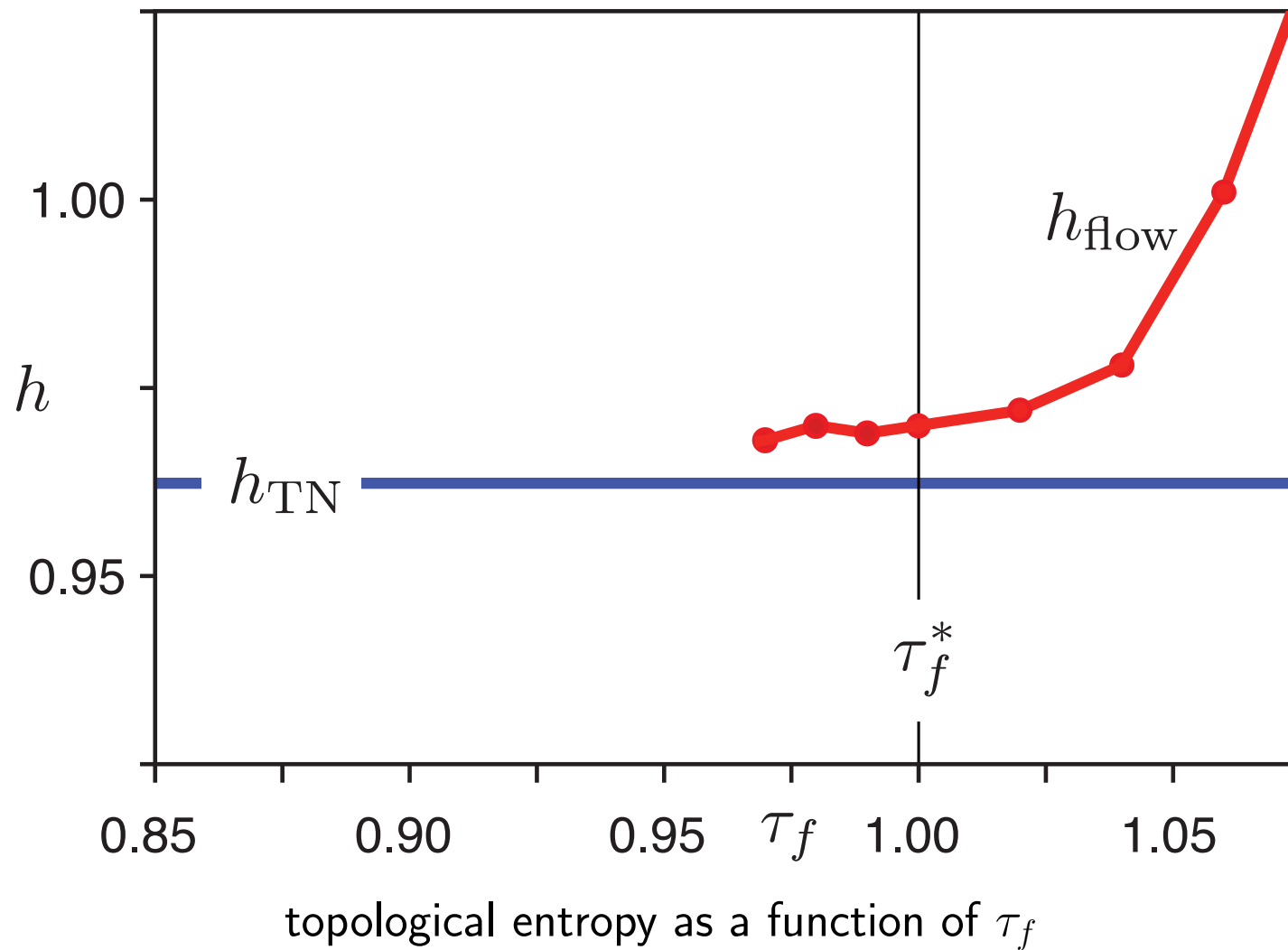


ACS braid

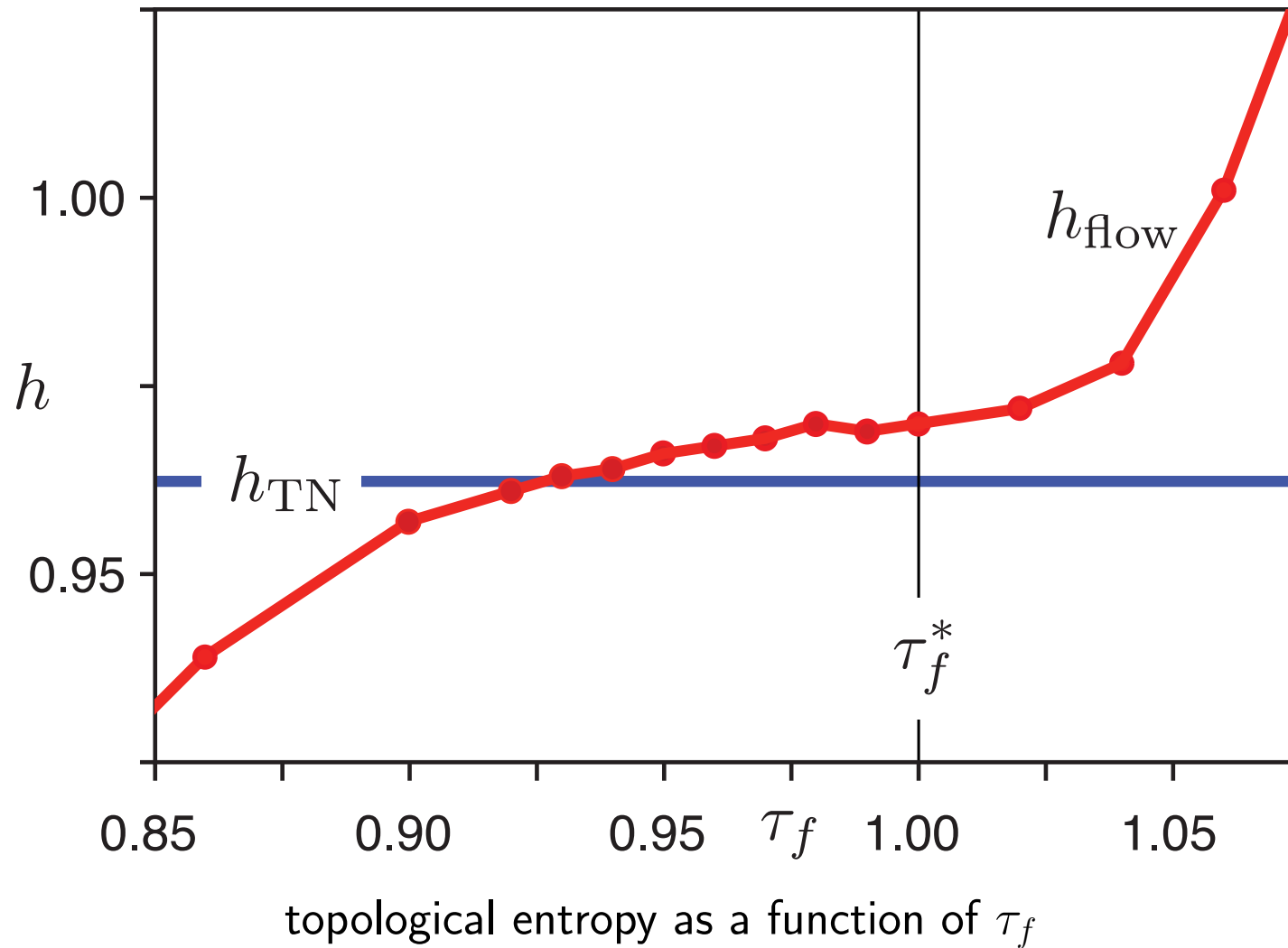


points started in an ACS

Topological entropy vs. parameter



Topological entropy vs. parameter

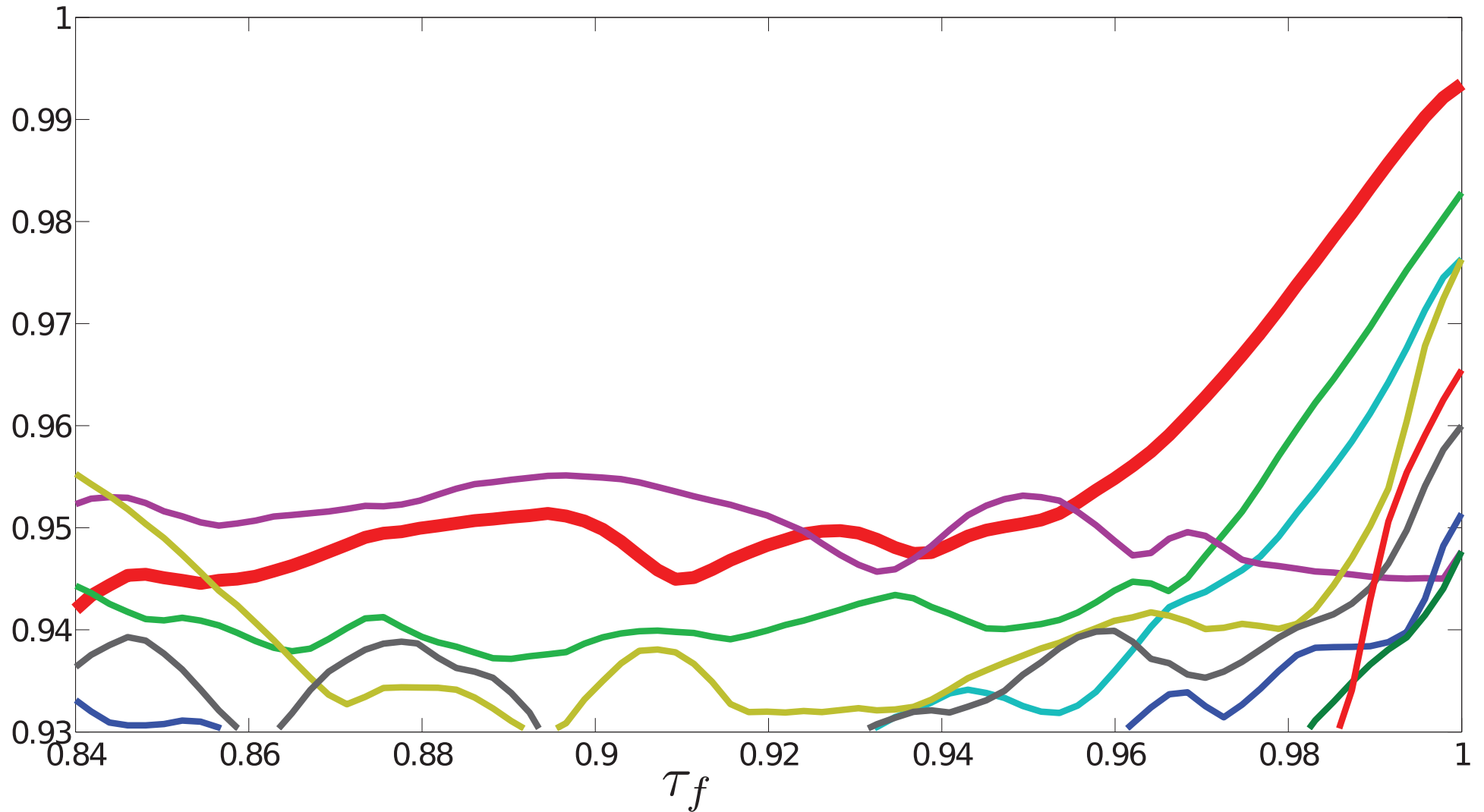


- h_{TN} continues to be a lower bound until about $\tau_f = 0.925$

Eigenvalues/eigenvectors vs. parameter

Eigenspectrum of P changes with the parameter τ_f

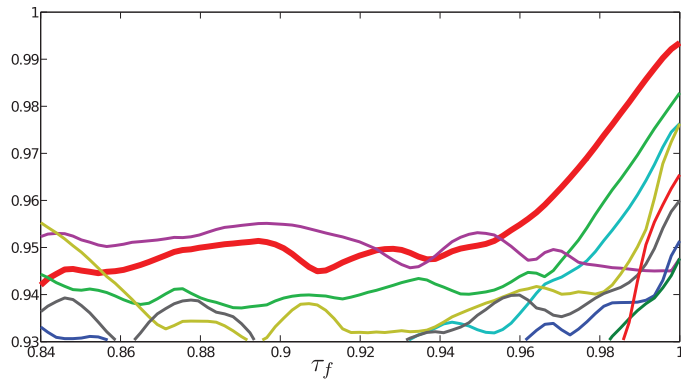
Eigenvalues/eigenvectors vs. parameter



Top eigenvalues of reversible R as parameter τ_f changes

Lines colored according to continuity of eigenvector

Eigenvalues/eigenvectors vs. parameter

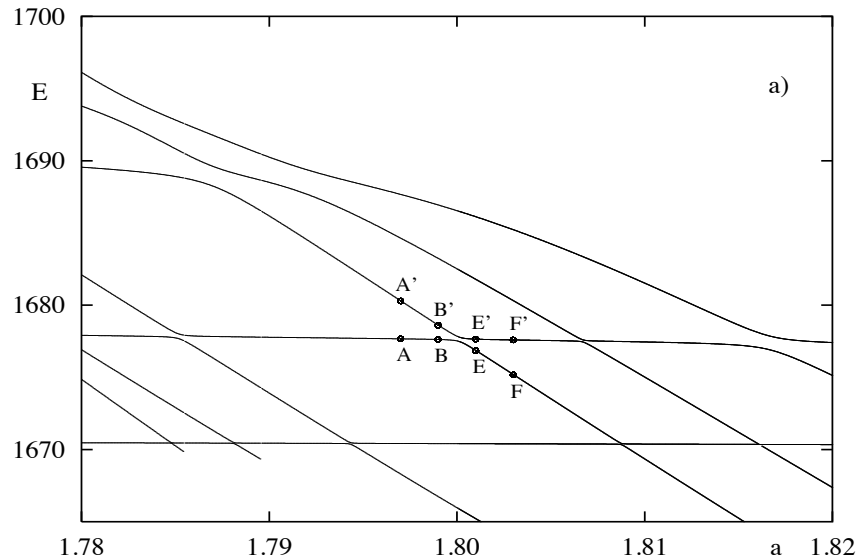


Genuine eigenvalue crossings?
Eigenvalues generically avoid crossings if there is no symmetry present

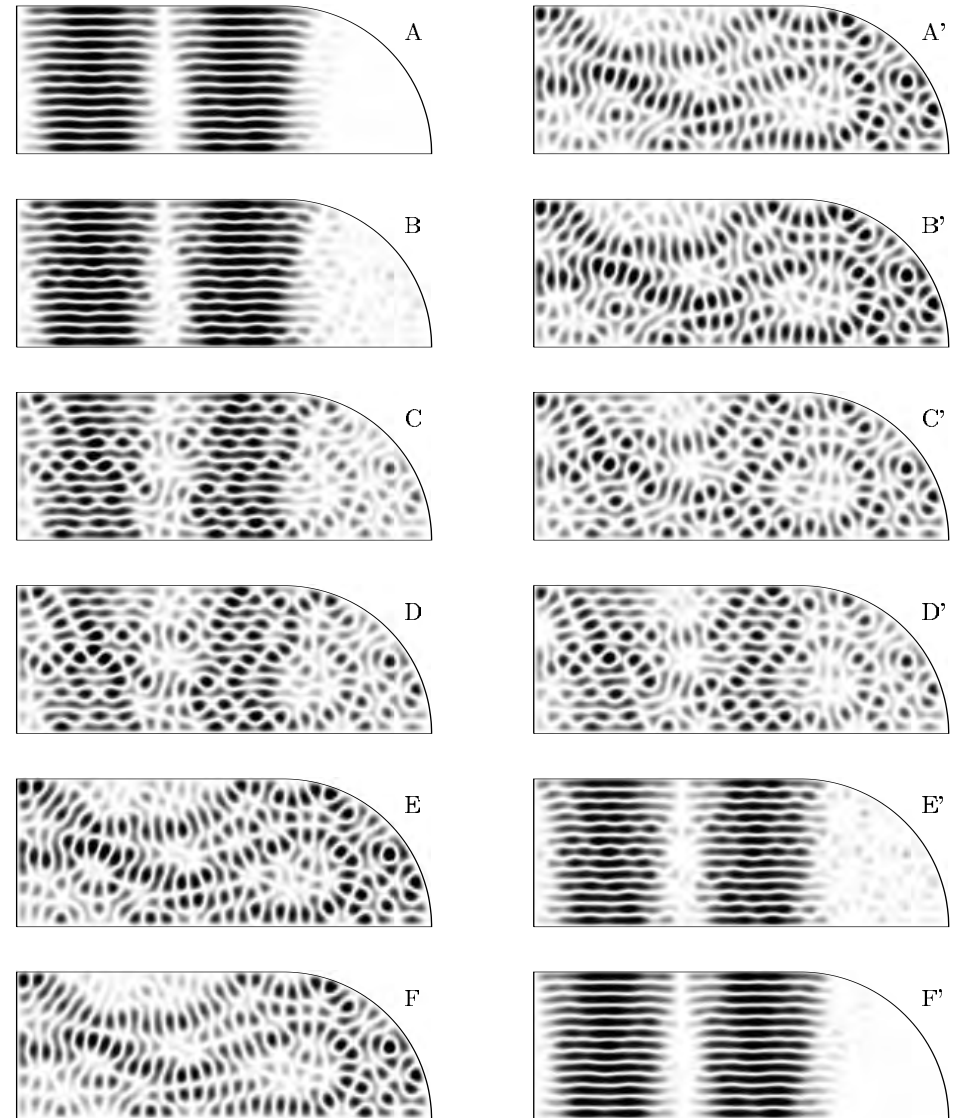
(Dellnitz, Melbourne, 1994)

But eigenvectors can 'cross' –
(Bäcker, 1998)

Aside: Eigenvalue avoidance in quantum mechanics



Energy vs. parameter



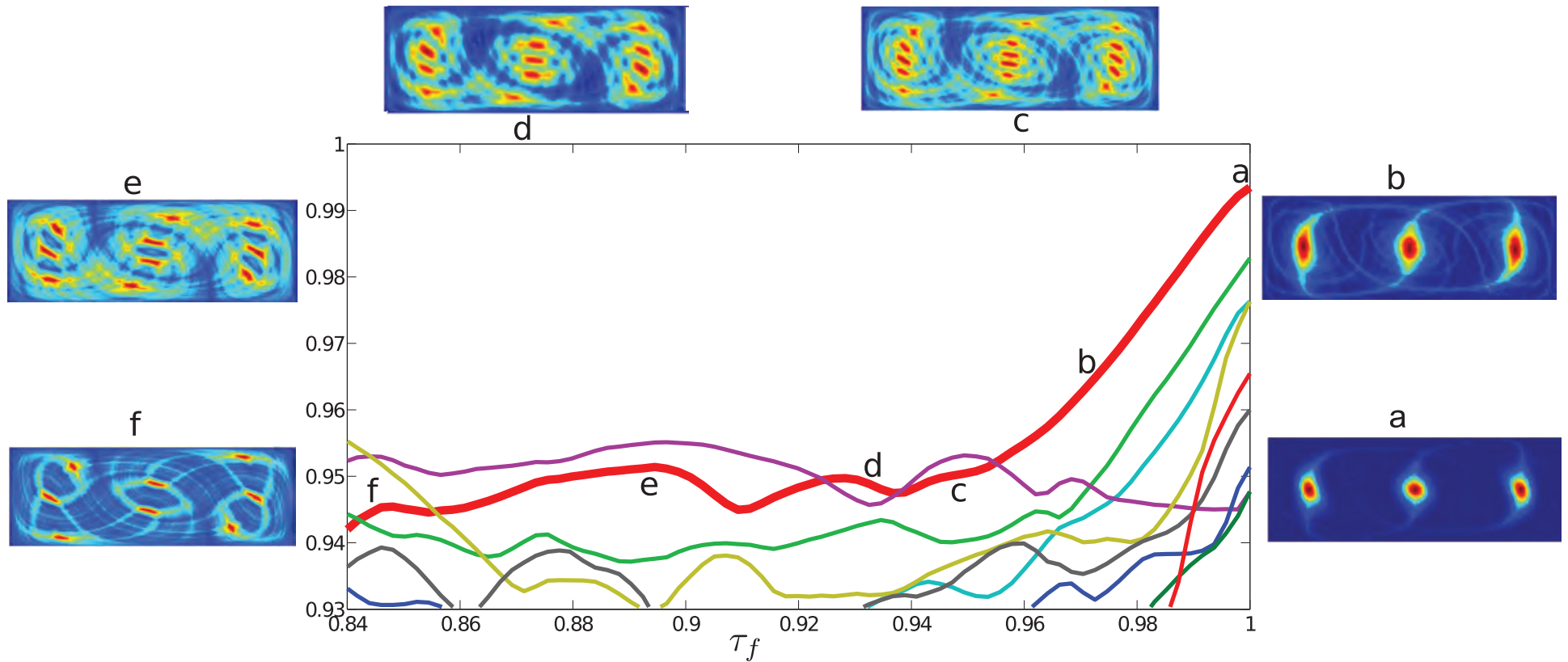
Eigenfunction crossing at 'near miss'

Phenomenon known since
von Neumann & Wigner [1929]

These computations from Bäcker [1998]

Also: Lax [2007] *Linear Algebra and
Its Applications*

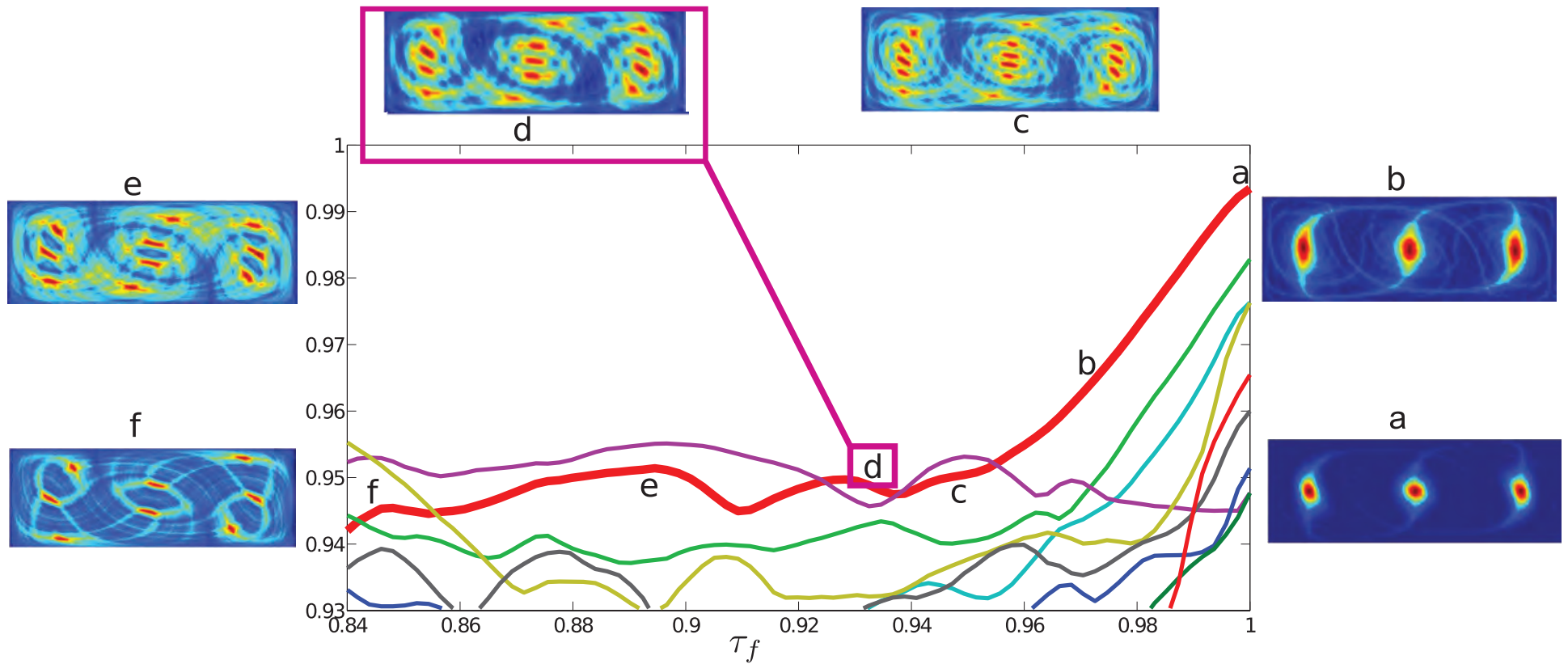
Eigenvalues/eigenvectors vs. parameter



change in eigenvector along thick red branch (a to f), as τ_f decreases.

Grover, Ross, Stremler, Kumar [2012] Chaos

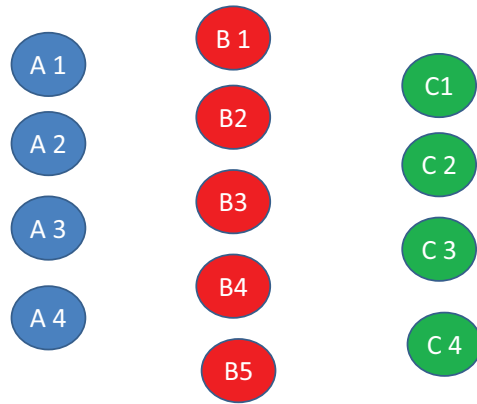
Eigenvalues/eigenvectors vs. parameter



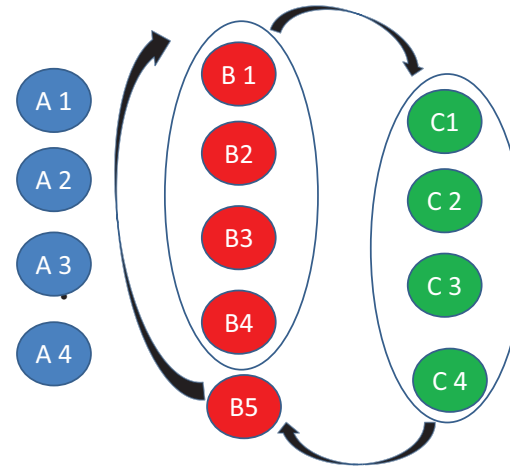
change in eigenvector along thick red branch (a to f), as τ_f decreases.

Grover, Ross, Stremler, Kumar [2012] Chaos

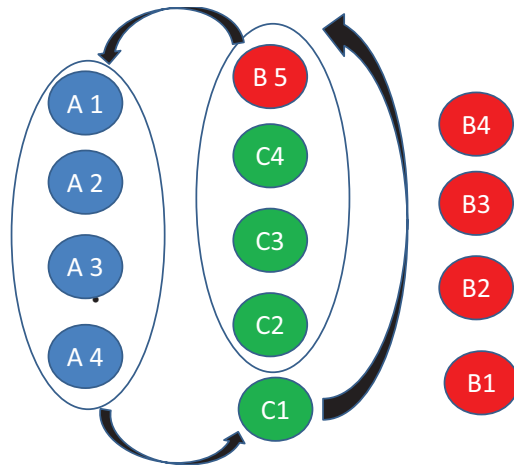
Bifurcation of ACSs



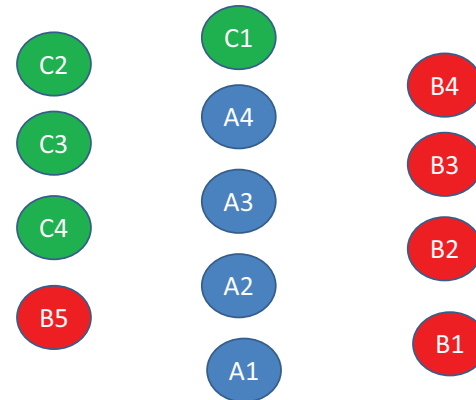
(a) Initial state



(b) First half-period

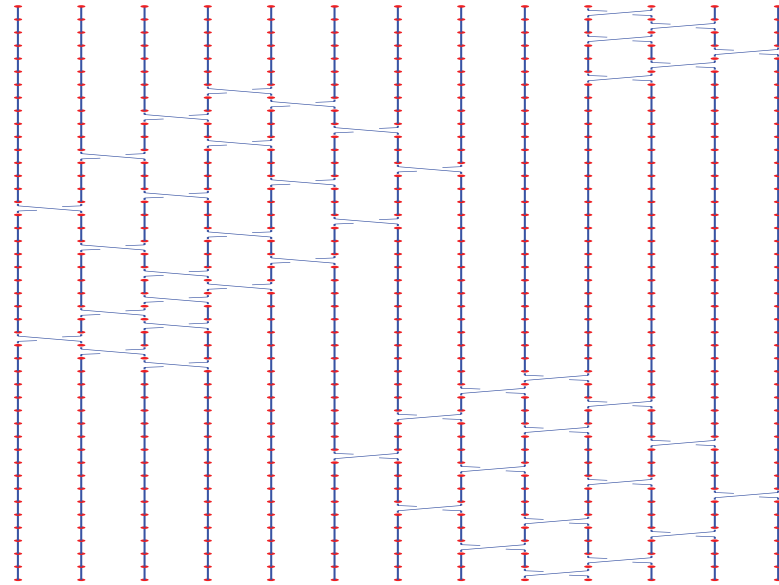


(c) Second half-period



(d) State after 1 period

Bifurcation of ACSs



representation of braid on 13 strands

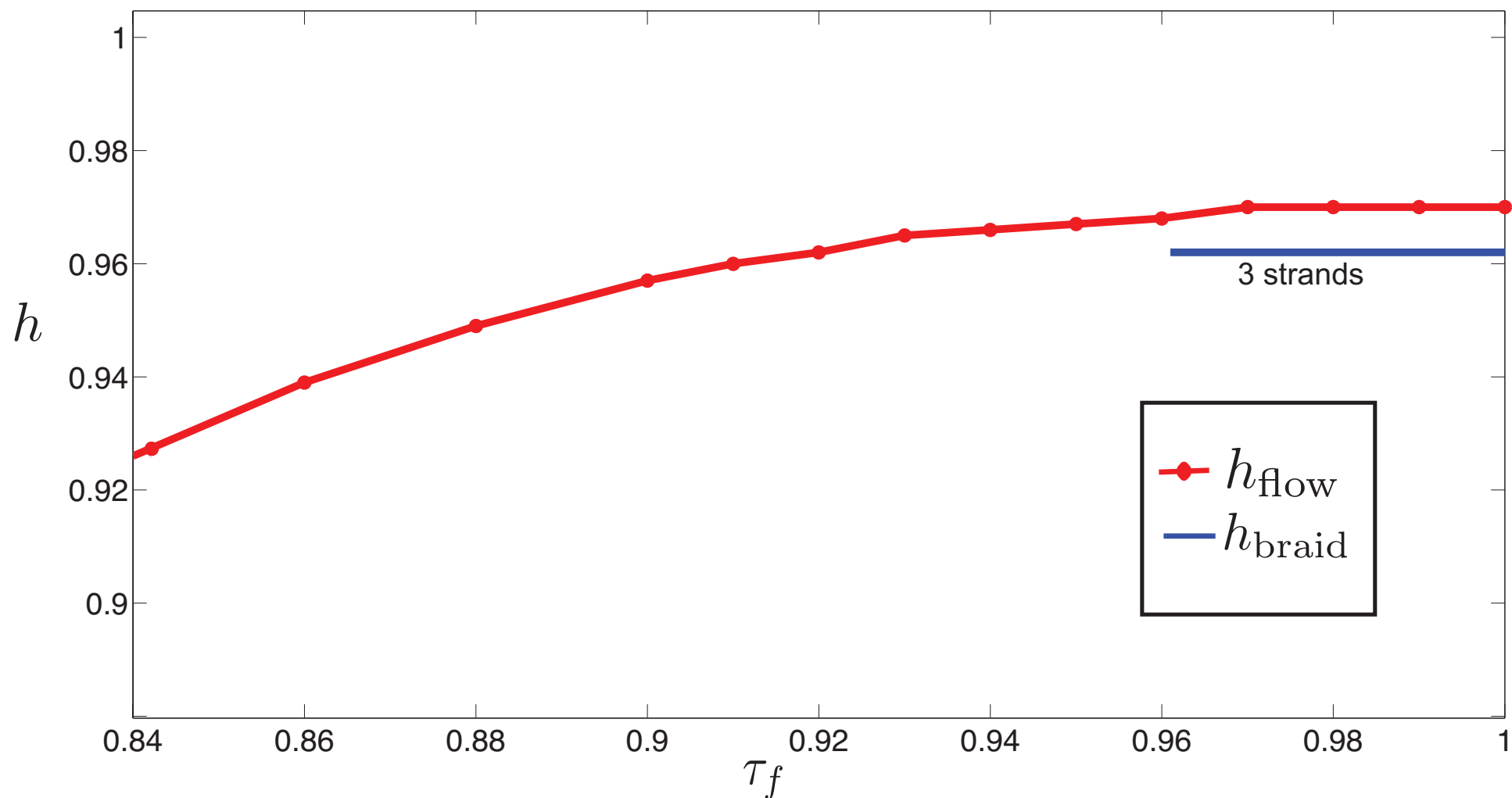
Braid word (action of this braid)

$$\sigma_{10} \sigma_{11} \sigma_{10} \sigma_{12} \sigma_{11} \sigma_{10} \sigma_{-4} \sigma_{-5} \sigma_{-3} \sigma_{-6} \sigma_{-4} \sigma_{-2} \sigma_{-7} \sigma_{-5} \sigma_{-3} \sigma_{-1} \sigma_{-6} \sigma_{-4} \sigma_{-2} \sigma_{-5} \sigma_{-3} \sigma_{-4} \cdots$$
$$\sigma_{-3} \sigma_{-2} \sigma_{-3} \sigma_{-1} \sigma_{-2} \sigma_{-3} \sigma_9 \sigma_8 \sigma_{10} \sigma_7 \sigma_9 \sigma_{11} \sigma_6 \sigma_8 \sigma_{10} \sigma_{12} \sigma_7 \sigma_9 \sigma_{11} \sigma_8 \sigma_{10} \sigma_9$$

From word, can determine if f.o. or pA (and topological entropy)

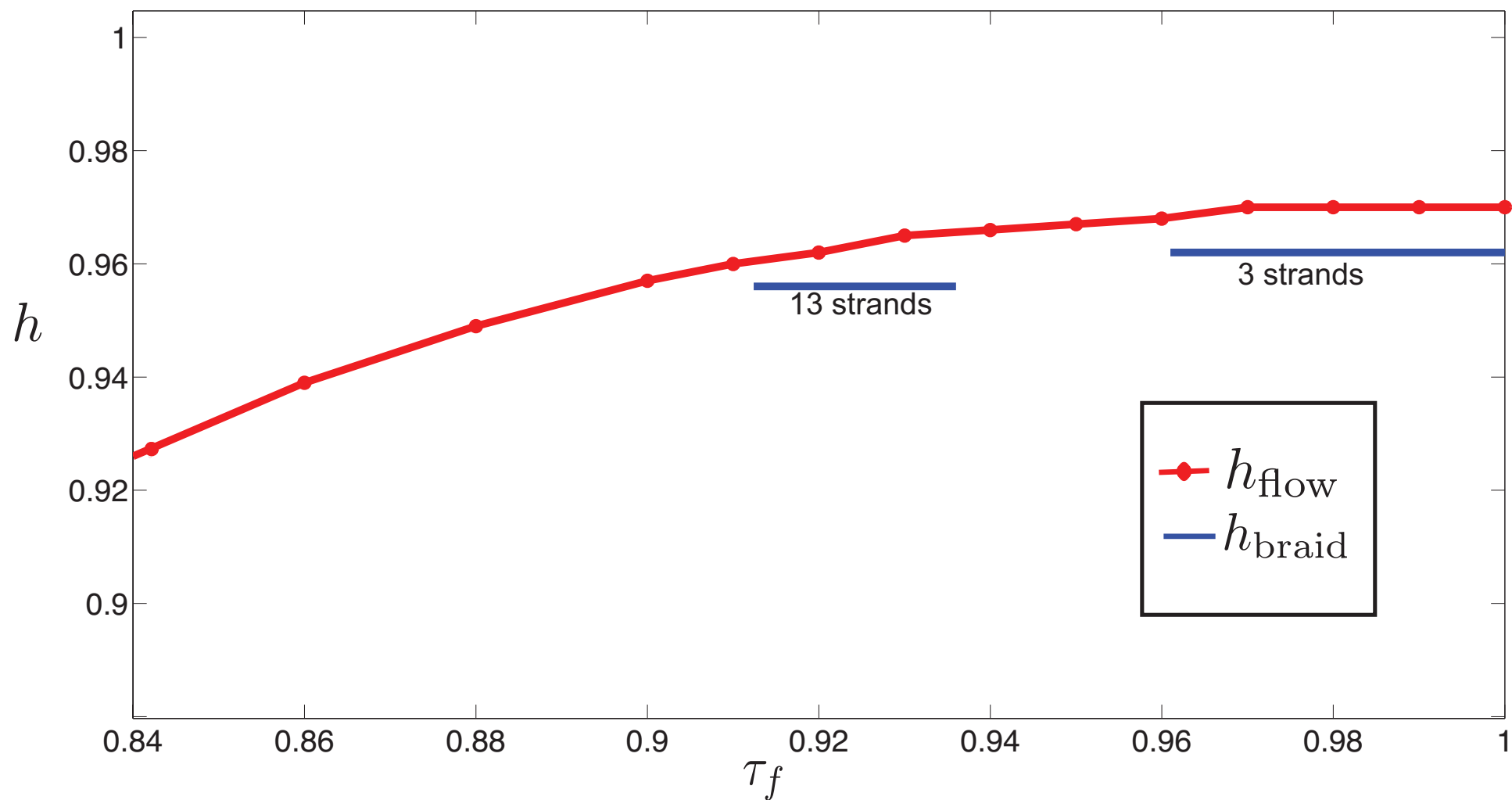
Use braidlab software of Jean-Luc Thiffeault (U. Wisconsin-Madison)

Sequence of ACS braids bounds entropy



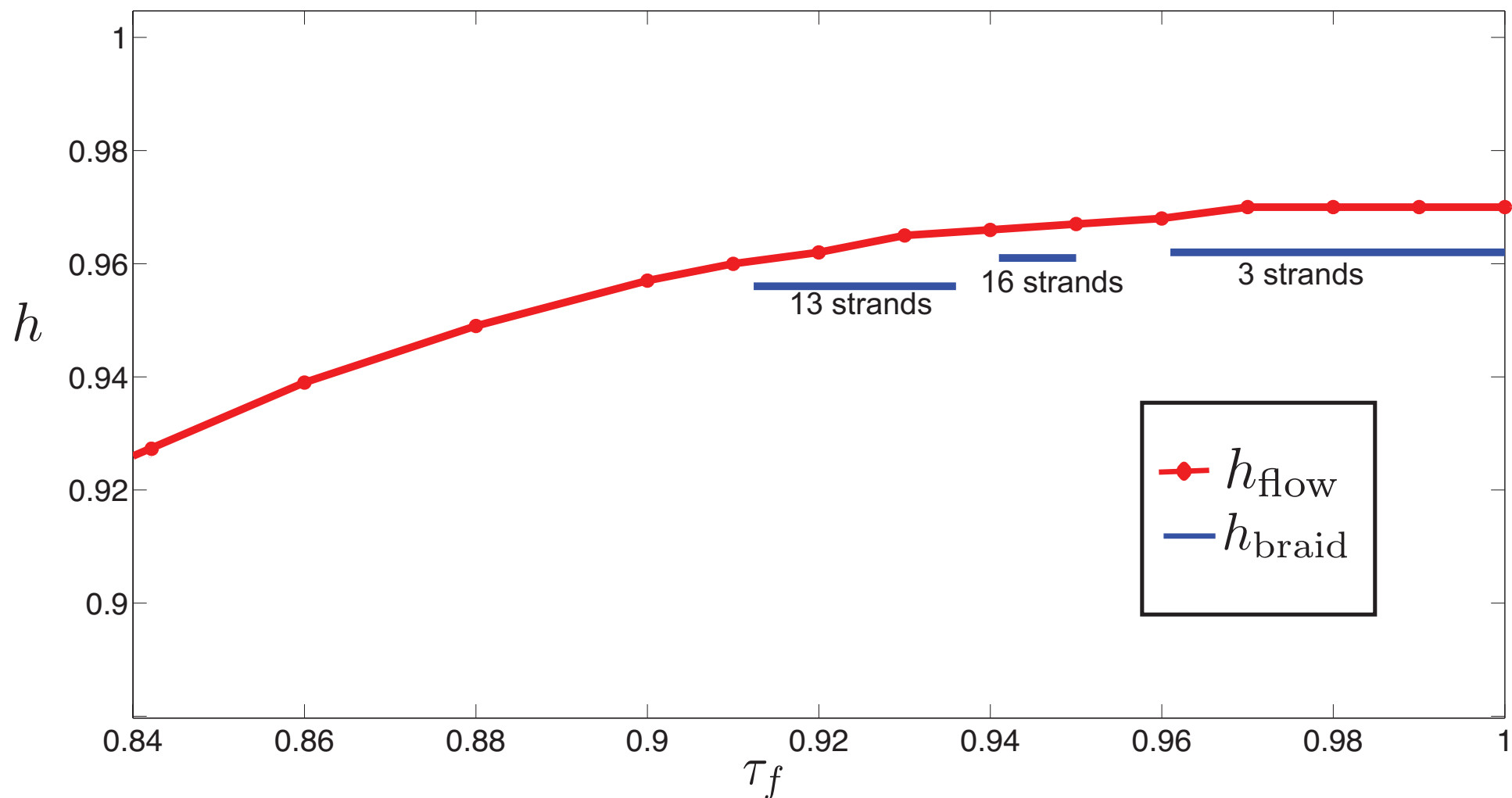
For various braids of ACSs, the calculated entropy is given, bounding from below the true topological entropy over the range where the braid exists

Sequence of ACS braids bounds entropy



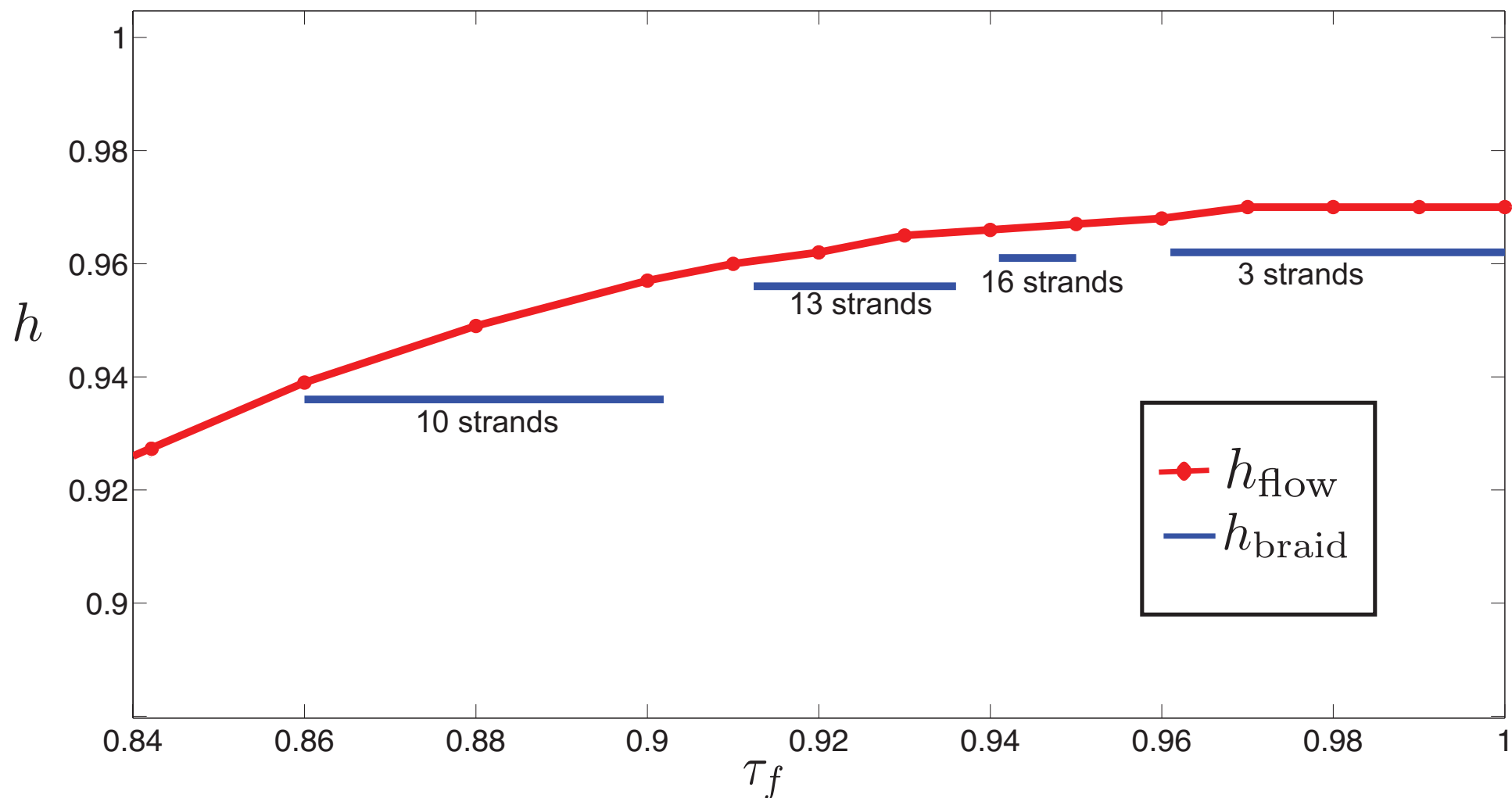
For various braids of ACSs, the calculated entropy is given, bounding from below the true topological entropy over the range where the braid exists

Sequence of ACS braids bounds entropy



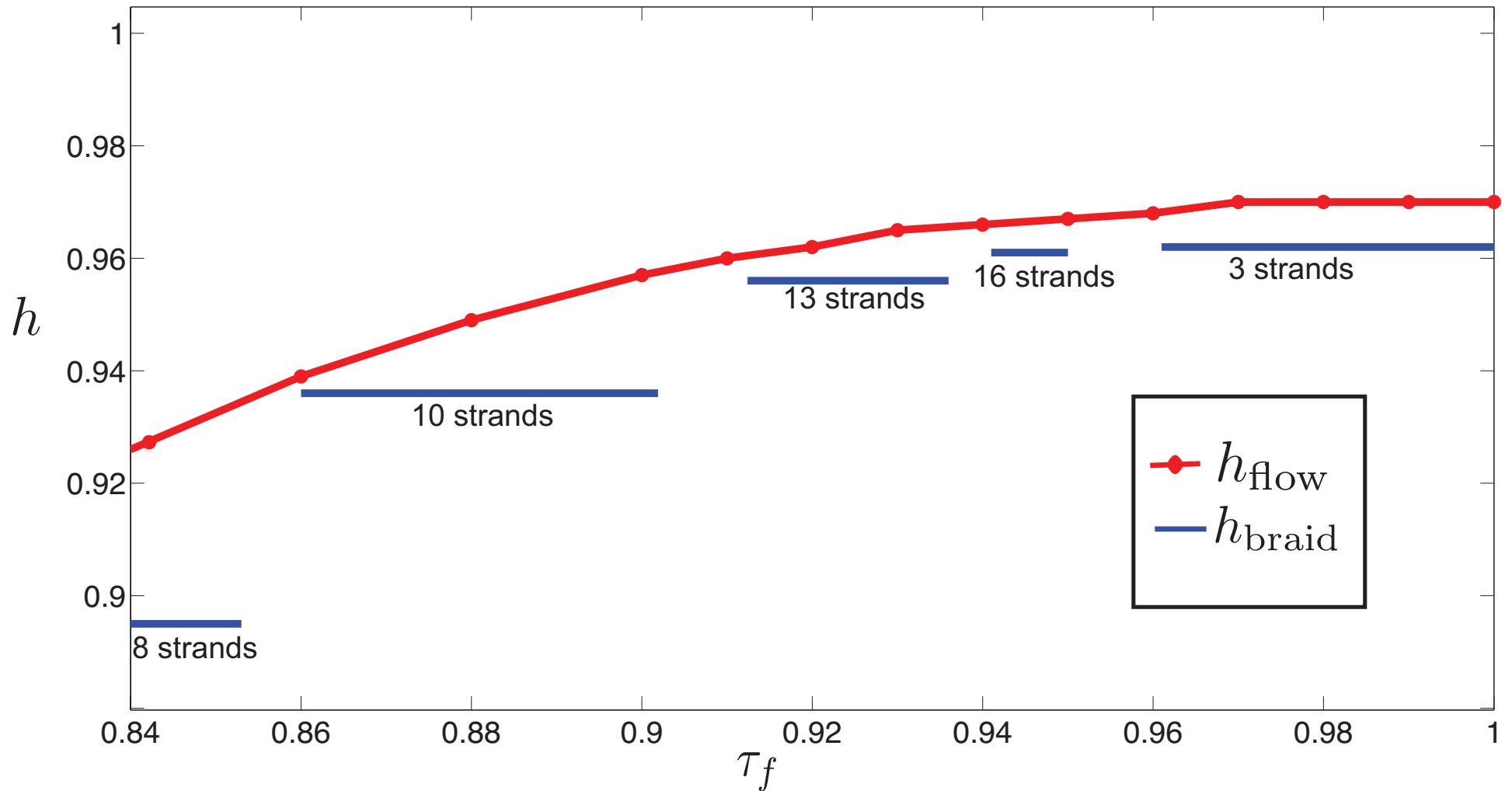
For various braids of ACSs, the calculated entropy is given, bounding from below the true topological entropy over the range where the braid exists

Sequence of ACS braids bounds entropy



For various braids of ACSs, the calculated entropy is given, bounding from below the true topological entropy over the range where the braid exists

Sequence of ACS braids bounds entropy



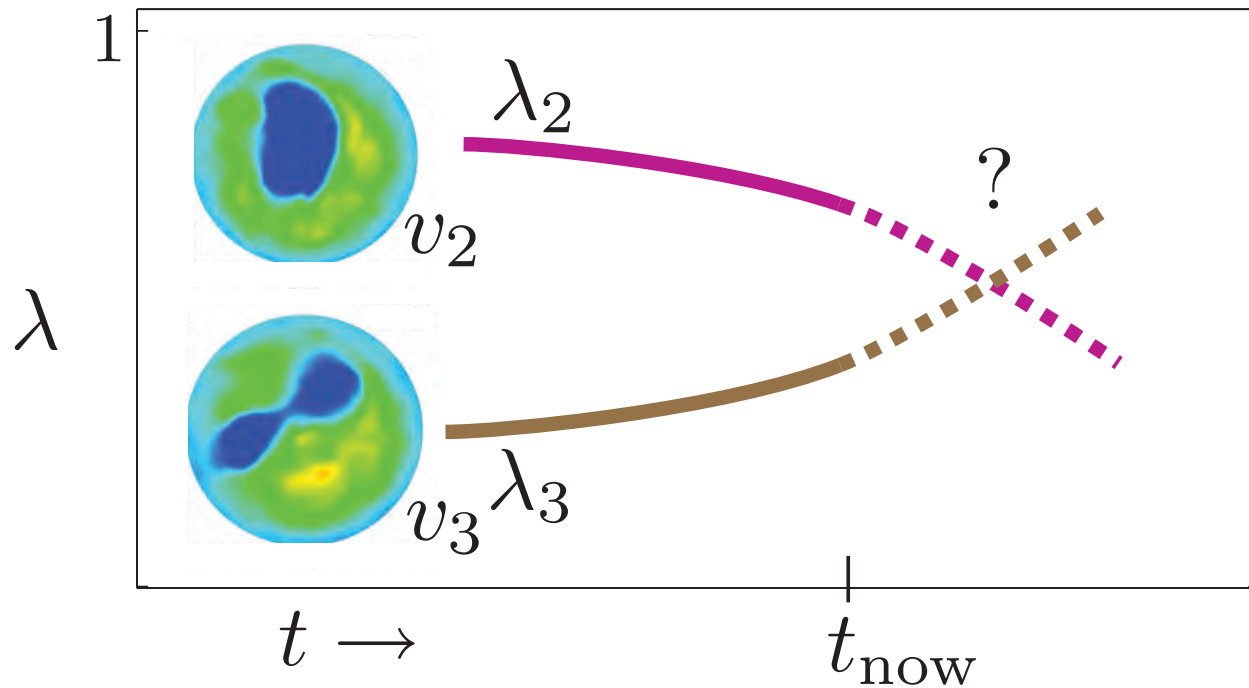
For various braids of ACSs, the calculated entropy is given, bounding from below the true topological entropy over the range where the braid exists

Speculation: trends in eigenvalues/modes for prediction

Predict critical transitions in geophysical transport?

Ozone data (Lekien and Ross [2010] Chaos)

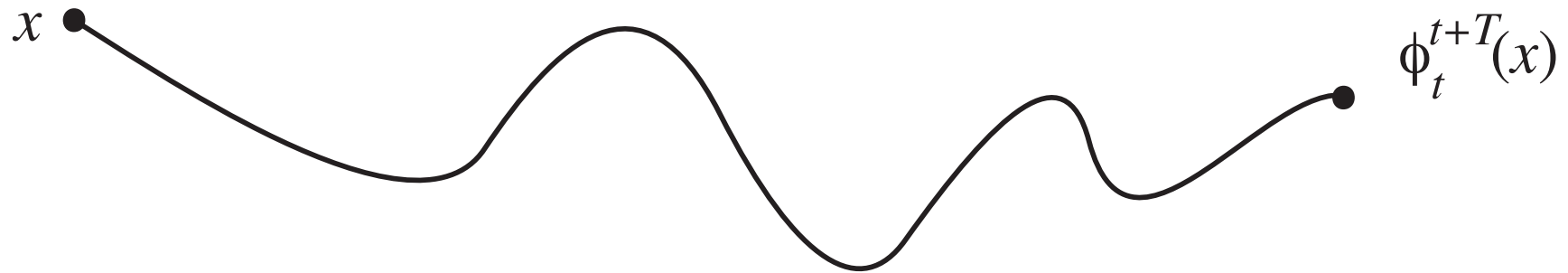
Predict critical transitions in geophysical transport?



- Different eigenmodes can correspond to dramatically different behavior.
- Some eigenmodes increase in importance while others decrease
- Can we predict dramatic changes in system behavior?
- e.g., predicting major changes in geophysical transport patterns??

Chaotic transport: aperiodic, finite-time setting

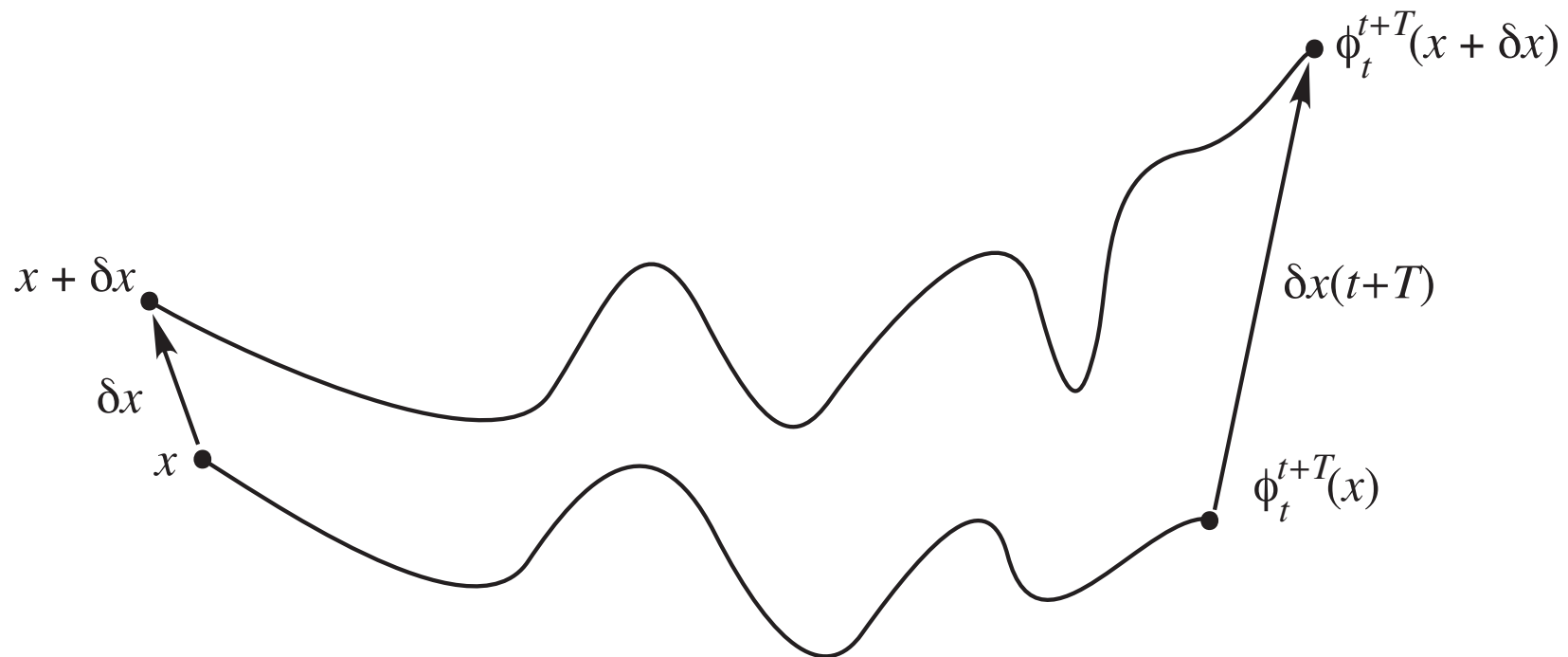
- Data-driven, finite-time, aperiodic setting
 - e.g., non-autonomous ODEs for fluid flow, $\dot{x} = u(x, t)$, $x \in \mathbb{R}^n$
- How do we get at transport?
- The flow map, $x \mapsto \phi_t^{t+T}(x)$, where $\phi_t^{t+T} : \mathbb{R}^n \rightarrow \mathbb{R}^n$



Identify regions of high sensitivity of initial conditions

- Small material line elements $\delta x(t)$ grow like

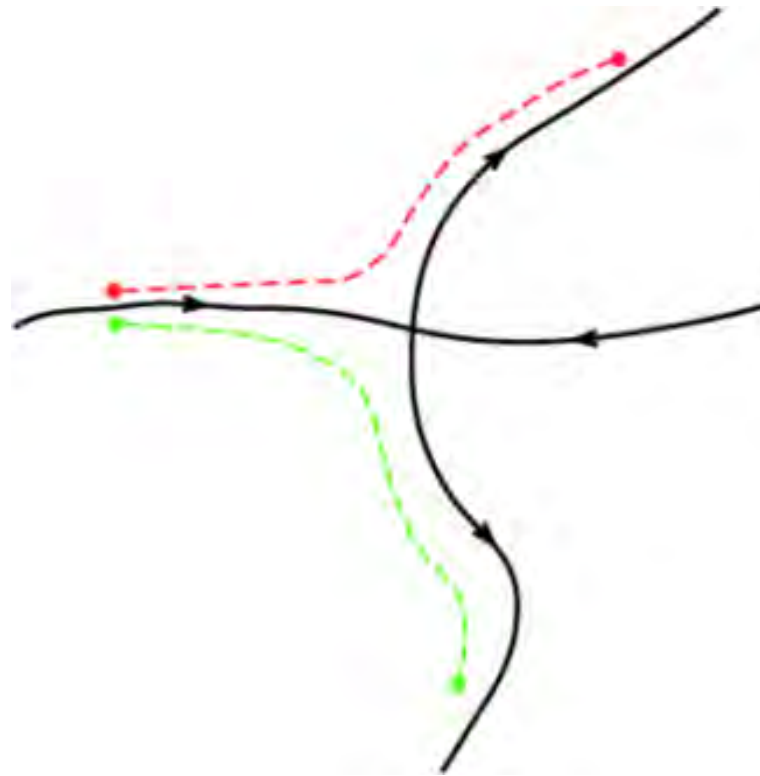
$$\begin{aligned}\delta x(t+T) &= \phi_t^{t+T}(x + \delta x(t)) - \phi_t^{t+T}(x) \\ &= D\phi_t^{t+T}(x)\delta x(t) + O(\|\delta x(t)\|^2)\end{aligned}$$



Identify regions of high sensitivity of initial conditions

- Small material line elements $\delta x(t)$ grow like

$$\begin{aligned}\delta x(t + T) &= \phi_t^{t+T}(x + \delta x(t)) - \phi_t^{t+T}(x) \\ &= D\phi_t^{t+T}(x)\delta x(t) + O(\|\delta x(t)\|^2)\end{aligned}$$



Invariant manifold analogs: FTLE-LCS approach

- right Cauchy-Green deformation tensor

$$C_t^T(x) = \left[D\phi_t^{t+T}(x) \right]^T D\phi_t^{t+T}(x)$$

- finite-time Lyapunov exponent (FTLE),

$$\begin{aligned}\sigma_t^T(x) &= \frac{1}{|T|} \log \left\| D\phi_t^{t+T}(x) \right\| \\ &= \frac{1}{|T|} \log \sqrt{\lambda_{\max}(C_t^T(x))}\end{aligned}$$

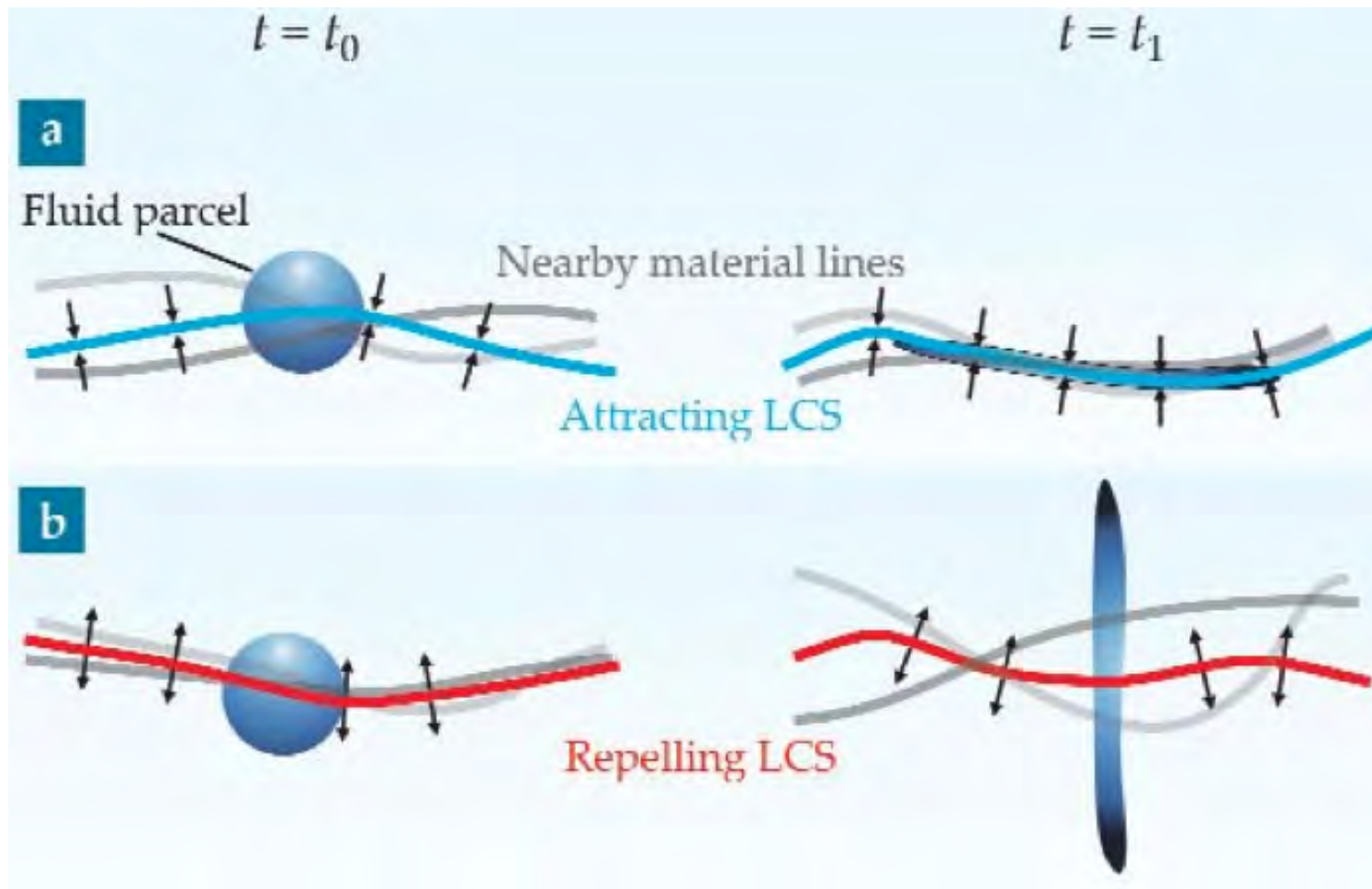
measures the maximum stretching rate over the interval T of trajectories starting near the point x at time t

- Ridges of σ_t^T reveal hyperbolic codim-1 surfaces; finite-time stable/unstable manifolds; **'Lagrangian coherent structures' or LCSs**⁴

⁴ cf. Bowman, 1999; Haller & Yuan, 2000; Haller, 2001; Shadden, Lekien, Marsden, 2005

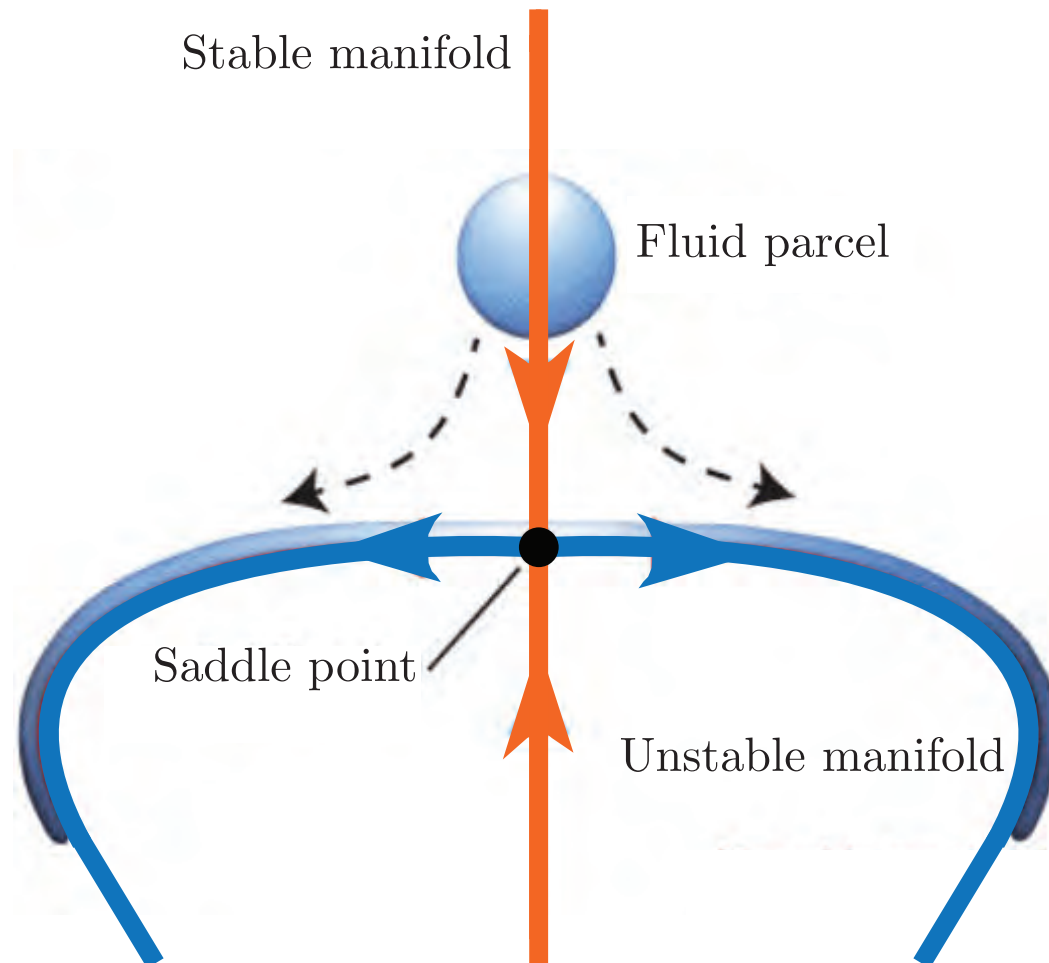
Repelling and attracting structures

- attracting structures for $T < 0$
repelling structures for $T > 0$



Repelling and attracting structures

- Most influential structures of Lagrangian deformation pattern
- Stable manifolds are repelling structures
Unstable manifolds are attracting structures

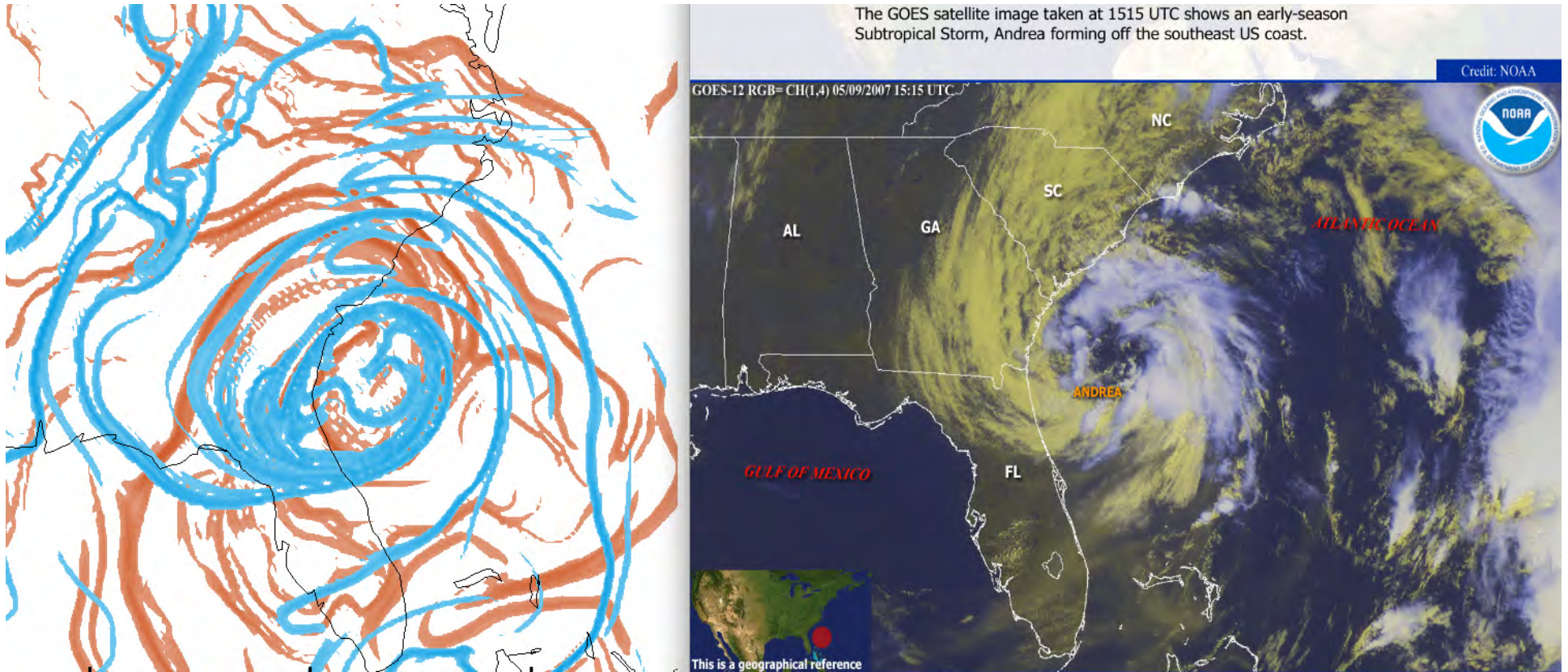


Atmospheric flows: continental U.S.

LCSs: orange = repelling, blue = attracting

2D curtain-like structures bounding 3D air masses

Atmospheric flows and lobe dynamics — hurricane



orange = repelling LCSs, blue = attracting LCSs

satellite

Andrea, first storm of 2007 hurricane season

cf. Sapsis & Haller [2009], Du Toit & Marsden [2010], Lekien & Ross [2010], Ross & Tallapragada [2012]

Atmospheric flows and lobe dynamics — hurricane



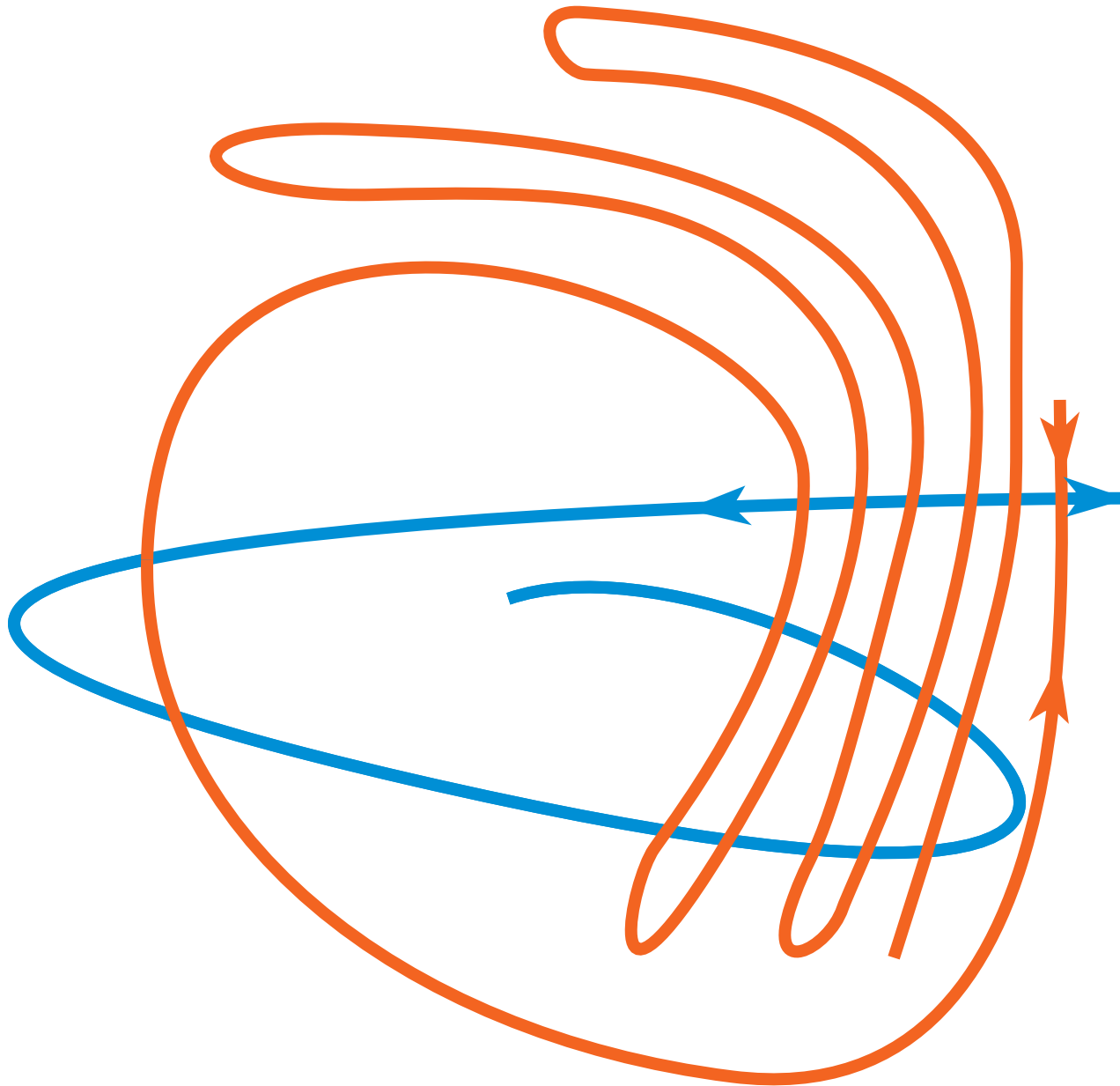
Andrea at one snapshot; LCS shown (orange = repelling, blue = attracting)

Atmospheric flows and lobe dynamics — hurricane



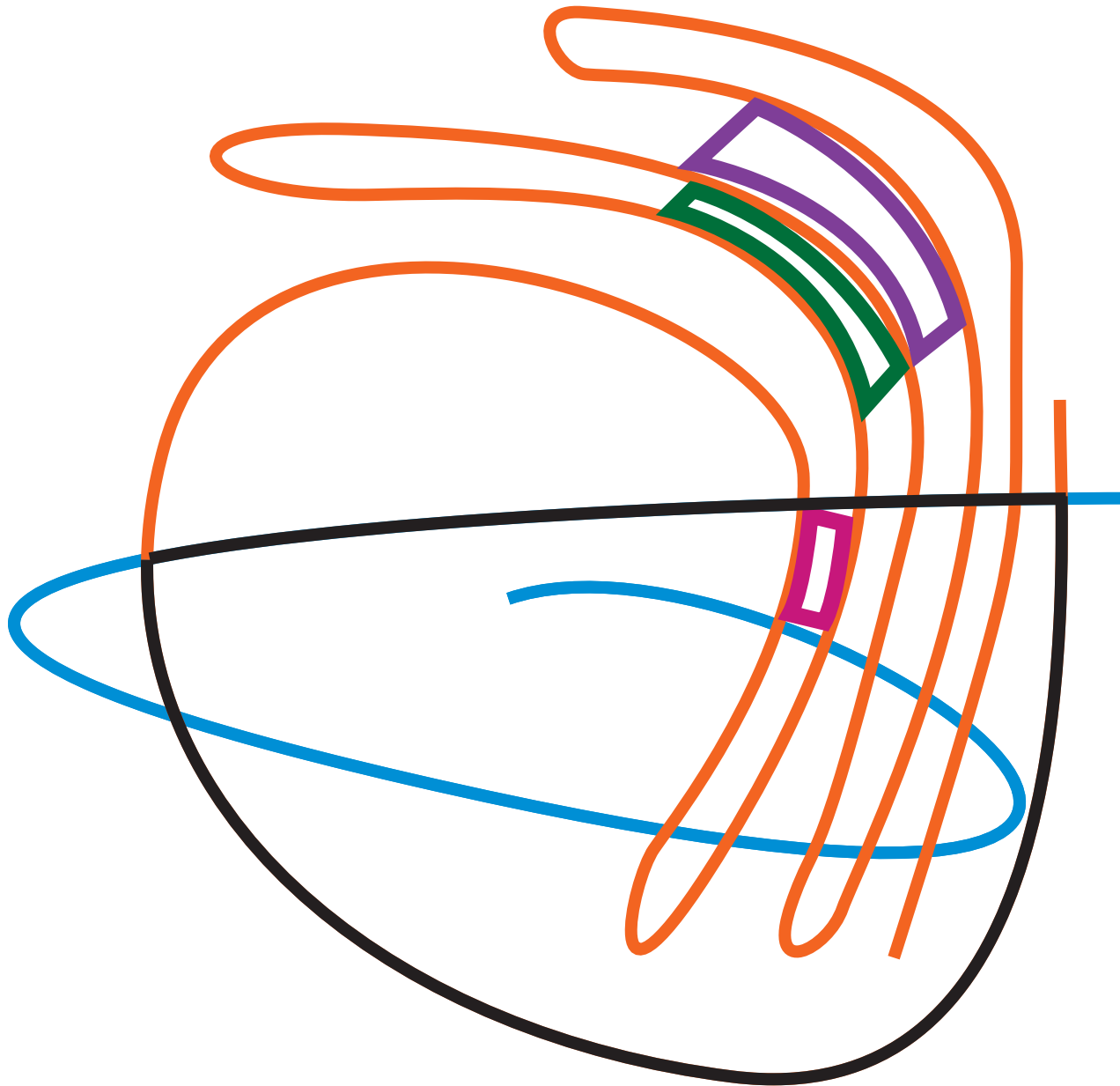
orange = repelling (stable manifold), blue = attracting (unstable manifold)

Atmospheric flows and lobe dynamics — hurricane



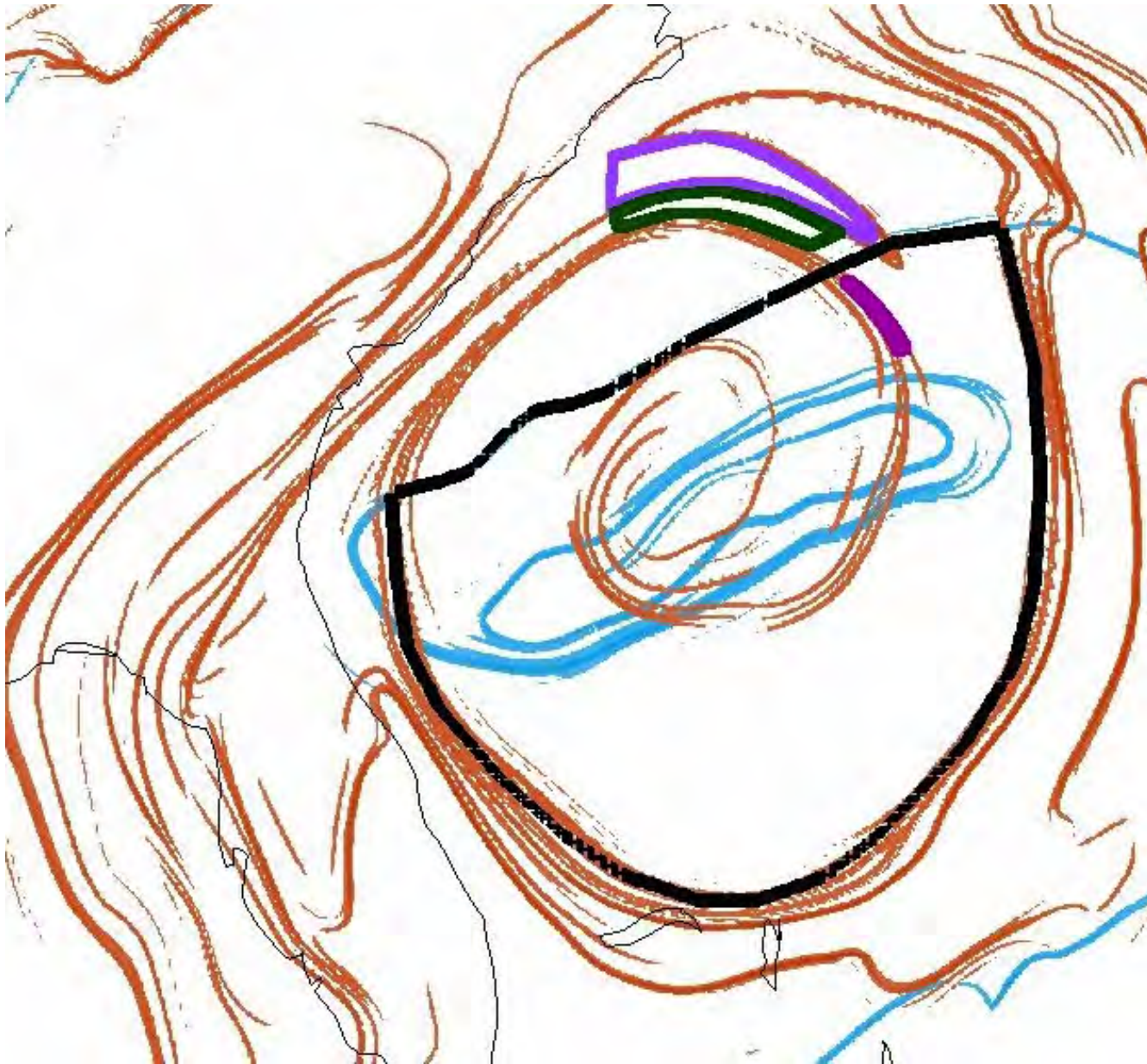
orange = repelling (stable manifold), blue = attracting (unstable manifold)

Atmospheric flows and lobe dynamics — hurricane



Portions of lobes colored; magenta = outgoing, green = incoming, purple = stays out

Atmospheric flows and lobe dynamics — hurricane

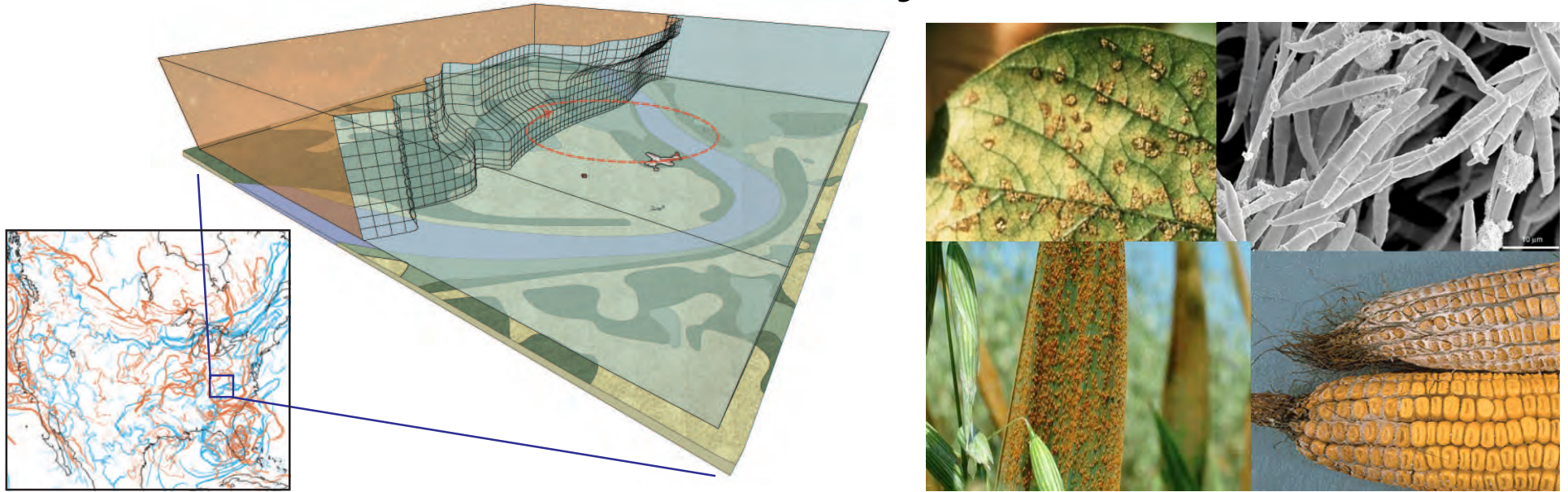


Portions of lobes colored; magenta = outgoing, green = incoming, purple = stays out

Atmospheric flows and lobe dynamics — hurricane

Sets behave as lobe dynamics dictates; also form pA braid

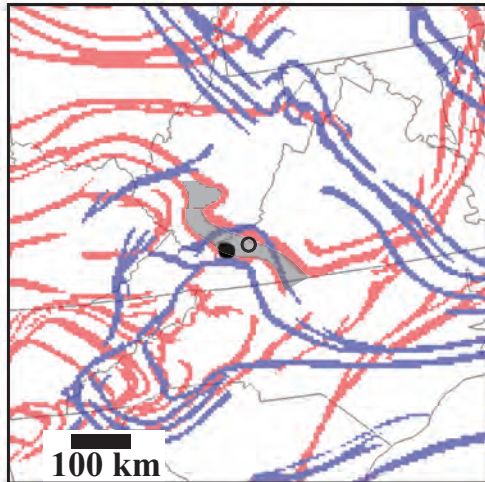
Airborne diseases moved about by coherent structures



Joint work with David Schmale, Plant Pathology / Agriculture at Virginia Tech

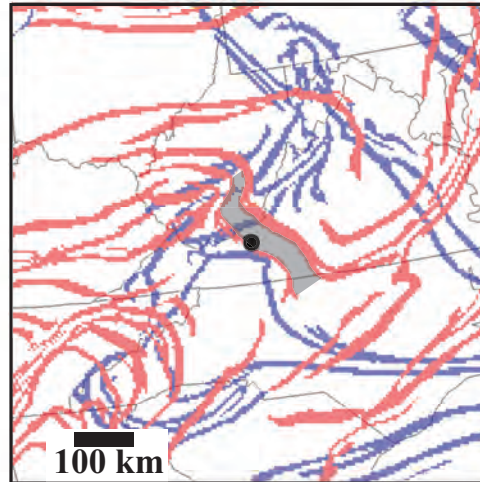
Coherent filament with high pathogen values

12:00 UTC 1 May 2007



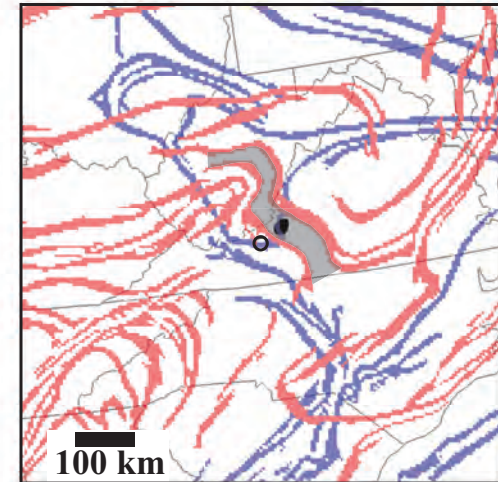
(a)

15:00 UTC 1 May 2007

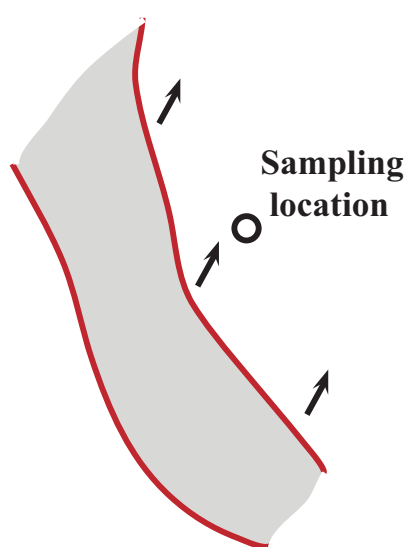


(b)

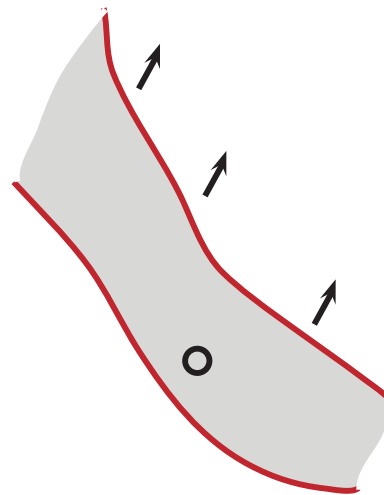
18:00 UTC 1 May 2007



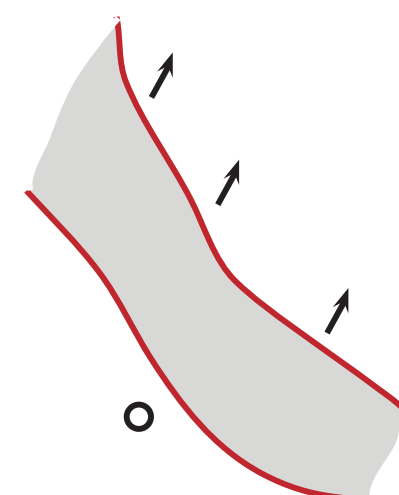
(c)



(d)



(e)



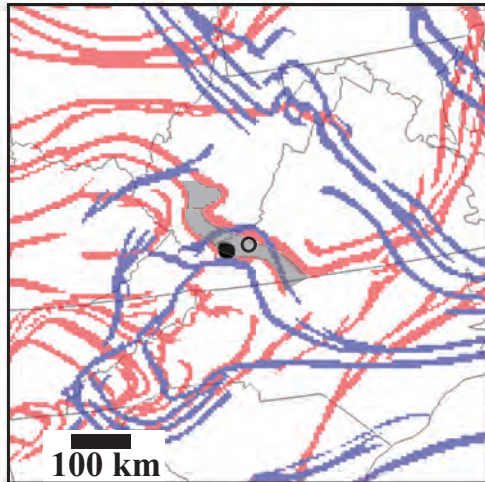
(f)

Coherent filament with high pathogen values

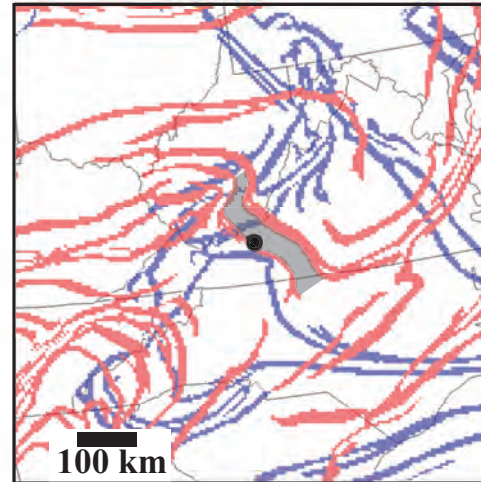
12:00 UTC 1 May 2007

15:00 UTC 1 May 2007

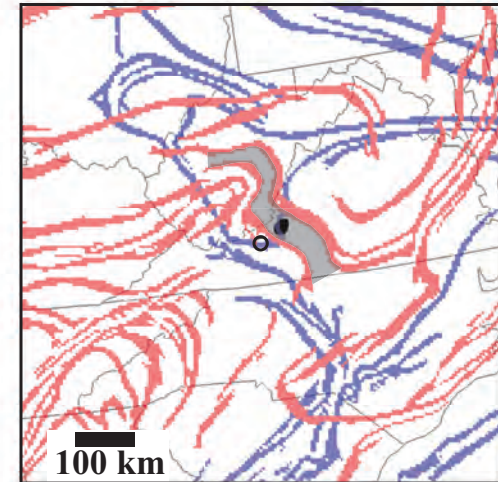
18:00 UTC 1 May 2007



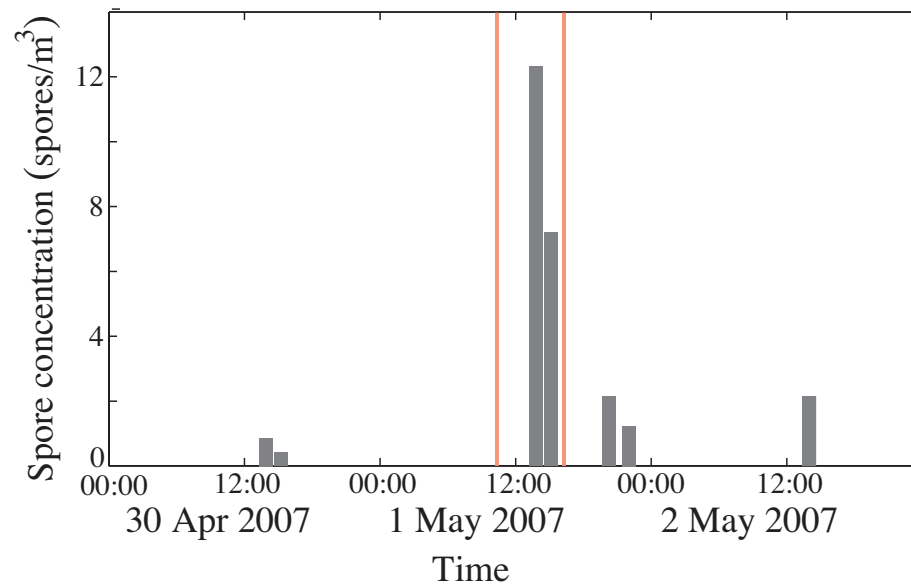
(a)



(b)



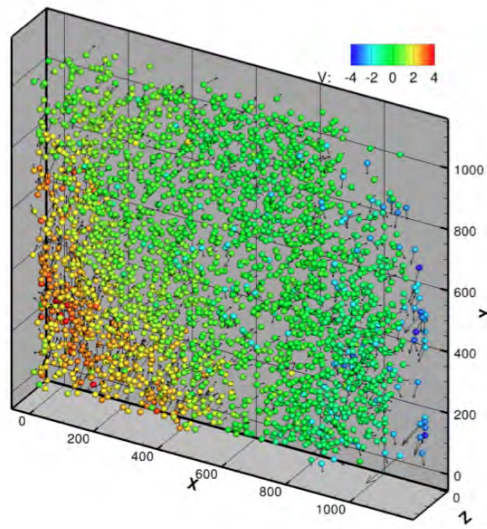
(c)



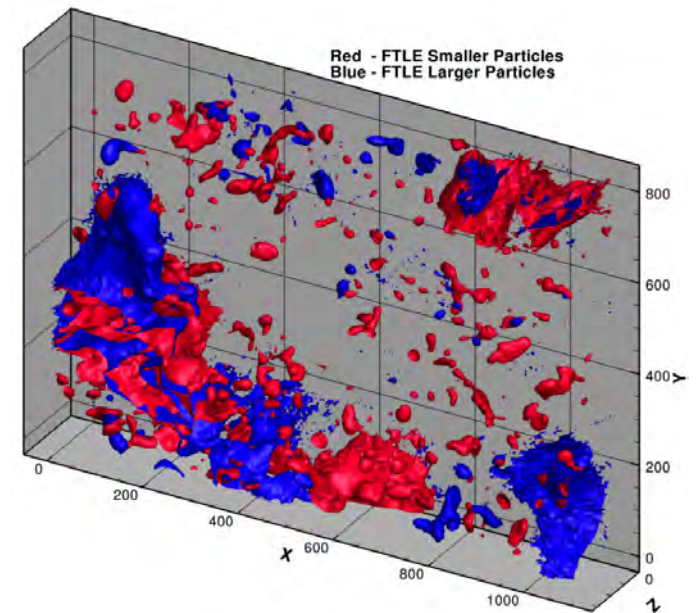
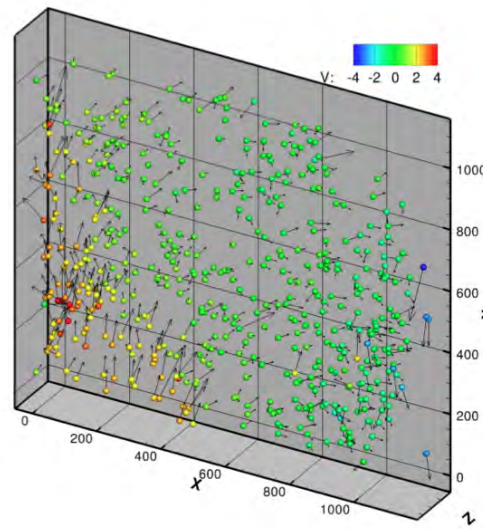
Laboratory fluid experiments

3D Lagrangian structure for non-tracer particles:
— Inertial particle patterns (do not follow fluid velocity)

Above 75 voxels



Above 175 voxels



e.g., allows further exploration of physics of multi-phase flows⁵

⁵Raben, Ross, Vlachos [2014,2015] Experiments in Fluids

Predicting spread of hazardous material, debris

- ALPHA - Advanced Lagrangian Predictions for Hazards Assessments⁶
- e.g., oil spills, Coast Guard search-and-rescue, airplane debris fields
- Transport at air-water interface is a hybrid of ocean-wind effects



Deep Horizons oil spill



ocean search-and-rescue

⁶NSF Hazards SEES project: MIT-Woods Hole-Virginia Tech-Berkeley

Parting words on transport and mixing in fluids

- What are robust descriptions of transport which work in data-driven aperiodic, finite-time settings?
 - Geometric methods
 - finite-time lobe dynamics / symbolic dynamics
 - Probabilistic methods
 - almost-invariant sets, almost-cyclic sets
 - bifurcation analysis via eigenstructure changes
 - Topological methods
 - periodic braids, Thurston-Nielsen classification
 - Interesting links between some of these notions
 - Connections with fluid modeling?

Thank you!

For papers, movies, etc., visit: shaneross.com

- Schmale & Ross [2015] Highways in the Sky: Scales of Atmospheric Transport of Plant Pathogens. *Annual Review of Phytopathology* 53, 591.
- BozorgMagham & Ross [2015] Atmospheric Lagrangian coherent structures considering unresolved turbulence and forecast uncertainty, *Comm. in Nonlin. Sci. Numer. Simulation* 22, 964
- Raben, Ross, Vlachos [2014] Computation of finite time Lyapunov exponents from time resolved particle image velocimetry data. *Experiments in Fluids* 55, 1638.
- Tallapragada & Ross [2013] A set oriented definition of the finite-time Lyapunov exponent and coherent sets. *Comm. in Nonlin. Sci. Numer. Simulation* 18, 1106.
- Grover, Ross, Stremler, Kumar [2012] Topological chaos, braiding and breakup of almost-invariant sets. *Chaos* 22, 043135.
- Stremler, Ross, Grover, Kumar [2011] Topological chaos and periodic braiding of almost-cyclic sets. *Physical Review Letters* 106, 114101.
- Lekien & Ross [2010] The computation of finite-time Lyapunov exponents on unstructured meshes and for non-Euclidean manifolds. *Chaos* 20, 017505.